JUSTUS-LIEBIG-
UNIVERSITÄT
GIESSEN

Fachbereich 06
Psychologie und Sportwissenschaft
35394 Gießen

Chromatic and luminance processing during eye movements in human early visual cortex

Synopsis zur kumulativen Dissertation
zur Erlangung des Doktorgrades der Naturwissenschaften
vorgelegt von Yuan Zhang

Betreuer und Erstgutachter: Prof. Dr. Karl Gegenfurtner
Zweitbetreuerin: Prof. Dr. Katja Dörschner-Boyaci

Summary

Human vision is not a passive process. Rather, our visual perception of the world emerges from a dynamic and adaptive interplay between sensory input and motor action, whereby perception continually guides movements, and these movements in turn reshape perceptual experience. Eye movements are essential for acquiring clear visual input in natural viewing. Despite substantial progress in understanding how eye movements are generated, controlled, and functionally organized, fundamental questions remain about how early visual processing is modulated by natural viewing behaviors, and how different types of eye movements influence neural mechanisms encoding color and luminance. This dissertation addresses these questions by combining precise neurophysiological measurement techniques with carefully controlled behavioral paradigms.

Our eyes move frequently to keep objects of interest projected onto the fovea for a clear image. Among these movements, saccades are rapid, ballistic shifts of gaze that move the eyes from one location to another, while smooth pursuit keeps a moving target within the foveal region through continuous, slow eye rotations that closely match the target's speed and direction. When the gaze is relatively stable and directed at a single point, the eye is in a state of fixation. These three types of eye movements are fundamental for acquiring visual information from the environment.

Visual scenes are encoded by the L, M, and S cones in the retina and then relayed via three pathways: the magnocellular pathway (L+M, luminance), the parvocellular pathway (L–M, red-green opponency), and the koniocellular pathway (S–[L+M], blue-yellow opponency). These pathways transmit information in parallel up to the primary visual cortex (V1), where their signals are subsequently processed through partially distinct yet interacting cortical circuits (for reviews, see Gegenfurtner, 2003; S. H. C. Hendry & Reid, 2000; Nassi & Callaway, 2009). Given that V1 is the first cortical site where luminance and chromatic signals converge and begin to interact, a key unresolved question is how these signals are modulated by different types of eye movements during natural viewing.

To explore the neural mechanisms underlying these processes, this thesis employed steady-state visual evoked potentials (SSVEPs) to track neural responses in the early visual cortex. SSVEPs are brain oscillations elicited by periodic visual stimulation (Adrian & Matthews, 1934; for review, see Norcia et al., 2015), originating primarily from V1 (Di Russo et al., 2007; Müller et al., 1997). SSVEPs possess high temporal resolution and exhibit narrowband spectral responses locked

precisely to the stimulation frequency, making them highly resistant to eye movement artifacts (e.g., J. Chen et al., 2017a, 2017b; J. Chen, Valsecchi, et al., 2019). Those properties make SSVEPs a reliable tool for studying visual processing in the human early visual cortex during eye movements.

In Study 1, we investigated the effect of chromatic (L–M) adaptation during prolonged fixation. Results showed that SSVEP responses to chromatic stimuli progressively decrease as stimulation duration increased, following an exponential decay with a half-life of approximately 20 seconds. In contrast, responses to luminance stimuli did not show any systematic adaptation. After characterizing this sustained visual adaptation, Study 2 then investigated transient modulations of visual cortical responses induced by saccadic eye movements. Results demonstrated comparable saccadic suppression effects on SSVEP responses to both chromatic (L–M) and luminance stimuli. Further modeling of contrast response functions revealed that saccades selectively reduced response gain without altering contrast gain, suggesting that visual attenuation involves a multiplicative mechanism operating similarly within both the parvocellular and magnocellular pathways. To enhance the quality of SSVEP data, the third study evaluated various EEG referencing methods and introduced the Laplacian reference as an optimal strategy for signal derivation. Results showed that the Laplacian reference significantly improved the signal-to-noise ratio (SNR) and reliability of neural measurements, while also being straightforward to implement across different experimental settings.

Taken together, these findings underscore the critical role of eye movements in modulating both luminance and chromatic signals within the early visual cortex. This work demonstrates that perception is dynamically shaped by the continuous interplay between sensory input and oculomotor behavior, offering new insights into how active vision operates under natural viewing conditions.

Contents

I. Synopsis

1. Introduction

Imagine walking your dog in nature, and finally reaching the perfect spot to play fetch. You see green grass dotted with flowers, and watch your dog dash into the bushes and return with enthusiasm. While you enjoy this vibrant scene, it's worth noting that your dog sees it quite differently: humans are trichromats, whereas dogs are dichromats with a red-green color deficiency, resulting in a more limited range of colors (Jacobs et al., 1993; Neitz et al., 1989). During this playful moment, your eyes are constantly active, engaging in various types of eye movements to get the image you're interested in. You smoothly track your dog's motion (smooth pursuit), hold your gaze steady while giving praise (fixation), and quickly shift your focus from the bush to the dog to cue the next round (saccades).

This leads to the first key question: How do we perceive such a rich and colorful scene? The vividness of our visual experience relies on two remarkable biological mechanisms. The first originates in the retina, where humans have evolved specialized photoreceptors and neural circuitry capable of preserving wavelength-specific information. These photoreceptors are cones, characterized by peak sensitivities (λ_{max}) in the yellow-green (around 560 nm, longwave-sensitive, L), green (around 530 nm, middlewave-sensitive, M), and blue (around 430 nm, shortwave-sensitive, S) regions of the spectrum (Baylor et al., 1987; Hunt & Peichl, 2014; Stockman & Sharpe, 2000). The second mechanism lies in the visual cortex, where cone signals are processed via functional pathways specialized for extracting information such as color, luminance, edges, and motion (for review, see Gegenfurtner, 2003). Specifically, there are pathways categorized as magnocellular, parvocellular, and koniocellular pathway. The magnocellular pathway is sensitive to luminance contrast and high temporal frequencies. In contrast, the parvocellular and koniocellular pathways operate at finer spatial and lower temporal resolutions, and are primarily involved in red-green and blue-yellow color processing, respectively (Derrington & Lennie, 1984; S. H. Hendry & Yoshioka, 1994; Page et al., 1994; Schiller et al., 1990). Chromatic and luminance signals are transmitted in parallel via these pathways from the retina through the lateral geniculate nucleus (LGN) to the primary visual cortex (V1), where their processing begins to integrate before becoming further distributed across higher cortical areas (for reviews, see Gegenfurtner, 2003; S. H. C. Hendry & Reid, 2000; Nassi & Callaway, 2009). Together, these pathways support the construction of a detailed and stable perception of the visual world. Importantly, however, it should be noted that these pathways are not completely

independent; interactions between them occur at multiple cortical stages (for review, see Gegenfurtner & Hawken, 1996).

The second key question that arises from the initial example is: Why and how do our eyes actively explore the visual scene? Cone photoreceptor density is highest in the fovea, the center of the visual field, and declines rapidly toward the periphery (Curcio & Allen, 1990; Østerberg, 1935). As a result, visual acuity (Anstis, 1974; Aubert & Foerster, 1857) and contrast sensitivity (Pointer & Hess, 1989; J. G. Robson & Graham, 1981) peak at the fovea and diminish with eccentricity. Despite the transient disruptions and energetic cost caused by eye movements, we rely on them constantly to place objects of interest onto this high-resolution region. Importantly, this advantage is not only due to retinal architecture but also because cortical processing prioritizes foveal input (Harvey & Dumoulin, 2011).

Human vision is not like a camera that passively receives input; it is dynamic, adaptive, and tightly coupled with the motor systems that guide where and how we look. Understanding visual perception therefore requires considering how sensory inputs are continuously shaped by active behaviors, such as eye movements, and by internal neural processes like adaptation, both of which jointly determine what we perceive, when, and with what fidelity. Although the neural mechanisms of eye movement generation and control are well understood (for reviews, see Binda & Morrone, 2018; Gegenfurtner, 2016; Lisberger, 2015; Rucci & Poletti, 2015; Schutz et al., 2011), it remains unclear how early stages of visual processing are influenced by natural eye movements, particularly in relation to their effects on chromatic and luminance signals.

This thesis addresses these questions by specifically investigating the neural responses in the early visual cortex during eye movement behaviors. By employing steady-state visual evoked potentials (SSVEPs), we focus on how chromatic and luminance information are modulated during fixation and saccadic eye movements, aiming to clarify the dynamic interplay between visual perception and oculomotor actions. The following sections introduce the key questions and specific aims of each study included in this work.

1.1 Chromatic and luminance signals processing during eye movements

As described in our initial example, primates are unique among mammals in their ability to process trichromatic color vision. The evolutionary pressure behind the development of trichromacy is thought to stem from the advantage of enhanced color discrimination in the red-green range, which aids in detecting and evaluating ripe fruits and young, nutritious leaves against the predominantly

green background of the rainforest (Dominy & Lucas, 2001; Mollon, 1989; B. C. Regan et al., 2001; Sumner & Mollon, 2000). Chromatic and luminance signals originate from the recombination of cone excitations through addition and subtraction mechanisms. These signals are relayed via three major post-receptoral pathways that project to the LGN and subsequently to the cortex (Derrington et al., 1984; Derrington & Lennie, 1984; Lee, 2011). The magnocellular pathway originates in the parasol ganglion cells that receive summed input from L- and M-cones. The parvocellular pathway begins in the midget ganglion cells that receive antagonistic, subtractive input from the L- and M-cones. The koniocellular pathway typically conveys signals originating from S-cone activity in opposition to combined M- and L-cone input. Notably, the parvocellular and koniocellular pathways are distinguished by very sustained responses, which may be advantageous for encoding stable surface properties such as color. In contrast, magnocellular cells are characterized by transient responses and are particularly sensitive to luminance-defined edges, functioning primarily as contrast detectors.

During natural viewing, saccadic, smooth pursuit, and fixational eye movements are highly coordinated for keeping the interested image foveated. These eye movements are fundamental for actively sampling the visual scene (for recent reviews, see Binda & Morrone, 2018; Lisberger, 2015; Rucci & Poletti, 2015; Schutz et al., 2011). To efficiently explore a visual scene, the eyes frequently make saccades. However, such rapid shifts can disrupt the retinal image. Saccadic suppression is a potential mechanism serving for the visual stability against the distortions caused by eye sweeps over the visual field quickly and frequently. This suppression effect follows a very tight time course and exhibits pathway-specific: visual sensitivity for seeing low-spatial-frequency, luminance-modulated brief stimuli declines approximately 100 ms before saccadic onset, reaches a minimum at the onset of the saccade, then rapidly recovers to normal levels 100 ms afterward (Latour, 1962; for reviews, see Binda & Morrone, 2018; Ibbotson & Krekelberg, 2011; Sommer & Wurtz, 2008). Behavioral evidence suggests that saccades preferentially suppress signals in the magnocellular pathway (Anand & Bridgeman, 2002; Bridgeman & Macknik, 1995; Bruno et al., 2006; Burr et al., 1994; Diamond et al., 2000; Hass & Horwitz, 2011; Knöll et al., 2011; Ross et al., 2001; Uchikawa & Sato, 1995), or at least, the suppression is stronger in the magnocellular pathway compared to parvocellular pathway (Braun et al., 2017, 2021). However, the evidence is mixed in neurophysiological studies. Human fMRI studies revealed a comparable saccadic suppression effect on luminance and color in the relatively early stages of visual processing, such as the LGN, V1, and V2 (Kleiser et al., 2004; Sylvester et al., 2005); whereas studies on non-human primates showed that saccade suppresses

luminance more strongly than color in early areas such as LGN (Bartlett et al., 1976; Reppas et al., 2002; Royal et al., 2006).

A major limitation of the fMRI approach is its low temporal resolution. Given that saccadic suppression occurs within tens of milliseconds, fMRI is suboptimal for capturing its rapid dynamics. SSVEPs offer a promising alternative, providing high temporal resolution and robust SNR characteristics (for review, see Norcia et al., 2015). SSVEPs are narrowband responses locked to the frequency of periodic stimulation and are relatively immune to eye movement artifacts (e.g., J. Chen et al., 2017a, 2017b; J. Chen, Valsecchi, et al., 2019). A recent study successfully used SSVEPs to track the temporal dynamics of neural responses during saccades (J. Chen, Valsecchi, et al., 2019), opening a path for testing whether early visual cortical areas exhibit pathway-specific suppression, particularly in the parvocellular pathway.

In contrast to saccades, smooth pursuit eye movements involve the continuous tracking of moving objects and have been associated with enhanced visual sensitivity, particularly in the chromatic domain. Behavioral studies have shown that pursuit improves sensitivity to red-green stimuli and to high spatial frequency luminance stimuli, relative to fixation (Schütz et al., 2008, 2009). Additionally, pursuit has been found to enhance temporal resolution for color signals (Terao et al., 2010). Physiological evidence from SSVEP studies further supports this enhancement: responses to chromatic stimuli are significantly amplified during pursuit, while responses to luminance stimuli remain largely unaffected (J. Chen et al., 2017b). Together, these findings suggest that smooth pursuit selectively boosts chromatic processing, likely via modulation of parvocellular activity in early visual cortex.

Finally, fixation refers to periods of relatively stable gaze directed at an object of interest. However, even during these intervals, small involuntary eye movements such as drift, tremor, and microsaccades continue to occur (Ditchburn & Ginsborg, 1952; Ratliff & Riggs, 1950; for recent review, see Klein & Ettinger, 2019). These subtle movements modulate visual input and help prevent the fading of the retinal image (Rucci et al., 2007; Rucci & Poletti, 2015). Among the various processes observable during fixation, chromatic adaptation is a particularly important one, as it supports color constancy by adjusting sensitivity based on the prevailing chromatic environment (for review, see Smithson, 2005). Chromatic adaptation occurs at multiple levels of the visual pathway, from the retina (Yeh et al., 1996) to the LGN (Chang et al., 2016) and visual cortex (Engel, 2005; Engel & Furmanski, 2001; Mullen et al., 2015). Chromatic adaptation also unfolds across different

time scales: a fast component in the range of milliseconds to seconds, and a slower component with time constants from 10 to 30 seconds (Fairchild & Lennie, 1992; Fairchild & Reniff, 1995; Rinner & Gegenfurtner, 2000; Werner et al., 2000). The rapid phase is likely mediated by local retinal mechanisms (Fairchild & Lennie, 1992; Kries, 1905; Rinner & Gegenfurtner, 2000; Werner, 2014), while the slow phase is less well understood but may involve subcortical or early cortical sites (Rinner & Gegenfurtner, 2000). Evidence from dichoptic studies suggests a cortical contribution to the slow phase, as similar adaptation effects were observed whether the same or opposite eye was tested (Werner et al., 2000). Taken together, these findings implicate the early visual cortex is a likely candidate for the neural basis of slow-phase chromatic adaptation.

1.2. Research aims and experimental overview

The overarching aim of this thesis is to investigate how natural eye movement behaviors modulate early visual processing of chromatic and luminance signals in the human brain. To achieve this, we employed SSVEPs to measure neural responses in V1. Specifically, we examined two kinds of eye movements: fixation and saccade. Study 1 examined the temporal dynamics of chromatic adaptation during prolonged fixation. Study 2 investigated the effect of saccadic suppression on neural responses to chromatic and luminance stimuli. Finally, Study 3 introduced and evaluated methodological improvements for SSVEP analysis, aimed at significantly enhancing signal quality and reliability. Collectively, these studies provide new insights into the distinct temporal dynamics and integration of chromatic (L–M) and luminance signals in the context of natural eye movement behavior.

In Study 1, we re-analyzed publicly available datasets in which participants passively fixated stimuli for 150 seconds. The prolonged SSVEP recordings allowed us to examine the time course of adaptation effect in the human early visual cortex. In Study 2, we used SSVEPs to track neural responses dynamically during saccadic eye movements. We created trials in which flickering stimuli were modulated either in luminance or isoluminant red-green signals, and participants made saccades back and forth between two spots positioned parallel to the flickers. By sliding the time window over EEG epochs that contains saccades, we were able to quantify the dynamic modulation of saccades on the parvocellular and magnocellular pathways in the human early visual cortex.

Study 3 introduced and validated Laplacian reference as an optimized method for analyzing SSVEP signals. We systematically compared Laplacian reference to three other commonly used EEG reference methods (i.e., monopolar reference, common average reference, and averaged-mastoids

reference) using seven publicly available datasets. Our results consistently demonstrated that Laplacian referencing significantly improves SSVEP data quality, as measured by enhanced SNRs and reliability.

Taken together, these studies deepen our understanding of how natural eye movements temporally modulate the processing of chromatic (L–M) and luminance signals in the human early visual cortex. The following chapters will describe the designs and results of each study in more detail.

2. Study 1: The time course of chromatic adaptation in human early visual cortex revealed by SSVEPs

(Zhang, Valsecchi, Gegenfurtner & Chen, 2023, Journal of Vision)

Study 1 investigated the red-green chromatic adaptation effect during fixation using SSVEPs. The time course of cortical responses to chromatic stimuli followed a clear exponential decay function, with a half-life of approximately 20 seconds, whereas the responses from luminance stimuli do not show any systematic adaptation.

We re-analyzed data from two publicly available datasets, comprising a total of 49 participants who passively viewed flickering stimuli modulated either in red-green chromaticity or luminance. Each trial lasted 150 seconds, with two repetitions per condition. Dataset #1 employed full-screen horizontal gratings (spatial frequency = 0.34 cycles/°) undergoing pattern-reversal flickering at 7.5 Hz, modulated either in isoluminant red-green chromaticity or luminance. Both stimulus types were tested at low and high contrast levels. Dataset #2 used black-and-white checkerboard patterns extended 8.15° horizontally and 8.15° vertically. The checkboards were presented at various pattern-reversal flicker frequencies: 5.2 Hz, 6.3 Hz, 7.5 Hz, 8.6 Hz, 10 Hz, 10.9 Hz, 12 Hz, and 13.3 Hz. SSVEP analyses focused on channels O1, Oz, and O2, which typically show maximal responses (e.g., J. Chen et al., 2017a, 2017b; J. Chen, McManus, et al., 2019; J. Chen & Gegenfurtner, 2021; Martinovic et al., 2018; Nunez et al., 2017). For each trial, the first second of data was excluded to remove onset transients (e.g., Liu-Shuang et al., 2016). Then the remaining signals were decomposed into thirty-seven successive 4-second epochs. The amplitude spectrum of the epoch was obtained by fast-Fourier transformation (*fft*.m in Matlab), and the response amplitude at a certain frequency was calculated by subtracting the average amplitude of adjacent frequency bins from the peak amplitude at the target frequency.

Figure 1A shows the time course of SSVEP amplitudes throughout the whole 150s duration for both chromatic and luminance stimuli in Dataset #1. For chromatic stimuli (*left* panel), the SSVEP amplitudes exhibited an exponential decay, with half-lives of 17.1 seconds (low contrast) and 21.5 seconds (high contrast), closely matching prior behavioral results (Rinner & Gegenfurtner's, 2000, 18.2s for color discrimination, and 19.6s for color appearance). In contrast, luminance-elicited responses showed no systematic adaptation at either contrast level (*right* panel). This lack of adaptation was further confirmed by the broader range of frequencies tested in Dataset #2 (Figure 1B).

These results suggest that slow-phase chromatic adaptation occurs already in the early visual cortex, which confirms previous speculations (Rinner & Gegenfurtner, 2000; Werner et al., 2000). The estimated ~20-second half-life of chromatic adaptation provides important temporal constraints for future SSVEP research in color vision. The absence of measurable adaptation in luminance responses, however, remains an open question.

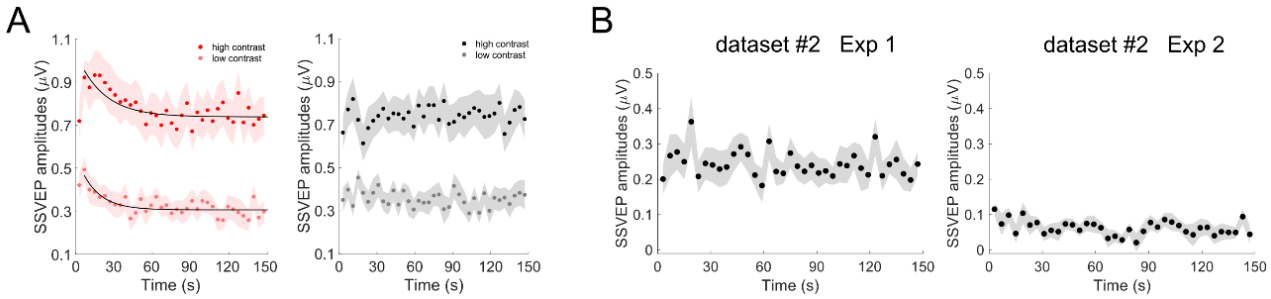

Figure 1. The time courses of the mean SSVEP amplitudes. (**A**) SSVEP amplitudes elicited by color (*left*) and luminance (*right*) stimuli at low and high contrast in Dataset #1. The black lines in the *left* penal are the fits by exponential decay functions to the data. (**B**) SSVEPs responses elicited by luminance-defined checkerboard patterns in experiments from Dataset #2. No clear sign of adaptation effect.

3. Study 2: The execution of saccadic eye movements suppresses visual processing of both color and luminance in the early visual cortex of humans

(Zhang, Valsecchi, Gegenfurtner & Chen, 2024, Journal of Neurophysiology)

The goal of Study 2 was to investigate whether saccadic suppression occurs exclusively in the magnocellular visual pathway or extends to the parvocellular pathway as well in the human early visual cortex. Additionally, we measured the suppression effect across various contrast levels, which enabled us to model SSVEP responses with contrast response functions.

We adopted the experimental design from Chen et al., (2019) (J. Chen, Valsecchi, et al., 2019). Two types of stimuli were used: isoluminant red-green and luminance-defined gratings, both with a spatial frequency of 1.03 cycles/°. Each stimulus was presented full-screen and flickered in a pattern-reversal mode at 7.5 Hz to elicit SSVEPs. Each trial lasted for 90 seconds. Participants were required to make horizontal saccades back and forth between two spots, at a rate of once every 1 to 2 seconds. They made saccades voluntarily without any instruction during the experiment. In Experiment 1, we tested two contrast levels for each stimulus type. In Experiment 2, each stimulus type was presented across ten contrast levels.

To improve signal quality and accurately characterize saccade-related modulations in SSVEPs, we developed a novel analysis pipeline termed *Eye movement-associated phase-aligned analysis*. A brief demonstration is shown in Figure 2A. This approach reduces non-phase-locked EEG activities by coherently averaging EEG segments aligned to saccade onset, separately for each observer and condition. Following phase alignment, the EEG signals were segmented using a 400 ms moving window advanced in 1 ms steps. A short-term FFT was then applied to each segment to extract the time course of saccade-related SSVEP responses. Compared to the traditional method used in previous study (J. Chen, Valsecchi, et al., 2019), this pipeline yielded significantly higher SNRs in the SSVEP responses.

Surprisingly, we found that saccades suppressed SSVEP responses to both chromatic and luminance stimuli. Figure 2B displays the time course of SSVEP responses from Experiment 1, collapsed across contrast levels. The suppression index reveals comparable transient suppression in both stimulus types (Figure 2C). This result suggests that saccadic suppression affects not only the magnocellular pathway but also the parvocellular pathway, indicating a more generalized mechanism of visual attenuation during saccades.

We then modeled the contrast response functions of SSVEP amplitudes under saccadic suppression for both chromatic and luminance stimuli. A Bayesian approach was employed for parameter estimation, with uniform priors assigned to all model parameters. Figure 2D illustrates the normalized SSVEP amplitudes and corresponding model fits across all conditions. By computing the differences of parameters' posterior distributions, we found that saccades primarily reduce the response gain without altering the contrast gain. Notably, this suppressive effect on response gain was comparable for both chromatic and luminance stimuli.

These findings provide new insight into the long-debated question of whether saccades selectively suppress the magnocellular pathway. Our results suggest that such disparity might arise in higher visual areas, as early visual cortex responses show similar suppression across both pathways. This pathway-general modulation at early cortical stages may contribute to the mechanisms that ultimately support stable and adaptive visual perception.

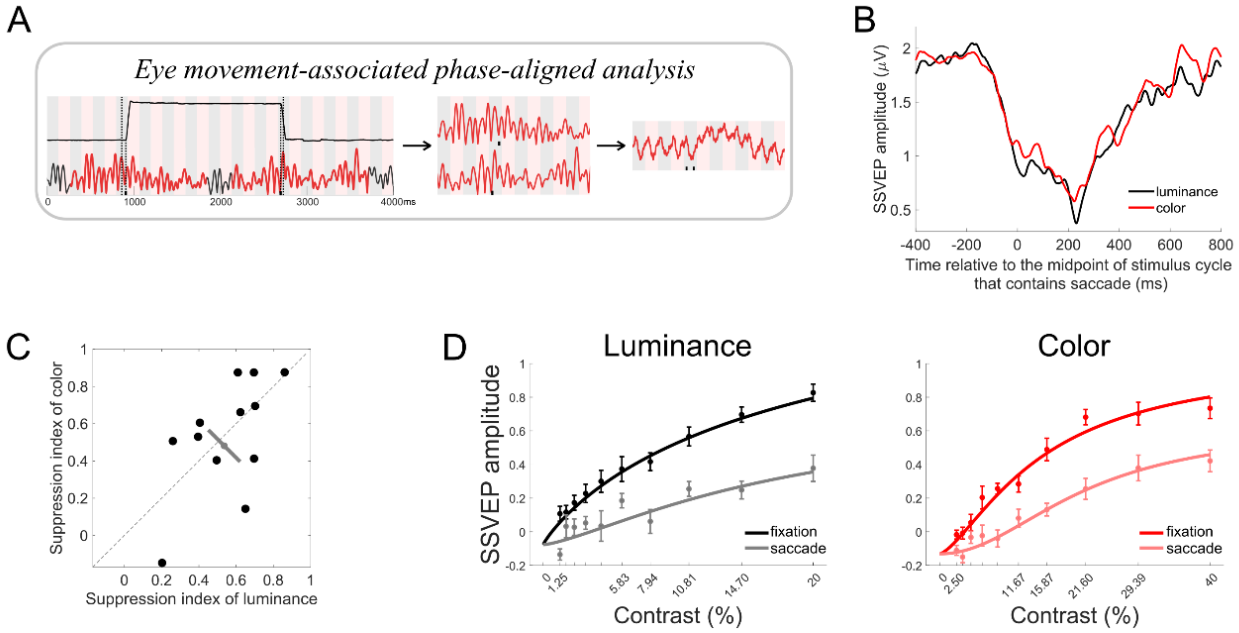

Figure 2. Comparable saccadic suppression on both color and luminance stimuli. (**A**) The demonstration of coherently average the EEG epochs in *Eye movement-associated phase-aligned analysis*. **(B)** Average SSVEP amplitude elicited by chromatic and luminance stimuli at different time points relative to the midpoint of the stimulus cycle that contains saccade among all observers. (**C**) Comparable saccadic suppression effect for chromatic and luminance stimuli. (**D**) Contrast response function of normalized SSVEP amplitudes at the time of fixation and saccade. Saccades reduced response gain for both types of stimuli.

4. Study 3: Laplacian reference is optimal for steady-state visual-evoked potentials

(Zhang, Valsecchi, Gegenfurtner & Chen, 2023, Journal of Neurophysiology)

The goal of Study 3 was to systematically evaluate different EEG referencing methods for SSVEP analysis and to introduce Laplacian reference, which subtracts the average of neighboring electrodes from the maximally responsive electrode, as an optimal approach for reducing common noise and enhancing SSVEP signal quality.

We re-analyzed SSVEP data from seven publicly available datasets, each recorded with either 32 or 64 EEG channels covering the whole scalp. As SSVEP responses in all datasets were activated most of the electrode Oz, our analyses focus on Oz only. We evaluated four (re-)reference methods: monopolar reference, common average reference, averaged-mastoids reference, and Laplacian reference. For the monopolar reference, signals at Oz were re-referenced to a single electrode (Fz or Cz). For the common average reference, the signals at Oz were re-referenced to the average of all channels, excluding EOG electrodes. For averaged-mastoids reference, we re-referenced the signals at Oz to the average of two electrodes near the mastoids (i.e., TP9/TP10 or M1/M2). For the Laplacian reference, signals from the central electrode were re-referenced to the average of 5–9 nearest neighboring electrodes. After preprocessing, EEG data for each condition were segmented into 5-second epochs and analyzed using the Fast Fourier Transform (FFT). We primarily assessed data quality using two metrics: SNR and reliability. SNRs were computed as the amplitude at the target frequency divided by the average amplitude of ten adjacent frequency bins. The reliability was computed as the average *Pearson* correlation coefficient between SSVEP responses derived from two separate halves of the data, split by either epochs or trials within the same condition.

Our results showed that the Laplacian reference consistently outperformed the other three referencing methods in both SNR and reliability. Notably, it produced the highest SNRs not only at the fundamental stimulation frequency but also at its harmonics (Figure 3A). Furthermore, contrast response functions of the SNRs demonstrated that the enhancement provided by Laplacian reference was robust across a wide range of stimulus contrasts (Figure 3B). Given the substantial improvement in data quality, we hypothesized that the Laplacian reference would also reduce the required stimulation duration to achieve reliable SSVEP signals. This was confirmed by our analysis: to achieve a certain level of SNR (e.g., 5), Laplacian reference requires an epoch length of 18 seconds, whereas other reference methods need 1.5 to 3 times longer.

Taken together, these findings suggest that Laplacian reference is a highly effective and practical method for SSVEP analysis. It significantly enhances data quality in terms of both SNRs and reliability. Moreover, it is easy to implement in experimental settings and facilitates for more time-efficient data acquisition when a given SNR threshold is desired.

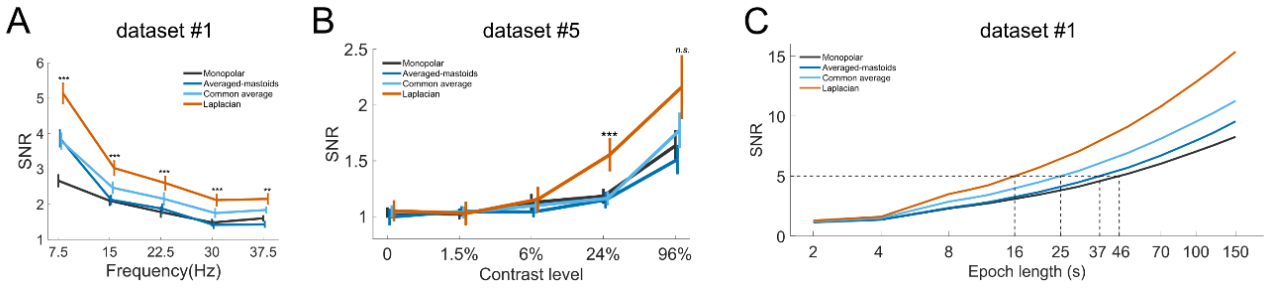

Figure 3. Laplacian reference outperforms the other three reference methods. (**A**) SNRs at stimulation frequency and harmonics below 45 Hz. (**B**) SNRs as a function of contrast. Laplacian reference can provide advantages in terms of SNRs across a wide range of contrast levels. (**C**). SNRs as a function of epoch lengths. To achieve a certain SNR (e.g., 5), Laplacian reference requires the shortest epoch.

5. Discussion

This thesis set out to investigate how eye movements modulate the early cortical processing of chromatic and luminance signals in the human visual system. The findings emphasize that visual perception is not a passive decoding of sensory input but a dynamic process shaped by continuous oculomotor behavior. In the following sections, we discuss two central themes: (1) how eye movements influence luminance and chromatic signal processing within the early visual cortex, and (2) how SSVEP analysis methods can be further optimized to more effectively capture these neural dynamics in vision research.

5.1. Modulation of chromatic and luminance processing across eye movements

Luminance and chromatic (L–M) signals originate at the photoreceptor level and are subsequently transmitted via the magnocellular and parvocellular pathways. With respect to adaptation and saccadic suppression, two long-standing assumptions have dominated the field: first, that chromatic and luminance signals are equally subject to adaptation, and second, that saccadic suppression selectively affects luminance processing. In Studies 1 and 2, we tested these assumptions using SSVEPs to measure visual responses during prolonged fixation and saccadic eye movements. Contrary to expectations, we observed a double dissociation: chromatic (L–M) responses showed robust adaptation during fixation, whereas luminance responses did not; meanwhile, saccades suppressed both chromatic and luminance signals to a comparable extent.

First, our findings challenge the view that adaptation affects chromatic and luminance signals similarly. Study 1 showed that pattern-reversal SSVEPs elicited by chromatic stimuli exhibited a

clear, time-dependent decay with a half-life of approximately 20 seconds. In contrast, luminance-driven SSVEPs showed no systematic adaptation across the same time course. To our knowledge, few studies have examined slow adaptation effects in SSVEPs elicited by grating stimuli similar to those tested in Study 1. One early study reported some preliminary observations (Blakemore & Campbell, 1969). They showed that after viewing a high contrast grating for 30s or 60s, the VEPs to a low contrast grating were reduced. This result, however, was based on a single observer. Also, they used high spatial frequency stimuli (12 c/deg), whereas the stimuli in Study 1 have low spatial frequency (0.34 c/deg). It will therefore be interesting to test whether spatial frequency is a determining factor for the presence of an adaptation effect in SSVEPs to luminance gratings. A later study found that neural responses to achromatic gratings are attenuated after adapting to a mask at certain contrast (Robson & Kulikowski, 2012). However, they did not examine the slow adaptation effect and the time course.

In motion SSVEP studies using luminance-based stimuli, adaptation effects appear to depend on stimulus direction. Heinrich & Bach (2003) found an absence of adaptation after exposure to motion reversals (flickering between motion expansion and contraction). When the adaptation stimuli were moving only in a single direction, instead of moving back and forth, adaptation did occur (Ales & Norcia, 2009; Heinrich & Bach, 2003). For example, Ales & Norcia (2009) presented an adaptor moving in a single direction for 25 seconds, and then tested SSVEPs to moving stimuli oscillating left and right. They found that responses in the adapted direction were reduced but not in the un-adapted direction, and this induced an asymmetry in the population responses. Therefore, in the domain of motion SSVEPs, direction-specific motion adaptation has been observed, whereas non-direction-specific adaptation may not occur in the early visual cortex as indicated by SSVEPs. At this stage, we don't know exactly why luminance-gratings did not induce an adaptation effect in the current result. Based on findings from motion SSVEP studies, we speculate that adaptation might be revealed using "unidirectional" stimulation, i.e., adapting to either a black or white field alone.

The chromatic adaptation effect observed in Study 1 aligns with prior psychophysical findings (Gupta et al., 2020; Rinner & Gegenfurtner, 2000; Werner et al., 2000) and provides clear electrophysiological evidence of slow-phase color adaptation in human early visual cortex. A few previous studies recorded single-neuron activity in response to prolonged stimulation in animals and reported slow-phase adaptation effects. The time constant of adaptation to luminance gratings in the visual cortex of cat is around 6 seconds (Albrecht et al., 1984; Ohzawa et al., 1985; Vautin & Berkley,

1977). Sclar et al. (1989) also reported that activities of simple cells in monkey visual cortex declined for the initial 10-20 seconds during adaptation. Although these studies did not use color stimuli, their reported time courses align with our findings from Study 1. A few previous studies investigated the effect of chromatic adaptation in SSVEPs (D. Regan, 1968) and VEPs (Duncan et al., 2012; Rabin et al., 1994). Regan (1968a) and Rabin et al. (1994) found that there is an instant adaptation effect of a color field on cortical responses to another color. The instant adaptation effect also varied with flickering frequency (D. Regan, 1968) and color similarity between the adapting and testing color (Rabin et al., 1994). They, however, did not test the slow phase of adaptation. Duncan et al. (2012) examined the effect of adapting one color for 2 minutes on the VEP responses to other colors, however, they did not investigate the time course of adaptation (Duncan et al., 2012).

Second, our results from Study 2 also contradict the widespread assumption that saccadic suppression selectively targets the magnocellular (luminance) pathway. Whereas previous psychophysical studies have suggested that saccadic suppression is either absent or significantly weaker for color stimuli (Anand & Bridgeman, 2002; Braun et al., 2017, 2021; Bridgeman & Macknik, 1995; Bruno et al., 2006; Burr et al., 1994; Diamond et al., 2000; Hass & Horwitz, 2011; Knöll et al., 2011; Ross et al., 2001; Uchikawa & Sato, 1995), our findings reveal that chromatic and luminance SSVEPs are equally suppressed in early visual cortex.

This observation contributes to the broader debate regarding the origin of saccadic suppression. The prominent theory attributes suppression to motor-related signals, specifically, corollary discharge from pre-motor areas such as the superior colliculus or frontal eye fields (Binda & Morrone, 2018). An alternative view attributes suppression to purely visual masking effects (Castet et al., 2001). Although Study 2 was not designed to resolve this debate, but it is interesting to point out the findings in a recent study by Idrees et al. (Idrees et al., 2020). They showed that selective suppression of low spatial frequency luminance stimuli can be observed even when no saccade was required and only the visual flow was presented to the observer. Furthermore, the selective suppression effect can be easily violated by using a fine texture background. Their result indicates that the selective suppression of low spatial frequency information reported in the literature (Burr et al., 1994; Volkmann et al., 1978) is probably a visual phenomenon and does not provide enough evidence for the magnocellular suppression hypothesis. This is consistent with our main message in Study 2 that, at least in the early visual cortex, there is no evidence for selective suppression of the magnocellular pathway.

If both our results and prior fMRI findings (Kleiser et al., 2004; Sylvester et al., 2005) suggest that suppression effects are comparable for both color and luminance stimuli in early visual cortex, an important question arises: where do perceptual difference originate? Notably, previous fMRI studies have examined neural activities in higher visual areas such as V5 and MT, revealing a stronger saccadic suppression effect for luminance-defined stimuli compared to color-defined stimuli (Kleiser et al., 2004; Sylvester et al., 2005). This observation may indicate that saccades exert a more pronounced suppression of luminance processing in the higher-level visual cortex beyond V1/V2. However, due to the limited temporal resolution of fMRI, further investigations are warranted to delve deeper into this matter. Alternatively, some studies have shown that visual motor neurons in the superior colliculus exhibit spatial-frequency-specific saccadic suppression effects (C. Y. Chen & Hafed, 2017). A recent study showed selective suppression of low spatial frequencies can also occur in the complete absence of saccades, when rapid image shifts are introduced on the retina (Idrees et al., 2020). Further studies are needed to pinpoint the neural origins of this perceptual discrepancy.

Moreover, our modeling results in Study 2 reveal that saccadic suppression operates via a multiplicative reduction in response gain, rather than a shift in contrast gain. This finding parallels recent psychophysical results (Li et al., 2021), which show that overt pre-saccadic attention modulates response gain, whereas covert attention modulates both response and contrast gain. Our results are also consistent with neurophysiological studies in non-human primates showing that microsaccades reduce firing rates in the superior colliculus through a gain control mechanism (C. Y. Chen et al., 2015). Together, these findings suggest that saccades suppress visual input through a dynamic gating process that is time-locked, gain-selective, and evident across both chromatic and luminance pathways in the early visual cortex.

Above all, the use of SSVEPs enabled us to track cortical responses with high temporal resolution across time. However, a key question remains: why did our measurements reveal no adaptation for luminance signals and comparable saccadic suppression across both pathways—contrary to what might be expected from previous findings?

Regarding the absence of luminance adaptation, one possibility relates to the transient and sustained response in visual processing. It is well known that neural processing of luminance is relatively transient, whereas the processing of color tends to be sustained (Kulikowski & Walsh, 1993; A. G. Robson & Kulikowski, 2012; Schiller & Malpeli, 1978; Schwartz & Loop, 1982; Shapley et al., 1981; Valberg & Lee, 1991). The lack of slow adaptation for luminance response might be a characteristic

for transient response. In addition, SSVEPs in the current study were produced by pattern-reversal stimuli, which have been shown to elicit transient responses more than on-off stimuli (Strasburger et al., 1993). It is thus possible that luminance SSVEPs with on-off stimulation may show a slow adaptation effect.

With regard to saccadic suppression, our results showed robust modulation in both chromatic and luminance SSVEPs. Given that SSVEPs primarily originate from V1, the first cortical site to receive chromatic and luminance input, this finding suggests that saccadic suppression at this level operates through a non-selective, shared gating mechanism. Saccadic eye movements are controlled by a distributed network involving both subcortical structures (e.g., superior colliculus) and cortical areas such as V1, the lateral intraparietal area (LIP), inferotemporal cortex (IT), frontal eye fields (FEF), and the basal ganglia (Krauzlis, 2005). Given this hierarchical architecture, it is plausible that selective suppression effects reported in previous psychophysical studies may emerge at later stages of cortical processing. At the level of V1, however, where chromatic and luminance signals begin to converge for subsequent processing, our findings indicate that saccadic modulation operates in a pathway-general manner.

5.2. Optimizing SSVEPs analysis for vision research

Due to their high SNR and robustness to artifacts, SSVEPs have been widely employed in human sensory and cognitive neuroscience, clinical applications, and brain-computer interface (BCI) designs (Norcia et al., 2015; Vialatte et al., 2010). In Study 3, we found that the Laplacian reference enhances SSVEP signal quality compared to other referencing methods such as monopolar, averaged-mastoid, and common average reference. Moreover, in Study 2, we proposed an innovative method termed *Eye movement-associated phase-aligned analysis* to reduce non-phase-locked noise when applying SSVEPs in conjunction with eye movements.

One major advantage of SSVEPs is their ability to generate neural responses with high signal-to-noise ratio (SNR) at predefined narrowband frequencies, typically originating from localized visual areas near occipital electrodes (e.g., Oz). However, this spatial specificity makes them less compatible with conventional referencing methods (e.g., monopolar, common average, or averaged mastoids), while favoring Laplacian referencing, which is more sensitive to shallow, local sources (Yao, 2002; Zhai & Yao, 2004). Results from Study 3 indicated that the Laplacian reference yields high-quality SSVEP data while requiring only a few recording electrodes. It can also be applied to

any electrode across the scalp. Furthermore, with prior knowledge of the maximally activated electrode, the Laplacian reference requires only a cluster of nearby electrodes, offering a practical solution in certain experimental contexts.

Other more sophisticated SSVEP analysis methods have been used in specific contexts, for example the Reliable Components Analysis (Dmochowski et al., 2015) and the rhythmic entrainment source separation method (Cohen & Gulbinaite, 2017). These methods require data from all EEG electrodes over the head, and have also other requirements or assumptions. For example, the rhythmic entrainment source separation was developed based on the assumption that steady-state activity is spectrally and spatially stationary over time, and also requires high-quality data with many time points. The Reliable Components Analysis decomposes all-channel EEG data into a small number of reliable components by maximizing trial-to-trial consistency, which requires dozens of homogeneous and phase-locked trials. If these requirements are satisfied, Reliable Components Analysis may outperform the Laplacian reference when these conditions are met.

As SSVEPs are widely used for BCI designs, many studies have sought to optimize reference method to improve signal recognition accuracy. A large number of optimization methods that combines data from multiple EEG channels with various algorithms have been proposed (Sözer & Fidan, 2018; Wu & Su, 2014). For detecting SSVEP signals at specific frequencies in BCI applications, these methods would in principle result in higher detecting accuracy compared to a reference method as simple as the Laplacian. For example, the Generated Reference Filter method has been shown to provide higher accuracy than Laplacian and common average reference (Sözer & Fidan, 2018). For the spatial filter like common average reference and Laplacian reference methods, the classification results from Laplacian reference outperforms common average reference (Syam et al., 2017). However, stimuli used in neuroscience research are very different from BCI research. Future studies are needed to examine whether these algorithms developed in the BCI field also benefit SSVEP studies in neuroscience research.

Another advantage of SSVEPs is it relatively immune to eye movement artifacts, allowing studies for employing SSVEPs along with eye movements (e.g., J. Chen et al., 2017a, 2017b; J. Chen, Valsecchi, et al., 2019). Our novel pipeline from Study 2, *Eye movement-associated phase-aligned analysis*, significantly improvs data quality in SSVEP analysis. This method is based on the concept of coherently averaging SSVEP signals to minimize noise (Ales & Norcia, 2009; Candy et al., 2001; Gilmore et al., 2007; Hale et al., 2005; Liu-Shuang et al., 2016; Lygo et al., 2021). We used saccade

onset timing to identify the midpoint of the stimulus cycle for extracting phase-aligned EEG epochs. This alignment ensured that saccade onsets were evenly distributed within a single cycle, allowing coherent averaging to reduce non-phase-locked noise and enhance the SSVEP signal. However, this approach effectively treats each cycle as a single unit, which may limit the ability to resolve finer neural dynamics within that cycle. Future studies could address this limitation by increasing the stimulus temporal frequency to shorten the cycle duration if needed.

6. Conclusions and future work

This thesis investigated how eye movements modulate the processing of chromatic and luminance signals in the human early visual cortex using SSVEPs. We found that: (1) slow-phase chromatic adaptation occurs at early cortical stages, providing direct evidence that supports previous psychophysical speculations; and (2) saccades suppress both parvocellular and magnocellular pathways to a comparable extent, operating through a multiplicative modulation mechanism. Additionally, this thesis contributes methodologically by (1) introducing Laplacian reference as an optimized method for SSVEPs analysis, and (2) developing a novel analysis pipeline — *Eye movement-associated phase-aligned analysis* — that effectively integrates eye movement and SSVEPs data. Both methodological advances significantly improve the signal quality and reliability of SSVEP measurements across experiments. Collectively, these findings demonstrate that visual processing is dynamically shaped by the interplay between sensory inputs and eye movement behaviors across time and context.

Several promising directions remain open for future research. First, the absence of luminance adaptation in early visual cortex warrants further investigation, particularly regarding its potential dependence on stimulus properties such as spatial frequency or temporal structure. Second, future studies could complement the current EEG-based findings with methods offering higher spatial resolution, such as MEG or high-field fMRI, to better localize the neural substrates of chromatic and luminance processing. Third, the newly developed *Eye movement-associated phase-aligned analysis* pipeline could be extended to more naturalistic paradigms, including dynamic scenes or active viewing conditions where eye movements and attention freely interact. Finally, bridging methodological advances from brain–computer interface research to cognitive neuroscience remains a promising avenue for improving SSVEP signal decoding and interpretation.

7. References

Adrian, E. D., & Matthews, B. H. C. (1934). THE BERGER RHYTHM: POTENTIAL CHANGES FROM THE OCCIPITAL LOBES IN MAN. *Brain*, *57*(4), 355–385.

Albrecht, D. G., Farrar, S. B., & Hamilton, D. B. (1984). Spatial contrast adaptation characteristics of neurones recorded in the cat's visual cortex. *The Journal of Physiology*, *347*(1), 713–739.

Ales, J. M., & Norcia, A. M. (2009). Assessing direction-specific adaptation using the steady-state visual evoked potential: Results from EEG source imaging. *Journal of Vision*, *9*(7), 8–8.

Anand, S., & Bridgeman, B. (2002). An unbiased measure of the contributions of chroma and luminance to saccadic suppression of displacement. *Experimental Brain Research*, *142*(3), 335–341.

Anstis, S. M. (1974). A chart demonstrating variations in acuity with retinal position. *Vision Research*, *14*(7), 589–592.

Aubert & Foerster. (1857). Untersuchungen über den Raumsinn der Retina. *Archiv Für Ophthalmologie*, *3*(2), 1–37.

Bartlett, J. R., Doty, R. W., Lee, B. B., & Sakakura, H. (1976). Influence of saccadic eye movements on geniculostriate excitability in normal monkeys. *Experimental Brain Research*, *25*(5).

Baylor, D. A., Nunn, B. J., & Schnapf, J. L. (1987). Spectral sensitivity of cones of the monkey Macaca fascicularis. *The Journal of Physiology*, *390*(1), 145–160.

Binda, P., & Morrone, M. C. (2018). Vision During Saccadic Eye Movements. *Annual Review of Vision Science*, *4*(1), 193–213.

Blakemore, C., & Campbell, F. W. (1969). On the existence of neurones in the human visual system selectively sensitive to the orientation and size of retinal images. *The Journal of Physiology*, *203*(1), 237–260.

Braun, D. I., Schütz, A. C., & Gegenfurtner, K. R. (2017). Visual sensitivity for luminance and chromatic stimuli during the execution of smooth pursuit and saccadic eye movements. *Vision Research*, *136*, 57–69.

Braun, D. I., Schütz, A. C., & Gegenfurtner, K. R. (2021). Age effects on saccadic suppression of luminance and color. *Journal of Vision*, *21*(6), 11.

Bridgeman, B., & Macknik, S. L. (1995). Saccadic suppression relies on luminance information. *Psychological Research*, *58*(3), 163–168.

Bruno, A., Brambati, S. M., Perani, D., & Morrone, M. C. (2006). Development of Saccadic Suppression in Children. *Journal of Neurophysiology*, *96*(3), 1011–1017.

Burr, D. C., Morrone, M. C., & Ross, J. (1994). Selective suppression of the magnocellular visual pathway during saccadic eye movements. *Nature*, *371*(6497), 511–513.

Campbell, F. W., & Maffei, L. (1970). Electrophysiological evidence for the existence of orientation and size detectors in the human visual system. *The Journal of Physiology*, *207*(3), 635–652.

Candy, T. R., Skoczenski, A. M., & Norcia, A. M. (2001). Normalization Models Applied to Orientation Masking in the Human Infant. *The Journal of Neuroscience*, *21*(12), 4530–4541.

Castet, E., Jeanjean, S., & Masson, G. S. (2001). 'Saccadic suppression'- no need for an active extra-retinal mechanism. *Trends in Neurosciences*, *24*(6), 316–318.

Chang, D. H. F., Hess, R. F., & Mullen, K. T. (2016). Color responses and their adaptation in human superior colliculus and lateral geniculate nucleus. *NeuroImage*, *138*, 211–220.

Chen, C. Y., & Hafed, Z. M. (2017). A neural locus for spatial-frequency specific saccadic suppression in visual-motor neurons of the primate superior colliculus. *Journal of Neurophysiology*, *117*(4), 1657–1673.

Chen, C. Y., Ignashchenkova, A., Thier, P., & Hafed, Z. M. (2015). Neuronal Response Gain Enhancement prior to Microsaccades. *Current Biology*, *25*(16), 2065–2074.

Chen, J., & Gegenfurtner, K. R. (2021). Electrophysiological evidence for higher-level chromatic mechanisms in humans. *Journal of Vision*, *21*(8), 12.

Chen, J., McManus, M., Valsecchi, M., Harris, L. R., & Gegenfurtner, K. R. (2019). Steady-state visually evoked potentials reveal partial size constancy in early visual cortex. *Journal of Vision*, *19*(6), 8.

Chen, J., Valsecchi, M., & Gegenfurtner, K. R. (2017a). Attention is allocated closely ahead of the target during smooth pursuit eye movements: Evidence from EEG frequency tagging. *Neuropsychologia*, *102*, 206–216.

Chen, J., Valsecchi, M., & Gegenfurtner, K. R. (2017b). Enhanced brain responses to color during smooth-pursuit eye movements. *Journal of Neurophysiology*, *118*(2), 749–754.

Chen, J., Valsecchi, M., & Gegenfurtner, K. R. (2019). Saccadic suppression measured by steady-state visual evoked potentials. *Journal of Neurophysiology*, *122*(1), 251–258.

Cohen, M. X., & Gulbinaite, R. (2017). Rhythmic entrainment source separation: Optimizing analyses of neural responses to rhythmic sensory stimulation. *NeuroImage*, *147*, 43–56.

Curcio, C. A., & Allen, K. A. (1990). Topography of ganglion cells in human retina. *Journal of Comparative Neurology*, *300*(1), 5–25.

Derrington, A. M., Krauskopf, J., & Lennie, P. (1984). Chromatic mechanisms in lateral geniculate nucleus of macaque. *The Journal of Physiology*, *357*(1), 241–265.

Derrington, A. M., & Lennie, P. (1984). Spatial and temporal contrast sensitivities of neurones in lateral geniculate nucleus of macaque. *The Journal of Physiology*, *357*(1), 219–240.

Di Russo, F., Pitzalis, S., Aprile, T., Spitoni, G., Patria, F., Stella, A., Spinelli, D., & Hillyard, S. A. (2007). Spatiotemporal analysis of the cortical sources of the steady-state visual evoked potential. *Human Brain Mapping*, *28*(4), 323–334.

Diamond, M. R., Ross, J., & Morrone, M. C. (2000). Extraretinal Control of Saccadic Suppression. *The Journal of Neuroscience*, *20*(9), 3449–3455.

Ditchburn, R., & Ginsborg, B. (1952). Vision with a stabilized retinal image. *Nature*, *170*(4314), 36–37.

Dmochowski, J. P., Greaves, A. S., & Norcia, A. M. (2015). Maximally reliable spatial filtering of steady state visual evoked potentials. *NeuroImage*, *109*, 63–72.

Dominy, N. J., & Lucas, P. W. (2001). Ecological importance of trichromatic vision to primates. *Nature*, *410*(6826), 363–366.

Duncan, C. S., Roth, E. J., Mizokami, Y., McDermott, K. C., & Crognale, M. A. (2012). Contrast adaptation reveals increased organizational complexity of chromatic processing in the visual evoked potential. *Journal of the Optical Society of America A*, *29*(2), A152.

Engel, S. A. (2005). Adaptation of Oriented and Unoriented Color-Selective Neurons in Human Visual Areas. *Neuron*, *45*(4), 613–623.

Engel, S. A., & Furmanski, C. S. (2001). Selective Adaptation to Color Contrast in Human Primary Visual Cortex. *The Journal of Neuroscience*, *21*(11), 3949–3954.

Fairchild, M. D., & Lennie, P. (1992). Chromatic adaptation to natural and incandescent illuminants. *Vision Research*, *32*(11), 2077–2085.

Fairchild, M. D., & Reniff, L. (1995). Time course of chromatic adaptation for color-appearance judgments. *Journal of the Optical Society of America A*, *12*(5), 824.

Gegenfurtner, K. R. (2003). Cortical mechanisms of colour vision. *Nature Reviews Neuroscience*, *4*(7), 563–572.

Gegenfurtner, K. R. (2016). The interaction between vision and eye movements. *Perception*, *45*(12), 1333–1357.

Gegenfurtner, K. R., & Hawken, M. J. (1996). Interaction of motion and color in the visual pathways. *Trends in Neurosciences*, *19*(9), 394–401.

Gilmore, R. O., Hou, C., Pettet, M. W., & Norcia, A. M. (2007). Development of cortical responses to optic flow. *Visual Neuroscience*, *24*(6), 845–856.

Gupta, G., Gross, N., Pastilha, R., & Hurlbert, A. (2020). *The time course of chromatic adaptation under immersive illumination* [Preprint]. Neuroscience.

Hale, J., Harrad, R. A., McKee, S. P., Pettet, M. W., & Norcia, A. M. (2005). A VEP Measure of the Binocular Fusion of Horizontal and Vertical Disparities. *Investigative Opthalmology & Visual Science*, *46*(5), 1786.

Harvey, B. M., & Dumoulin, S. O. (2011). The Relationship between Cortical Magnification Factor and Population Receptive Field Size in Human Visual Cortex: Constancies in Cortical Architecture. *The Journal of Neuroscience*, *31*(38), 13604–13612.

Hass, C. A., & Horwitz, G. D. (2011). Effects of microsaccades on contrast detection and V1 responses in macaques. *Journal of Vision*, *11*(3), 3–3.

Heinrich, S. P., & Bach, M. (2003). Adaptation characteristics of steady-state motion visual evoked potentials. *Clinical Neurophysiology*, *114*(7), 1359–1366.

Hendry, S. H. C., & Reid, R. C. (2000). The Koniocellular Pathway in Primate Vision. *Annual Review of Neuroscience*, *23*(1), 127–153.

Hendry, S. H., & Yoshioka, T. (1994). A neurochemically distinct third channel in the macaque dorsal lateral geniculate nucleus. *Science (New York, N.Y.)*, *264*(5158), 575–577.

Hunt, D. M., & Peichl, L. (2014). S cones: Evolution, retinal distribution, development, and spectral sensitivity. *Visual Neuroscience*, *31*(2), 115–138.

Ibbotson, M., & Krekelberg, B. (2011). Visual perception and saccadic eye movements. *Current Opinion in Neurobiology*, *21*(4), 553–558.

Idrees, S., Baumann, M. P., Franke, F., Münch, T. A., & Hafed, Z. M. (2020). Perceptual saccadic suppression starts in the retina. *Nature Communications*, *11*(1), 1977.

Jacobs, G. H., Deegan II, J. F., Crognale, M. A., & Fenwick, J. A. (1993). Photopigments of dogs and foxes and their implications for canid vision. *Visual Neuroscience*, *10*(1), 173–180.

Klein, C., & Ettinger, U. (Eds.). (2019). *Eye Movement Research: An Introduction to its Scientific Foundations and Applications*. Springer International Publishing.

Kleiser, R., Seitz, R. J., & Krekelberg, B. (2004). Neural Correlates of Saccadic Suppression in Humans. *Current Biology*, *14*(5), 386–390.

Knöll, J., Binda, P., Morrone, M. C., & Bremmer, F. (2011). Spatiotemporal profile of peri-saccadic contrast sensitivity. *Journal of Vision*, *11*(14), 15–15.

Krauzlis, R. J. (2005). The Control of Voluntary Eye Movements: New Perspectives. *The Neuroscientist*, *11*(2), 124–137.

Kries, J. (1905). Die gesichtsempfindungen. *Nagel's Handbuch Der Physiologie Des Menschen*, *3*, 109–282.

Kulikowski, J. J., & Walsh, V. (1993). Colour vision: isolating mechanisms in overlapping streams. *Progress in Brain Research*, *95*, 417–426.

Latour, P. L. (1962). Visual threshold during eye movements. *Vision Research*, *2*(7–8), 261–262.

Lee, B. B. (2011). Visual pathways and psychophysical channels in the primate. *The Journal of Physiology*, *589*(1), 41–47.

Li, H.-H., Pan, J., & Carrasco, M. (2021). Different computations underlie overt presaccadic and covert spatial attention. *Nature Human Behaviour*, *5*(10), 1418–1431.

Lisberger, S. G. (2015). Visual Guidance of Smooth Pursuit Eye Movements. *Annual Review of Vision Science*, *1*(1), 447–468.

Liu-Shuang, J., Torfs, K., & Rossion, B. (2016). An objective electrophysiological marker of face individualisation impairment in acquired prosopagnosia with fast periodic visual stimulation. *Neuropsychologia*, *83*, 100–113.

Lygo, F. A., Richard, B., Wade, A. R., Morland, A. B., & Baker, D. H. (2021). Neural markers of suppression in impaired binocular vision. *NeuroImage*, *230*, 117780.

Martinovic, J., Wuerger, S. M., Hillyard, S. A., Müller, M. M., & Andersen, S. K. (2018). Neural mechanisms of divided feature-selective attention to colour. *NeuroImage*, *181*, 670–682.

Mollon, J. D. (1989). "Tho' she kneel'd in that place where they grew…" The uses and origins of primate colour vision. *Journal of Experimental Biology*, *146*(1), 21–38.

Mullen, K. T., Chang, D. H. F., & Hess, R. F. (2015). The selectivity of responses to red-green colour and achromatic contrast in the human visual cortex: an fMRI adaptation study. *European Journal of Neuroscience*, *42*(11), 2923–2933.

Müller, M. M., Teder, W., & Hillyard, S. A. (1997). Magnetoencephalographic recording of steadystate visual evoked cortical activity. *Brain Topography*, *9*(3), 163–168.

Nassi, J. J., & Callaway, E. M. (2009). Parallel processing strategies of the primate visual system. *Nature Reviews Neuroscience*, *10*(5), 360–372.

Neitz, J., Geist, T., & Jacobs, G. H. (1989). Color vision in the dog. *Visual Neuroscience*, *3*(2), 119–125.

Norcia, A. M., Appelbaum, L. G., Ales, J. M., Cottereau, B. R., & Rossion, B. (2015). The steady-state visual evoked potential in vision research: A review. *Journal of Vision*, *15*(6), 4.

Nunez, V., Shapley, R. M., & Gordon, J. (2017). Nonlinear dynamics of cortical responses to color in the human cVEP. *Journal of Vision*, *17*(11), 9.

Ohzawa, I., Sclar, G., & Freeman, R. D. (1985). Contrast gain control in the cat's visual system. *Journal of Neurophysiology*, *54*(3), 651–667.

Østerberg, G. (1935). Topography of the Layer of Rods and Cones in the Human Retina. *Acta Ophthalmologica*, *13*, 6–97.

Page, W. K., King, W. M., Merigan, W., & Maunsell, J. (1994). Magnocellular or parvocellular lesions in the lateral geniculate nucleus of monkeys cause minor deficits of smooth pursuit eye movements. *Vision Research*, *34*(2), 223–239.

Pointer, J. S., & Hess, R. F. (1989). The contrast sensitivity gradient across the human visual field: With emphasis on the low spatial frequency range. *Vision Research*, *29*(9), 1133–1151.

Pongrácz, P., Ujvári, V., Faragó, T., Miklósi, Á., & Péter, A. (2017). Do you see what I see? The difference between dog and human visual perception may affect the outcome of experiments. *Behavioural Processes*, *140*, 53–60.

Rabin, J., Switkes, E., Crognale, M., Schneck, M. E., & Adams, A. J. (1994). Visual evoked potentials in three-dimensional color space: Correlates of spatio-chromatic processing. *Vision Research*, *34*(20), 2657–2671.

Ratliff, F., & Riggs, L. A. (1950). Involuntary motions of the eye during monocular fixation. *Journal of Experimental Psychology*, *40*(6), 687.

Regan, B. C., Julliot, C., Simmen, B., Viénot, F., Charles–Dominique, P., & Mollon, J. D. (2001). Fruits, foliage and the evolution of primate colour vision. *Philosophical Transactions of the Royal Society of London. Series B: Biological Sciences*, *356*(1407), 229–283.

Regan, D. (1968). Chromatic adaptation and steady-state evoked potentials. *Vision Research*, *8*(2), 149–158.

Reppas, J. B., Usrey, W. M., & Reid, R. C. (2002). Saccadic Eye Movements Modulate Visual Responses in the Lateral Geniculate Nucleus. *Neuron*, *35*(5), 961–974.

Rinner, O., & Gegenfurtner, K. R. (2000). Time course of chromatic adaptation for color appearance and discrimination. *Vision Research*, *40*(14), 1813–1826.

Robson, A. G., & Kulikowski, J. J. (2012). Objective assessment of chromatic and achromatic pattern adaptation reveals the temporal response properties of different visual pathways. *Visual Neuroscience*, *29*(6), 301–313.

Robson, J. G., & Graham, N. (1981). Probability summation and regional variation in contrast sensitivity across the visual field. *Vision Research*, *21*(3), 409–418.

Ross, J., Morrone, M. C., Goldberg, M. E., & Burr, D. C. (2001). Changes in visual perception at the time of saccades. *Trends in Neurosciences*, *24*(2), 113–121.

Royal, D. W., Sáry, Gy., Schall, J. D., & Casagrande, V. A. (2006). Correlates of motor planning and postsaccadic fixation in the macaque monkey lateral geniculate nucleus. *Experimental Brain Research*, *168*(1–2), 62–75.

Rucci, M., Iovin, R., Poletti, M., & Santini, F. (2007). Miniature eye movements enhance fine spatial detail. *Nature*, *447*(7146), 852–855.

Rucci, M., & Poletti, M. (2015). Control and Functions of Fixational Eye Movements. *Annual Review of Vision Science*, *1*(1), 499–518.

Schiller, P. H., Logothetis, N. K., & Charles, E. R. (1990). Role of the color-opponent and broad-band channels in vision. *Visual Neuroscience*, *5*(04), 321–346.

Schiller, P. H., & Malpeli, J. G. (1978). Functional specificity of lateral geniculate nucleus laminae of the rhesus monkey. *Journal of Neurophysiology*, *41*(3), 788–797.

Schütz, A. C., Braun, D. I., & Gegenfurtner, K. R. (2009). Improved visual sensitivity during smooth pursuit eye movements: Temporal and spatial characteristics. *Visual Neuroscience*, *26*(3), 329–340.

Schutz, A. C., Braun, D. I., & Gegenfurtner, K. R. (2011). Eye movements and perception: A selective review. *Journal of Vision*, *11*(5), 9–9.

Schütz, A. C., Braun, D. I., Kerzel, D., & Gegenfurtner, K. R. (2008). Improved visual sensitivity during smooth pursuit eye movements. *Nature Neuroscience*, *11*(10), Article 10.

Schwartz, S. H., & Loop, M. S. (1982). Evidence for transient luminance and quasi-sustained color mechanisms. *Vision Research*, *22*(4), 445–447.

Sclar, G., Lennie, P., & DePriest, D. D. (1989). Contrast adaptation in striate cortex of macaque. *Vision Research*, *29*(7), 747–755.

Shapley, R., Kaplan, E., & Soodak, R. (1981). Spatial summation and contrast sensitivity of X and Y cells in the lateral geniculate nucleus of the macaque. *Nature*, *292*(5823), 543–545.

Siniscalchi, M., d'Ingeo, S., Fornelli, S., & Quaranta, A. (2017). Are dogs red–green colour blind? *Royal Society Open Science*, *4*(11), 170869.

Smithson, H. E. (2005). Sensory, computational and cognitive components of human colour constancy. *Philosophical Transactions of the Royal Society B: Biological Sciences*, *360*(1458), 1329–1346.

Sommer, M. A., & Wurtz, R. H. (2008). Brain Circuits for the Internal Monitoring of Movements. *Annual Review of Neuroscience*, *31*(1), 317–338.

Sözer, A. T., & Fidan, C. B. (2018). Novel spatial filter for SSVEP-based BCI: A generated reference filter approach. *Computers in Biology and Medicine*, *96*, 98–105.

Spekreijse, H., Van der Tweel, L. H., & Zuidema, Th. (1973). Contrast evoked responses in man. *Vision Research*, *13*(8), 1577–1601.

Stockman, A., & Sharpe, L. T. (2000). The spectral sensitivities of the middle- and long-wavelength-sensitive cones derived from measurements in observers of known genotype. *Vision Research*, *40*(13), 1711–1737.

Strasburger, H., Murray, I., & Remky, A. (1993). Sustained and transient mechanisms in the steady-state visual evoked potential: onset presentation compared to pattern reversal. *Clinical Vision Sciences*, *8*, 211–211.

Sumner, P., & Mollon, J. D. (2000). Catarrhine Photopigments are Optimized for Detecting Targets Against a Foliage Background. *Journal of Experimental Biology*, *203*(13), 1963–1986.

Syam, S. H.-F., Lakany, H., Ahmad, R. B., & Conway, B. A. (2017). Comparing Common Average Referencing to Laplacian Referencing in Detecting Imagination and Intention of Movement for Brain Computer Interface. *MATEC Web of Conferences*, *140*, 01028.

Sylvester, R., Haynes, J.-D., & Rees, G. (2005). Saccades Differentially Modulate Human LGN and V1 Responses in the Presence and Absence of Visual Stimulation. *Current Biology*, *15*(1), 37–41.

Terao, M., Watanabe, J., Yagi, A., & Nishida, S. (2010). Smooth Pursuit Eye Movements Improve Temporal Resolution for Color Perception. *PLoS ONE*, *5*(6), e11214.

Uchikawa, K., & Sato, M. (1995). Saccadic suppression of achromatic and chromatic responses measured by increment-threshold spectral sensitivity. *Journal of the Optical Society of America A*, *12*(4), 661.

Valberg, A., & Lee, B. B. (Eds.). (1991). *From Pigments to Perception: Advances in Understanding Visual Processes*. Springer US.

Vautin, R. G., & Berkley, M. A. (1977). Responses of single cells in cat visual cortex to prolonged stimulus movement: neural correlates of visual aftereffects. *Journal of Neurophysiology*, *40*(5), 1051–1065.

Vialatte, F.-B., Maurice, M., Dauwels, J., & Cichocki, A. (2010). Steady-state visually evoked potentials: Focus on essential paradigms and future perspectives. *Progress in Neurobiology*, *90*(4), 418–438.

Volkmann, F. C., Riggs, L. A., White, K. D., & Moore, R. K. (1978). Contrast sensitivity during saccadic eye movements. *Vision Research*, *18*(9), 1193–1199.

Werner, A. (2014). Spatial and temporal aspects of chromatic adaptation and their functional significance for colour constancy. *Vision Research*, *104*, 80–89.

Werner, A., Sharpe, L. T., & Zrenner, E. (2000). Asymmetries in the time-course of chromatic adaptation and the significance of contrast. *Vision Research*, *40*(9), 1101–1113.

Wu, Z., & Su, S. (2014). A Dynamic Selection Method for Reference Electrode in SSVEP-Based BCI. *PLoS ONE*, *9*(8), e104248.

Yao, D. (2002). The theoretical relation of scalp Laplacian and scalp current density of a spherical shell head model. *Physics in Medicine and Biology*, *47*(12), 2179–2185.

Yeh, T., Lee, B. B., & Kremers, J. (1996). The time course of adaptation in macaque retinal ganglion cells. *Vision Research*, *36*(7), 913–931.

Zhai, Y., & Yao, D. (2004). A Radial-Basis Function Based Surface Laplacian Estimate for a Realistic Head Model. *Brain Topography*, *17*(1), 55–62.

II. Publications

1. The time course of chromatic adaptation in human early visual cortex revealed by SSVEPs

The time course of chromatic adaptation in human early visual cortex revealed by SSVEPs

Yuan Zhang School of Psychology, Shanghai University of Sport, Shanghai, China

Matteo Valsecchi Dipartimento di Psicologia, Universitá di Bologna, Bologna, Italy

Karl R. Gegenfurtner Abteilung Allgemeine Psychologie and Center for Mind, Brain & Behavior, Justus-Liebig-Universität Giessen, Giessen, Germany

Jing Chen School of Psychology, Shanghai University of Sport, Shanghai, China

Previous studies have identified at least two components of chromatic adaptation: a rapid component with a time scale between tens of milliseconds to a few seconds, and a slow component with a half-life of about 10 to 30 seconds. The basis of the rapid adaptation probably lies in receptor adaptation at the retina. The neural substrate for the slow adaptation remains unclear, although previous psychophysical results hint at the early visual cortex. A promising approach to investigate adaptation effects in the visual cortex is to analyze steady-state visual evoked potentials (SSVEPs) elicited by chromatic stimuli, which typically use long durations of stimulation. Here, we re-analyzed the data from two previous pattern-reversal SSVEP studies. In these experiments (N = 49 observers in total), SSVEPs were elicited by counter-phase flickering color- or luminance-defined grating stimuli for 150 seconds in each trial. By analyzing SSVEPs with short time windows, we found that chromatic SSVEP responses decreased with increasing stimulation duration and reached a lower asymptote within a minute of stimulation. The luminance SSVEPs did not show any systematic adaptation. The time course of chromatic SSVEPs can be well described by an exponential decay function with a half-life of about 20 seconds, which is very close to previous psychophysical reports. Despite the difference in stimuli between the current and previous studies, the coherent time course may indicate a more general adaptation mechanism in the early visual cortex. In addition, the current result also provides a guide for future color SSVEP studies in terms of either avoiding or exploiting this adaptation effect.

Introduction

Chromatic adaptation is a central characteristic of color vision, and a major contributory mechanism to color constancy (for review, see Smithson, 2005). Multiple neural mechanisms contribute to color adaptation along the neural processing pathway from the retina (Yeh, Lee, & Kremers, 1996), the lateral geniculate nucleus (LGN) (Chang, Hess, & Mullen, 2016) to the visual cortex (Engel, 2005; Engel & Furmanski, 2001; Mullen, Chang, & Hess, 2015). Color adaptation can also occur at multiple time scales. Previous studies have reported a rapid adaptation component with a time scale in milliseconds to seconds, and also a slow component with a time constant between 10 to 30 seconds (Fairchild & Lennie, 1992; Fairchild & Reniff, 1995; Rinner & Gegenfurtner, 2000; Werner, Sharpe, & Zrenner, 2000). The neural substrate of the rapid adaptation most likely lies in local receptor adaptation at the retina (Fairchild & Lennie, 1992; Kries, 1905; Rinner & Gegenfurtner, 2000; Werner, 2014). The neural basis of the slow adaptation, however, is poorly understood. Rinner & Gegenfurtner (2000) speculated that it may be at the subcortical or early cortical level, because slow adaptation occurs both for color discrimination and appearance. Werner et al. (2000) used dichoptic presentations to examine the contribution of subcortical and cortical mechanisms to chromatic adaptation. They observed a similar adaptation effect in the cross-eye adaptation condition (i.e., adapting one eye and testing the other eye), compared with the same-eye adaptation condition

Citation: Zhang, Y., Valsecchi, M., Gegenfurtner, K. R., & Chen, J. (2023). The time course of chromatic adaptation in human early visual cortex revealed by SSVEPs. *Journal of Vision*, *23*(5):17, 1–13, https://doi.org/10.1167/jov.23.5.17.

https://doi.org/10.1167/jov.23.5.17 Received January 19, 2022; published May 24, 2023 ISSN 1534-7362

(i.e., adapting and testing the same eye). Their result suggested a cortical contribution to chromatic adaptation (Werner et al., 2000). Based on these studies, the early visual cortex is a likely candidate for the neural basis of slow-phase chromatic adaptation.

To test whether slow chromatic adaptation occurs in the early visual cortex of humans, a promising approach is to analyze steady-state visually evoked potentials (SSVEPs) elicited by chromatic stimuli. SSVEPs are oscillatory brain responses to rhythmic visual stimulation, originating mainly from the early visual cortex, especially the primary visual cortex (for review, see Norcia, Appelbaum, Ales, Cottereau, & Rossion, 2015). Recently, chromatic SSVEP have been used to investigate a whole range of topics, including color and attention (Martinovic, Wuerger, Hillyard, Müller, & Andersen, 2018; Russo & Spinelli, 1999; Wang & Wade, 2011), higher-order color mechanisms (Chen & Gegenfurtner, 2021; Kaneko, Kuriki, & Andersen, 2020), eye movements and color (Chen, Valsecchi, & Gegenfurtner, 2017b), and the effect of color on higher-level visual perception (Or, Retter, & Rossion, 2019). A similar paradigm called cVEP (chromatic VEP) has also been widely used to investigate color processing (Duncan, Roth, Mizokami, McDermott, & Crognale, 2012; Highsmith & Crognale, 2010; Nunez, Shapley, & Gordon, 2017; Nunez, Shapley, & Gordon, 2018; Regan, 1970; Siegfried, Tepas, Sperling, & Hiss, 1965; Skiba, Duncan, & Crognale, 2014; Xing et al., 2015). The cVEP studies used the same periodic flickering stimulation, but usually presented the result in time domain rather than in frequency domain as SSVEP studies. For both cVEP and SSVEP studies, the stimulation duration is usually long, from tens of seconds to a few minutes. There is some evidence showing that slow adaptation occurs in such a setup. For example, Duncan et al. (2012) examined the effect of two-minute adaptation on the VEP responses to colors and indeed revealed reduced responses after adaptation. However, the time course of adaptation has not been investigated.

To address these questions, we re-analyzed the data from two previous pattern-reversal SSVEP studies (Chen, Valsecchi, & Gegenfurtner, 2017a; Chen et al., 2017b). Dataset 1 used luminance-defined gratings and equiluminant red-green gratings to elicit SSVEP responses. The aim of the original study was to examine the effect of smooth pursuit eye movements on chromatic SSVEPs; and the result showed that smooth pursuit enhances chromatic pattern-reversal SSVEPs (Chen et al., 2017b). Dataset 2 used multiple frequencies to tag neural responses at multiple locations. The aim of the original study was to examine attentional allocation during smooth pursuit; and the result showed that attention is allocated closely ahead of the tracking target (Chen et al., 2017a). Here, to investigate the potential adaptation effect during prolonged stimulation (150 seconds in both studies), we reanalyzed only the control condition where no eye movements were executed in both datasets.

Unlike previous color adaptation studies which used a uniform adaptation field (e.g., Rinner & Gegenfurtner, 2000), the pattern-reversal SSVEPs here were elicited by red-green gratings with stable average color over time. Despite the difference, we observed a similar adaptation effect with the same half-life of about 20 seconds. The current result suggests that slow-phase chromatic adaptation might happen already in early visual cortex, as indicated by pattern-reversal SSVEP signals. Moreover, the result has implications for the design of future color SSVEP studies, which could either avoid or exploit the chromatic adaptation effect.

Methods

We re-analyzed data from two of our previous publications (Chen et al., 2017a; Chen et al., 2017b). The studies are briefly described here, and further details can be found in the original articles.

Dataset 1

Dataset 1 was from the previous study (Chen et al., 2017b), which is publicly available at https://zenodo.org/record/808197. The study had 25 observers (15 females and 10 males). In the experiment, the observer either fixated at the screen center or executed smooth pursuit eye movements to a moving target, against a full-screen background that was counter-phase flickering at a reversal rate of 7.5 Hz (7.5 reversals per second). The flickering background was a horizontal grating with a spatial frequency of 0.34 cycles/°, at a size of 61° × 38° on the whole screen. The grating could be modulated in either luminance or isoluminant red-green chromaticity (Figure 1A). Each trial lasted 150 seconds, and each observer underwent eight trials in total. Here for the purpose of investigating adaptation, we only re-analyzed the four trials in the fixation condition (two trials with luminance grating, and two trials with red-green color grating) to exclude any potential effect of eye movements on adaptation.

Dataset 2

Dataset 2 was from the first and second experiments of the study (Chen et al., 2017a), which is publicly available at: https://zenodo.org/record/817545. In both experiments, the observers either fixated at the screen center or executed smooth pursuit eye movements to an array of flickering targets, which were moving across the screen back and forth. Here, we re-analyzed only the fixation trials. In experiment 1, observers (N = 12) underwent two fixation trials and each trial

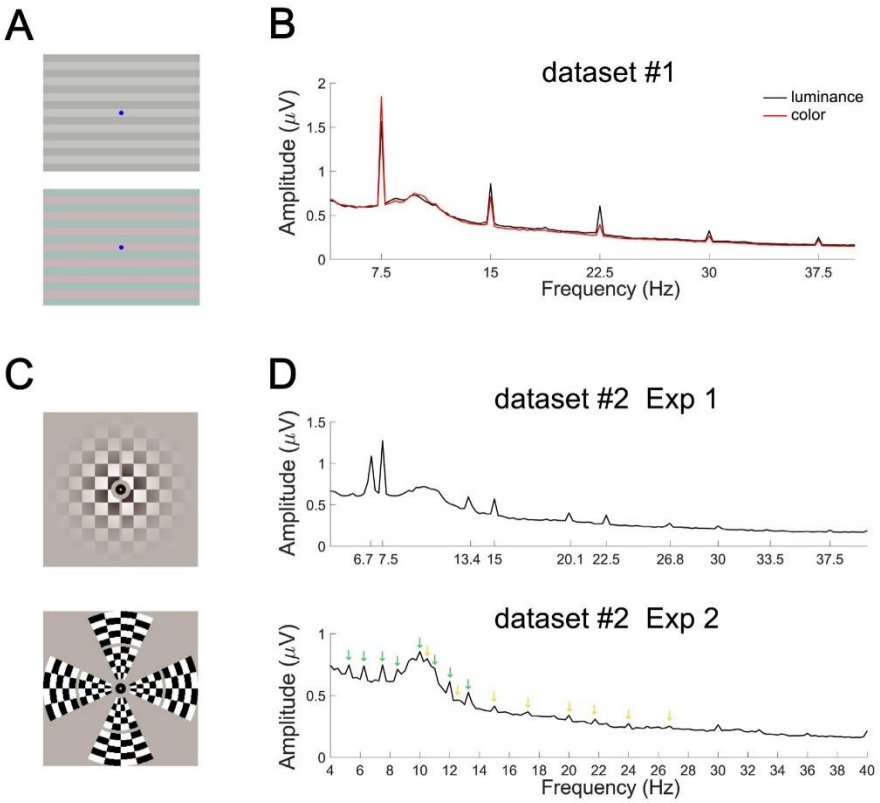

Figure 1. Stimuli and SSVEP responses. (**A**) Stimuli used in the dataset 1 (Chen et al., 2017b). (**B**) Grand-average amplitude spectrum over all observers (N = 25) for color and luminance stimuli. The response at 7.5 Hz and harmonics (e.g., 15, 22.5 Hz) is clearly visible. (**C**) Stimuli used in experiment 1 (top) and experiment 2 (bottom) in dataset 2 (Chen et al., 2017a). (**D**) Grand-average amplitude spectrums in dataset 2. For experiment 1, the responses are clear at 6.7 Hz and 7.5 Hz and their harmonics. For experiment 2, the response is visible at all eight stimulation frequencies (marked by green arrows at 5.2, 6.3, 7.5, 8.6, 10.0, 10.9, 12.0, and 13.3 Hz) and their second higher harmonics (marked by yellow arrows).

lasted 150 seconds. The stimuli were black-and-white checkerboard patterns extended 8.15° horizontally and 8.15° vertically, and were filtered through a 2D Gaussian window (SD = 1.46°). The checkerboards at the left and right sides were pattern-reversal flickering at either 6.7 Hz or 7.5 Hz. In experiment 2, observers (N = 12) underwent two fixation trials, each lasting 150 seconds. The stimuli were eight black-and-white checkerboard sectors centered along the four cardinal directions. Sectors were flickering at eight different frequencies separately (i.e., 5.2 Hz, 6.3 Hz, 7.5 Hz, 8.6 Hz, 10 Hz, 10.9 Hz, 12 Hz, and 13.3 Hz).

Data analysis

The analysis procedures were largely the same as in Chen et al. (2017a). The 32-channel electroencephalography (EEG) signals were first re-referenced to the average. In each trial, we discarded the first 1-second to remove the abrupt onset (e.g., Liu-Shuang, Torfs, & Rossion, 2016). Then the remaining signals were decomposed into 37 successive four-second epochs. Each epoch was detrended by removing the linear fit (Bach & Meigen, 1999). The amplitude spectrum of the epoch was obtained by fast-Fourier transformation (*fft*.m in Matlab). Response amplitude at a certain frequency was calculated by subtracting the baseline noise from the peak amplitude at the target frequency. In the analysis of dataset 1, we used the average amplitude of four bins near the target frequency as baseline. SSVEP amplitude for a certain condition was then calculated by taking the average of amplitudes over the fundamental frequency and two higher harmonics (i.e., 7.5, 15, and 22.5 Hz). We used these three frequencies because previous studies

have indicated that 10 to 20 Hz signals are the best to capture neural activities in the parvocellular pathway (Kremers, Aher, Popov, Mirsalehi, & Huchzermeyer, 2021; Regan, 1968a). In the analysis of dataset 2, we used the average amplitude of 2 bins near the target frequency as baseline (i.e., two immediately adjacent bins were not included to avoid frequency leakage). We first calculated the SNRs of SSVEP responses at all the flicker frequencies and their harmonics by dividing the baseline. According to the results of one-sample *t*-tests on SNRs, we only chose the harmonics where the SNRs were significant (SNRs > 1, $P < .05$) for further analyses. For experiment 1, the first to third harmonics of 7.5 and 6.7 Hz were used. For experiment 2, the first harmonics of all frequencies (i.e., 5.2, 6.3, 7.5, 8.6, 10.0, 10.9, 12.0, and 13.3 Hz) and second of 7.5, 8.6, 10, 12, 13.3 Hz were used. SSVEP amplitude was calculated by taking the average of amplitudes over these frequencies. In all the SSVEP analyses, only the O1, Oz, and O2 channels were used because they are the channels showing maximal responses (this is the case in our other studies with similar setups, Chen et al., 2017a; Chen et al., 2017b; Chen, McManus, Valsecchi, Harris, & Gegenfurtner, 2019; Chen & Gegenfurtner, 2021; and in similar studies from other groups, e.g., Martinovic et al., 2018; Nunez et al., 2017).

The resulting time course of SSVEP responses to color flicker was fitted with an exponential decay function: $SSVEP = S_0 + A \times e^{-kt}$. For the fitting, we excluded the first data point in the time course, because

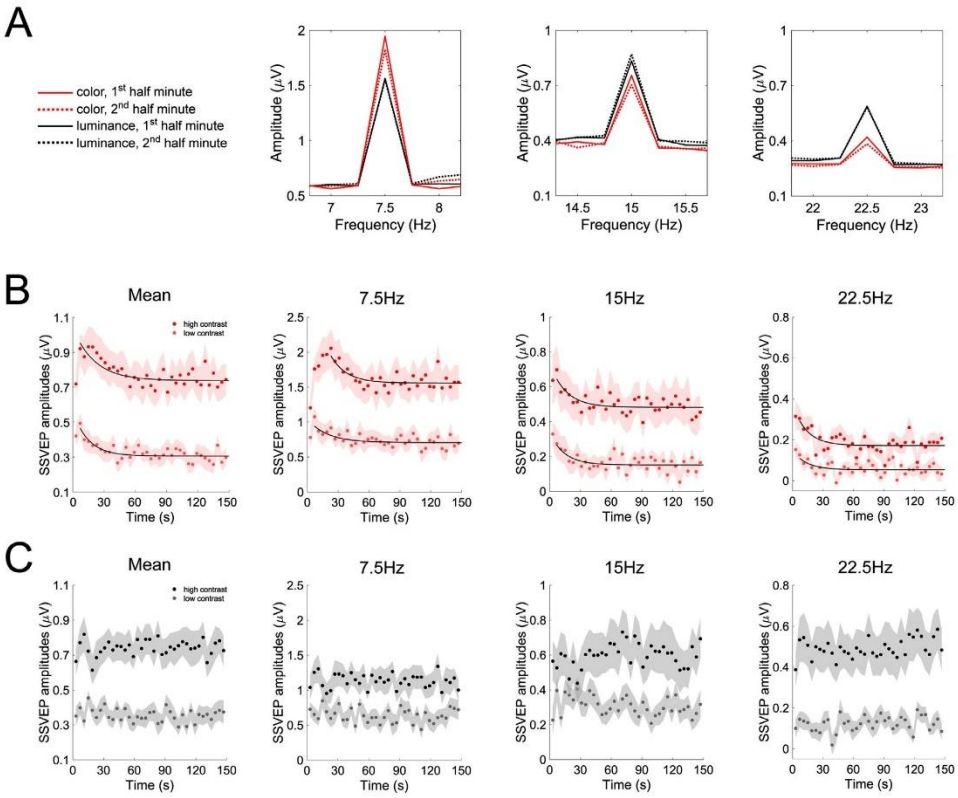

Figure 2. Time course of the adaptation effect in dataset 1. (A) Grand-average amplitude spectrum for color- and luminance-defined gratings during two intervals in each trial (i.e., first half versus second half-minute) at 7.5 Hz, 15 Hz, and 22.5 Hz. (B, C) Time course of SSVEP amplitudes elicited by color (B) and luminance (C) at low and high contrast. The first column is the mean SSVEP amplitudes of all three harmonics, and other columns are the amplitudes of individual harmonics (i.e., 7.5 Hz, 15 Hz, and 22.5 Hz). The black lines in B are the fit by an exponential decay function to the data. The half-life for mean SSVEP amplitudes is 17.1 seconds and 21.5 seconds for low and high contrast, respectively. Each dot shows the SSVEP amplitudes at every four-second epoch. Shaded areas indicate standard errors across observers.

the peak was typically given by the second time point (Figure 2B). The response at the first data point was smaller, probably because of contamination from the initial abrupt event-related response (which should have been minimized because we rejected the first second after stimulus onset) or because SSVEPs require some time to reach the steady-state entrainment (based on our visual inspections on waveforms, it takes about two seconds). Fitting was done on the average data, because EEG data of individual observers are noisy. To measure the half-life of the decay function, we calculated the time required for the decay function to drop to half of the amplitude (i.e., the peak minus the minimum).

Results

To estimate the adaptation effect in pattern-reversal SSVEPs elicited by chromatic and luminance flickers, we re-analyzed our previous datasets with short-term frequency analysis (4 seconds window). Figure 2 shows the result of dataset 1. Figure 2A plots the average spectrum at the reversal rate of 7.5 Hz, and its harmonics at 15 Hz and 22.5 Hz. One-sample t-tests on SNR values of all these peaks (SNR calculated by taking the peak amplitude divided by the average amplitude at nearby 4 bins) revealed that all the responses are

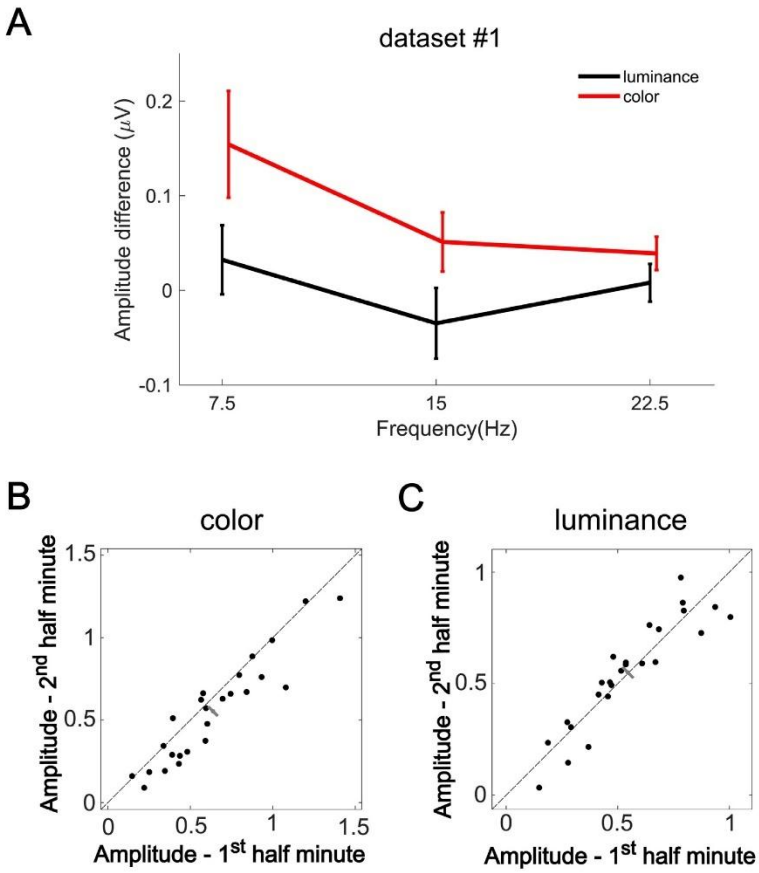

Figure 3. The adaptation effect in dataset 1. (A) The amplitude difference (i.e., the first half-minute minus the second half) at 7.5 Hz and its harmonics (15, 22.5 Hz) for color and luminance. The difference (i.e., adaptation effect) is more substantial for color than for luminance. Error bars represent standard errors across observers. (B, C) Adaptation effect in individual observers. Each data point denotes a single observer. For color-defined gratings (B), most data points fell below the diagonal line, revealing a significant adaptation effect. For luminance-defined gratings (C), there was no adaptation effect. Black bars denote 95% confidence intervals of the mean along the negative-slope diagonal line.

significant (all SNRs > 1, *P*s < .001). The plots show the spectra separately for the time window of the first half-minute of each trial (i.e., the 1st to 8th epochs, from 1 to 33 seconds) and the second half-minute (i.e., the nineth to sixteenth epochs, 33 to 65 seconds). Overall, the responses decrease across the two time intervals for color (i.e., showing adaptation effect), but not for luminance. Figures 2B and 2C show the mean (i.e., the mean of 7.5, 15, and 22.5 Hz) and the individual harmonics' SSVEP amplitudes as a function of time throughout the whole 150-second duration, for both high-contrast and low-contrast conditions. The overall pattern of SSVEPs to color looks remarkably similar to the color adaptation effect described previously with behavioral measurements (Figure 3 of Rinner & Gegenfurtner, 2000; Werner et al., 2000). A simple exponential decay model describes the data quite well (Figure 2B). The half-life of the exponential decay function for mean SSVEP amplitudes at low and high contrast is 17.1 and 21.5 seconds, which is also very close to Rinner & Gegenfurtner's (2000) result (18.2 seconds for color discrimination and 19.6 seconds for color appearance). For luminance, the mean SSVEP amplitudes at both low- and high-contrast stimuli do not show any adaptation effect, neither do the individual harmonics (Figure 2C). Because the mean SSVEP amplitudes at low and high contrast have a similar effect, we combined the two levels of contrast in further analyses. A 2 (type of stimulus: luminance versus color) × 2 (time interval: first versus second half-minute) repeated-measure analysis of variance revealed an interaction, $F(1, 24) = 14.05$, $p < .001$, $\eta_{p2} = 0.369$, indicating different effects of time for luminance and color stimuli. We then proceeded to analyze SSVEP responses between the 1st half minute and 2nd half minute for color and luminance stimuli separately (Figures 3B, 3C), color response decreased significantly ($t(24) = 3.95$, $p < .001$) whereas luminance response did not ($t(24) = 0.10$, $p = 0.923$). There was no clear adaptation effect for luminance response.

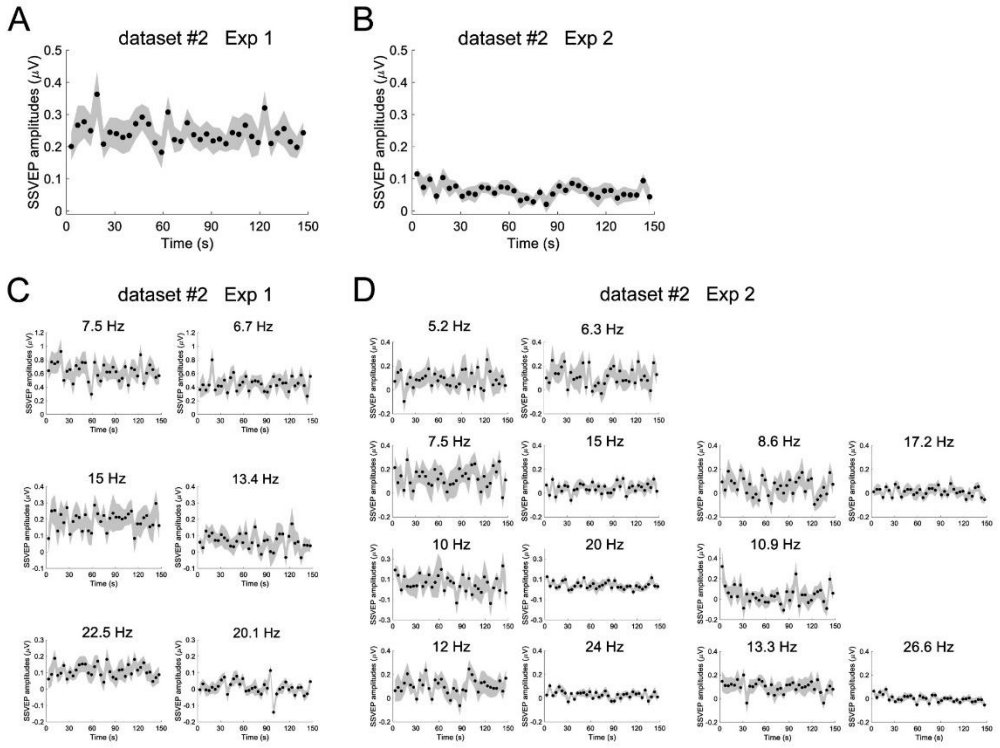

Figure 4. (A, B) The time course of the mean SSVEP amplitudes elicited by luminance-defined checkerboard patterns in two experiments of dataset 2. (C, D) The time course of SSVEP amplitudes of the individual harmonics in experiments 1 and 2, respectively. Each data point represents the SSVEP amplitudes at each four-second epoch. There is no clear sign of adaptation. Shaded areas indicate standard errors across observers.

Finally, we tested the adaptation effect separately at each harmonic frequency. For color stimuli, the SSVEP amplitudes at 7.5 Hz and 22.5 Hz showed significant adaptation effect (7.5 Hz: $t(24) = 4.60$, $p < 0.001$; 15 Hz: $t(24) = 1.64$, $p = 0.115$; 22.5 Hz: $t(24) = 2.22$, $p = 0.036$). For luminance stimuli, none of the harmonics showed significant effects (7.5 Hz: $t(24) = 0.87$, $p = 0.386$; 15 Hz: $t(24) = -0.94$, $p = 0.359$; 22.5 Hz: $t(24) = 0.40$, $p = 0.690$).

Because we used three harmonics to calculate SSVEP amplitudes, we further tested whether the adaptation effect in color SSVEPs depends on the harmonics. Figure 3A shows the adaptation effect (i.e., amplitude difference between the first and second half minute), separately at 7.5, 15, and 22.5 Hz. A 2 (time interval: first vs. second half minute) × 3 (harmonic frequency: 7.5 versus 15 versus 22.5 Hz) repeated-measure analyses of variance on color SSVEPs revealed a main effect for time interval, $F(1, 24) = 14.99$, $p < 0.001$, $\eta_{p2} = 0.384$, indicating an adaptation effect, and a main effect for harmonic frequency, $F(2, 48) = 58.68$, $p < 0.001$, $\eta_{p2} = 0.710$, indicating smaller SSVEP amplitudes at higher harmonic frequencies. However, there was no interaction between harmonic frequency and time interval, $F(2, 48) = 1.12$, $p = 0.340$, $\eta_{p2} = 0.044$, which suggest that the adaptation effect in color SSVEPs does not depend on harmonics. For luminance pattern-reversal SSVEPs, there was a main effect for harmonic frequency, $F(2, 48) = 23.53$, $p < 0.001$, $\eta_{p2} = 0.495$, but no main effect for time interval, $F(1, 24) = 0.01$, $p = 0.930$, $\eta_{p2} = 0.0003$, and no interaction between harmonic frequency and time interval, $F(2,48) = 1.12$, $p = 0.340$, $\eta_{p2} = 0.044$. This suggests that there is no sign of adaptation effect for luminance SSVEPs, and the lack of adaptation is similar across the three harmonics.

To further confirm the lack of adaptation effect for luminance responses, we re-analyzed the pattern-reversal SSVEPs in two experiments of dataset 2. Figure 4 shows the SSVEP amplitudes as a function of time. Figures 4A and 4B show the mean SSVEP amplitudes of all harmonics in experiments 1 and 2, respectively; and Figures 4C and 4D show the SSVEP amplitudes at individual harmonics with significant responses (SNRs > 1, $ps < 0.05$). Consistent with the result of dataset 1, we did not observe any clear sign of adaptation for pattern-reversal SSVEPs elicited by luminance-defined stimuli. Comparing the overall SSVEP responses between the first half-minute and second half-minute intervals in both experiments (Figures 4A, 4B), neither showed any significant difference (Exp 1: $t(11) = 0.50$, $p = 0.630$; Exp 2: $t(11) = 1.39$, $p = 0.193$). We also tested the adaptation effect (i.e., SSVEP amplitudes decrease at the second half-minute compared with the first half-minute of each trial) at each harmonic (Figures 4C, 4D). In experiment 1, the effect at 7.5Hz was significant if no multiple comparison correction was applied ($t(11) = 2.61$, $p = 0.024$), but it did not hold after multiple comparison correction. Except for that, none of the harmonics in experiments 1 and 2 showed any significant adaptation (all $ps > 0.05$).

Discussion

By re-analyzing data from previous studies, we found chromatic pattern-reversal SSVEPs decreased with increasing stimulating duration. This is likely to reflect activity changes in the early visual cortex. The time course can be well fitted by an exponential decay function with a half-life of about 20 seconds and reached a lower asymptote within a minute. The 20-second half-life in SSVEPs is consistent with previous psychophysical reports, where the perceptual performance declined to half at around 10 to 30 seconds during chromatic adaptation (Gupta, Gross, Pastilha, & Hurlbert, 2020; Rinner & Gegenfurtner, 2000; Werner et al., 2000). The current result suggests that slow-phase chromatic adaptation happens already in the early visual cortex, which confirms previous speculations (Rinner & Gegenfurtner, 2000; Werner et al., 2000).

To our knowledge, such slow phase of color adaptation has not been identified in animal physiological studies. A few previous studies recorded single-neuron activities to prolonged stimulations in animals and reported slow phase adaptation effect. The time constant of adaptation to luminance gratings in the visual cortex of cat is around 6 seconds (Albrecht, Farrar, & Hamilton, 1984; Ohzawa, Sclar, & Freeman, 1985; Vautin & Berkley, 1977). Sclar, Lennie, and DePriest (1989) also reported that activities of simple cells in monkey visual cortex declined for the initial 10 to 20 seconds during adaptation. These studies did not use color stimuli, but their time course is consistent with our current finding.

One may question whether the pattern-reversal SSVEP signals in the current study could capture chromatic processing, since the reversal rate of 7.5Hz is relatively high. Previously, Regan has suggested that the SSVEP amplitude at 10-20 Hz was mainly generated by the parvocellular pathway, while signals above 30 Hz were mostly due to the magnocellular pathway (Regan, 1968a; Regan, 1968b; Regan, 1970; Regan, 2009). Similarly, Kremers and colleagues have shown that electroretinographic (ERG) responses at 12Hz reflects L-/M-cone opponency, and responses at 36Hz reflect luminance signals (Kremers, Rodrigues, de Lima Silveira, & da Silva Filho, 2010; Kremers et al. 2021). Therefore the frequencies we used (i.e., 7.5, 15, and 22.5 Hz) should be able to capture chromatic processing. A further issue is whether these responses (7.5Hz-22.5Hz) reflect activity of only one of the multiple chromatic

processing channels. Indeed, previous studies have generally found that color is processed through multiple temporal channels (Cass, Clifford, Alais, & Spehar, 2009; Cropper, 1994; Fylan, Holliday, Singh, Anderson, & Harding, 1997; Gegenfurtner & Hawken, 1996; Metha & Mullen, 1996; Morrone, Fiorentini, & Burr, 1996; Muthukumaraswamy & Singh, 2008; Sun et al., 2007), with at least a slower channel (~2Hz) and a fast channel (~8Hz). The adaptation effect reported here is probably a property of the fast channel, and further studies are required to test whether a similar adaptation effect is also present for the slow channel.

Note that there is a key difference between the stimuli we used to elicit pattern-reversal SSVEPs and the stimuli used in previous psychophysical studies (Gupta et al., 2020; Rinner & Gegenfurtner, 2000; Werner et al., 2000). Previous experiments used the DC offsets of color, changing the average color in the scene. Here the pattern-reversal SSVEP experiment used counter-phase flickering red-green gratings with the same average color over time (i.e., the average color never changed). As a result, what we revealed in SSVEP is an adaptation effect to color contrast, and this does not necessarily correspond to the adaptation effect studied in previous psychophysical experiments. However, they might at least in part share similar mechanism, given that the time courses are strikingly similar. Besides, their neural loci are most likely both at the cortical level (Albrecht et al., 1984; Engel & Furmanski, 2001; Gardner et al., 2005; Goddard, Chang, D. H. F., Hess, R. F., & Mullen, 2019; Goddard, Shooner, & Mullen 2022; Maffei, Fiorentini, & Bisti, 1973; Mullen et al., 2015; Ohzawa, Sclar, & Freeman, 1982; Saul & Cynader, 1989; Sclar et al., 1989; Solomon, Peirce, Dhruv, & Lennie, 2004; Webster & Mollon, 1994). We speculate that the adaptation effect we found might share a similar cortical mechanism with the adaptation effects in previous psychophysical experiments.

A few previous studies investigated the effect of chromatic adaptation in SSVEPs (Regan, 1968a) and VEPs (Duncan et al., 2012; Rabin, Switkes, Crognale, Schneck, & Adams, 1994). Regan (1968a) and Rabin et al. (1994) found that there is an instant adaptation effect of a color field on cortical responses to another color. The instant adaptation effect also varied with flickering frequency (Regan, 1968a) and color similarity between the adapting and testing color (Rabin et al., 1994). They, however, did not test the slow phase of adaptation. Duncan et al. (2012) examined the effect of adapting one color for two minutes on the VEP responses to other colors. They found that two minutes of adaptation reduces amplitude to colors in neighboring angles in color space but has minimal effect on amplitude to colors at orthogonal angles. Their results provided evidence for higher-order chromatic mechanisms, similar to psychophysical results (Bouet & Knoblauch, 2004; Gegenfurtner & Kiper, 1992; Hansen & Gegenfurtner, 2013; Krauskopf & Gegenfurtner, 1992; Webster & Mollon, 1991) and also a recent SSVEPs study (Chen & Gegenfurtner, 2021). However, Duncan et al. (2012) did not investigate the time course of adaptation within these two minutes. Our results show that adaptation is largely complete within one minute, such that an adaptation period of one minute is sufficient to elicit adaptation in color SSVEPs in future studies.

One remarkable aspect of our data is that pattern-reversal SSVEPs elicited by luminance-defined stimuli did not show any systematic adaptation at all. To our knowledge, few studies have investigated slow adaptation effects in SSVEP elicited by grating stimuli similar to ours. One early study reported some preliminary observations (Blakemore & Campbell, 1969). They showed that after viewing a high-contrast grating for 30 or 60 seconds, the VEPs to a low-contrast grating were reduced. This result, however, was based on a single observer. Also, they used high spatial frequency stimuli (12 c/deg), whereas the current study used stimuli with low spatial frequency (0.34 c/deg). It will therefore be interesting to test whether spatial frequency is a determining factor for the presence of an adaptation effect in SSVEPs to luminance gratings. A later study found that neural responses to achromatic gratings are attenuated after adapting to a mask at certain contrast (Robson & Kulikowski, 2012). However, they did not examine the slow adaptation effect and the time course. For SSVEPs elicited by motion stimuli, Heinrich & Bach (2003) found an absence of adaptation after exposure to motion reversals (flickering between motion expansion and contraction). When the adaptation stimuli were moving only in a single direction, instead of moving back and forth, adaptation did occur (Ales & Norcia, 2009; Heinrich & Bach, 2003). For example, Ales & Norcia (2009) presented an adaptor moving in a single direction for 25 seconds and then tested SSVEPs to moving stimuli oscillating left and right. They found that responses in the adapted direction were reduced but not in the un-adapted direction, and this induced an asymmetry in the population responses. Therefore, in the domain of motion SSVEPs, direction-specific motion adaptation has been observed, whereas non-direction-specific adaptation may not occur in the early visual cortex as indicated by SSVEPs. At this stage, we don't know exactly why luminance-gratings did not induce an adaptation effect in the current result. Based on motion SSVEP, we speculate that adaptation might be revealed with "uni-direction" adaptation (i.e., adapting to a black or white field).

The lack of adaptation effect for luminance response may also be related to the transient and sustained response in visual processing. It is well known that neural processing of luminance is relatively transient, whereas the processing of color tends to be sustained

(Kulikowski & Walsh, 1993; Robson & Kulikowski, 2012; Schiller & Malpeli, 1978; Schwartz & Loop, 1982; Shapley, Kaplan, & Soodak, 1981; Valberg & Lee, 1991). The lack of slow adaptation for luminance response might be due to the transient nature of the response. In addition, SSVEPs in the current study were produced by pattern-reversal stimuli, which have been shown to elicit transient responses more than on-off stimuli (Strasburger, Murray, & Remky, 1993). It is thus possible that luminance SSVEPs with on-off stimulation may show a slow adaptation effect.

Although we believe our results show that adaptation affects luminance and color mechanisms differentially, one might also come to the conclusion that it is habituation that causes these differences. In our opinion, the difference between adaptation and habituation is difficult to resolve, and both terms have been used interchangeably in large parts of the literature (e.g., Krauskopf, Williams, & Heeley, 1982, versus Webster & Mollon, 1991). In the EEG or SSVEP literature, there is also no well-defined and accepted way to distinguish habituation from adaptation. Although most studies investigating habituation with SSVEPs did not consider the potential role of adaptation (Abdulhussein, An, Alsakaa, & Ming, 2022; Cao et al., 2020; Labecki, Nowicka, & Suffczynski, 2019; Shibata, Yamane, Otuka, & Iwata, 2008; Shibata, Yamane, Nishimura, Kondo, & Otuka, 2011), one study discussed this issue and explicitly said that their results can be explained by habituation as well as adaptation (Omland, Nilsen, & Sand, 2011). There was only one SSVEP study, as far as we know, that tried to manipulate habituation and adaptation in the experiment design (Dong, Du, & Bao, 2020). In their study, the change in visual sensitivity observed after exposure to the stimulus within a testing session (190 trials) was defined as "adaptation effect." In addition, their participants were tested every day for 11 days in a row. The change in visual sensitivity observed due to such long-term exposure (across a few days) was defined as "habituation effect." Based on their definition, what we reported in the current study should be "adaptation" rather than "habituation." However, because there is no well-accepted definition to distinguish the two, we think that further work is need to determine the contribution of habituation and adaptation to the present result.

The current result has important implications for designing color SSVEP studies in the future. First, SSVEP studies usually use long stimulation durations. Most previous color SSVEP studies employed a duration in the range of 20 to 150 seconds (Chen et al., 2017b; Chen & Gegenfurtner, 2021; Highsmith & Crognale, 2010; Kaneko et al., 2020; Nunez et al., 2017; Nunez et al., 2018; Or et al., 2019; Regan, 1968a; Xing et al., 2015), with a few in shorter duration from three to 12 seconds (Martinovic et al., 2018; Rabin et al., 1994; Skiba et al., 2014; Wang & Wade, 2011). Based on the current result, it seems optimal to use a relatively short duration of no more than 20 seconds if avoiding adaptation is preferred. Second, adaptation has been a widely used technique to investigate color processing in both psychophysical studies, as well as functional magnetic resonance imaging studies. In SSVEP studies, it is much less used. Our result suggests that an adaptation duration of 30 to 60 seconds should be sufficient. Third, caution should be taken if future studies want to directly compare color and luminance SSVEPs, because their adaptation time courses are different.

Keywords: color, luminance, chromatic adaptation, time course, steady-state visual evoked potentials

Acknowledgments

Supported by the National Natural Science Foundation of China [grant number 31900758]. KG was supported by the Deutsche Forschungsgemeinschaft (DFG, German Research Foundation)—project number 222641018—SFB/TRR 135 Project C2, and the European Research Council Advanced Grant Color3.0 project number 884116.

Commercial relationships: none.
Corresponding author: Jing Chen.
Email: chenjingps@gmail.com.
Address: School of Psychology, Shanghai University of Sport, Shanghai, China.

References

Abdulhussein, M. A., An, X., Alsakaa, A. A., & Ming, D. (2022). Lack of habituation in migraine patients and evoked potential types: Analysis study from EEG signals. *Journal of Information and Optimization Sciences, 43*(4), 855–891, https://doi.org/10.1080/02522667.2022.2095958.

Albrecht, D. G., Farrar, S. B., & Hamilton, D. B. (1984). Spatial contrast adaptation characteristics of neurones recorded in the cat's visual cortex. *Journal of Physiology, 347*(1), 713–739, https://doi.org/10.1113/jphysiol.1984.sp015092.

Ales, J. M., & Norcia, A. M. (2009). Assessing direction-specific adaptation using the steady-state visual evoked potential: Results from EEG source imaging. *Journal of Vision, 9*(7), 8–8, https://doi.org/10.1167/9.7.8.

Bach, M., & Meigen, T. (1999). Do's and don'ts in Fourier analysis of steady-state potentials. *Documenta Ophthalmologica, 99*(1), 69–82, https://doi.org/10.1023/A:1002648202420.

Blakemore, C., & Campbell, F. W. (1969). On the existence of neurones in the human visual system selectively sensitive to the orientation and size of retinal images. *Journal of Physiology, 203*(1), 237–260, https://doi.org/10.1113/jphysiol.1969.sp008862.

Bouet, R., & Knoblauch, K. (2004). Perceptual classification of chromatic modulation. *Visual Neuroscience, 21*(3), 283–289, https://doi.org/10.1017/S0952523804213141.

Cao, Z., Ding, W., Wang, Y.-K., Hussain, F. K., Al-Jumaily, A., & Lin, C.-T. (2020). Effects of repetitive SSVEPs on EEG complexity using multiscale inherent fuzzy entropy. *Neurocomputing, 389*, 198–206, https://doi.org/10.1016/j.neucom.2018.08.091.

Cass, J., Clifford, C. W. G., Alais, D., & Spehar, B. (2009). Temporal structure of chromatic channels revealed through masking. *Journal of Vision, 9*(5), 17–17, https://doi.org/10.1167/9.5.17.

Chang, D. H. F., Hess, R. F., & Mullen, K. T. (2016). Color responses and their adaptation in human superior colliculus and lateral geniculate nucleus. *NeuroImage, 138*, 211–220, https://doi.org/10.1016/j.neuroimage.2016.04.067.

Chen, J., & Gegenfurtner, K. R. (2021). Electrophysiological evidence for higher-level chromatic mechanisms in humans. *Journal of Vision, 21*(8), 12, https://doi.org/10.1167/jov.21.8.12.

Chen, J., McManus, M., Valsecchi, M., Harris, L. R., & Gegenfurtner, K. R. (2019). Steady-state visually evoked potentials reveal partial size constancy in early visual cortex. *Journal of Vision, 19*(6), 8, https://doi.org/10.1167/19.6.8.

Chen, J., Valsecchi, M., & Gegenfurtner, K. R. (2017a). Attention is allocated closely ahead of the target during smooth pursuit eye movements: Evidence from EEG frequency tagging. *Neuropsychologia, 102*, 206–216, https://doi.org/10.1016/j.neuropsychologia.2017.06.024.

Chen, J., Valsecchi, M., & Gegenfurtner, K. R. (2017b). Enhanced brain responses to color during smooth-pursuit eye movements. *Journal of Neurophysiology, 118*(2), 749–754, https://doi.org/10.1152/jn.00208.2017.

Cropper, S. J. (1994). Velocity discrimination in chromatic gratings and beats. *Vision Research, 34*(1), 41–48, https://doi.org/10.1016/0042-6989(94)90255-0.

Dong, X., Du, X., & Bao, M. (2020). Repeated contrast adaptation does not cause habituation of the adapter. *Frontiers in Human Neuroscience, 14*, 589634, https://doi.org/10.3389/fnhum.2020.589634.

Duncan, C. S., Roth, E. J., Mizokami, Y., McDermott, K. C., & Crognale, M. A. (2012). Contrast adaptation reveals increased organizational complexity of chromatic processing in the visual evoked potential. *Journal of the Optical Society of America A, 29*(2), A152, https://doi.org/10.1364/JOSAA.29.00A152.

Engel, S. A. (2005). Adaptation of oriented and unoriented color-selective neurons in human visual areas. *Neuron, 45*(4), 613–623, https://doi.org/10.1016/j.neuron.2005.01.014.

Engel, S. A., & Furmanski, C. S. (2001). Selective adaptation to color contrast in human primary visual cortex. *Journal of Neuroscience, 21*(11), 3949–3954, https://doi.org/10.1523/JNEUROSCI.21-11-03949.2001.

Fairchild, M. D., & Lennie, P. (1992). Chromatic adaptation to natural and incandescent illuminants. *Vision Research, 32*(11), 2077–2085, https://doi.org/10.1016/0042-6989(92)90069-U.

Fairchild, M. D., & Reniff, L. (1995). Time course of chromatic adaptation for color-appearance judgments. *Journal of the Optical Society of America A, 12*(5), 824, https://doi.org/10.1364/JOSAA.12.000824.

Fylan, F., Holliday, I. E., Singh, K. D., Anderson, S. J., & Harding, G. F. A. (1997). Magnetoencephalographic investigation of human cortical area V1 using color stimuli. *NeuroImage, 6*(1), 47–57, https://doi.org/10.1006/nimg.1997.0273.

Gardner, J. L., Sun, P., Waggoner, R. A., Ueno, K., Tanaka, K., & Cheng, K. (2005). Contrast adaptation and representation in human early visual cortex. *Neuron, 47*(4), 607–620, https://doi.org/10.1016/j.neuron.2005.07.016.

Gegenfurtner, K. R., & Hawken, M. J. (1996). Interaction of motion and color in the visual pathways. *Trends in Neurosciences, 19*(9), 394–401, https://doi.org/10.1016/S0166-2236(96)10036-9.

Gegenfurtner, K. R., & Kiper, D. C. (1992). Contrast detection in luminance and chromatic noise. *Journal of the Optical Society of America A, 9*(11), 1880, https://doi.org/10.1364/JOSAA.9.001880.

Goddard, E., Chang, D. H. F., Hess, R. F., & Mullen, K. T. (2019). Color contrast adaptation: FMRI fails to predict behavioral adaptation. *NeuroImage, 201*, 116032, https://doi.org/10.1016/j.neuroimage.2019.116032.

Goddard, E., Shooner, C., & Mullen, K. T. (2022). Magnetoencephalography contrast adaptation reflects perceptual adaptation. *Journal of Vision, 22*(10), 16, https://doi.org/10.1167/jov.22.10.16.

Gupta, G., Gross, N., Pastilha, R., & Hurlbert, A. (2020). The time course of chromatic

adaptation under immersive illumination [Preprint]. *Neuroscience,* https://doi.org/10.1101/2020.03.10.984567.

Hansen, T., & Gegenfurtner, K. R. (2013). Higher order color mechanisms: Evidence from noise-masking experiments in cone contrast space. *Journal of Vision, 13*(1), 26–26, https://doi.org/10.1167/13.1.26.

Heinrich, S. P., & Bach, M. (2003). Adaptation characteristics of steady-state motion visual evoked potentials. *Clinical Neurophysiology, 114*(7), 1359–1366, https://doi.org/10.1016/S1388-2457(03)00088-9.

Highsmith, J., & Crognale, M. A. (2010). Attentional shifts have little effect on the waveform of the chromatic onset VEP: Attentional effects on chromatic VEP. *Ophthalmic and Physiological Optics, 30*(5), 525–533, https://doi.org/10.1111/j.1475-1313.2010.00747.x.

Kaneko, S., Kuriki, I., & Andersen, S. K. (2020). Steady-state visual evoked potentials elicited from early visual cortex reflect both perceptual color space and cone-opponent mechanisms. *Cerebral Cortex Communications, 1*(1), tgaa059, https://doi.org/10.1093/texcom/tgaa059.

Krauskopf, J., & Gegenfurtner, K. (1992). Color discrimination and adaptation. *Vision Research, 32*(11), 2165–2175, https://doi.org/10.1016/0042-6989(92)90077-V.

Krauskopf, J., Williams, D. R., & Heeley, D. W. (1982). Cardinal directions of color space. *Vision Research, 22*(9), 1123–1131, https://doi.org/10.1016/0042-6989(82)90077-3.

Kremers, J., Aher, A. J., Popov, Y., Mirsalehi, M., & Huchzermeyer, C. (2021). The influence of temporal frequency and stimulus size on the relative contribution of luminance and L-/M-cone opponent mechanisms in heterochromatic flicker ERGs. *Documenta Ophthalmologica, 143*(2), 207–220, https://doi.org/10.1007/s10633-021-09837-9.

Kremers, J., Rodrigues, A. R., de Lima Silveira, L. C., & da Silva Filho, M. (2010). Flicker ERGs representing chromaticity and luminance signals. *Investigative Ophthalmology & Visual Science, 51*(1), 577, https://doi.org/10.1167/iovs.09-3899.

Kries, J. (1905). Die gesichtsempfindungen. *Nagel's Handbuch Der Physiologie Des Menschen, 3*, 109–282.

Kulikowski, J. J., & Walsh, V. (1993). Colour vision: Isolating mechanisms in overlapping streams. *Progress in Brain Research, 95*, 417–426, https://doi.org/10.1016/s0079-6123(08)60385-4.

Labecki, M., Nowicka, M. M., & Suffczynski, P. (2019). Temporal modulation of steady-state visual evoked potentials. *International Journal of Neural Systems, 29*(03), 1850050, https://doi.org/10.1142/S0129065718500508.

Liu-Shuang, J., Torfs, K., & Rossion, B. (2016). An objective electrophysiological marker of face individualisation impairment in acquired prosopagnosia with fast periodic visual stimulation. *Neuropsychologia, 83*, 100–113, https://doi.org/10.1016/j.neuropsychologia.2015.08.023.

Maffei, L., Fiorentini, A., & Bisti, S. (1973). Neural correlate of perceptual adaptation to gratings. *Science, 182*(4116), 1036–1038, https://doi.org/10.1126/science.182.4116.1036.

Martinovic, J., Wuerger, S. M., Hillyard, S. A., Müller, M. M., & Andersen, S. K. (2018). Neural mechanisms of divided feature-selective attention to colour. *NeuroImage, 181*, 670–682, https://doi.org/10.1016/j.neuroimage.2018.07.033.

Metha, A. B., & Mullen, K. T. (1996). Temporal mechanisms underlying flicker detection and identification for red–green and achromatic stimuli. *Journal of the Optical Society of America A, 13*(10), 1969, https://doi.org/10.1364/JOSAA.13.001969.

Morrone, M. C., Fiorentini, A., & Burr, D. C. (1996). Development of the temporal properties of visual evoked potentials to luminance and colour contrast in infants. *Vision Research, 36*(19), 3141–3155, https://doi.org/10.1016/0042-6989(96)00050-8.

Mullen, K. T., Chang, D. H. F., & Hess, R. F. (2015). The selectivity of responses to red-green colour and achromatic contrast in the human visual cortex: An fMRI adaptation study. *European Journal of Neuroscience, 42*(11), 2923–2933, https://doi.org/10.1111/ejn.13090.

Muthukumaraswamy, S. D., & Singh, K. D. (2008). Spatiotemporal frequency tuning of BOLD and gamma band MEG responses compared in primary visual cortex. *NeuroImage, 40*(4), 1552–1560, https://doi.org/10.1016/j.neuroimage.2008.01.052.

Norcia, A. M., Appelbaum, L. G., Ales, J. M., Cottereau, B. R., & Rossion, B. (2015). The steady-state visual evoked potential in vision research: A review. *Journal of Vision, 15*(6), 4, https://doi.org/10.1167/15.6.4.

Nunez, V., Shapley, R. M., & Gordon, J. (2017). Nonlinear dynamics of cortical responses to color in the human cVEP. *Journal of Vision, 17*(11), 9, https://doi.org/10.1167/17.11.9.

Nunez, V., Shapley, R. M., & Gordon, J. (2018). Cortical double-opponent cells in color perception: Perceptual scaling and chromatic visual evoked potentials. *I-Perception, 9*(1), 204166951775271, https://doi.org/10.1177/2041669517752715.

Ohzawa, I., Sclar, G., & Freeman, R. D. (1982). Contrast gain control in the cat visual cortex. *Nature, 298*(5871), 266–268, https://doi.org/10.1038/298266a0.

Ohzawa, I., Sclar, G., & Freeman, R. D. (1985). Contrast gain control in the cat's visual system. *Journal of Neurophysiology, 54*(3), 651–667, https://doi.org/10.1152/jn.1985.54.3.651.

Omland, P. M., Nilsen, K. B., & Sand, T. (2011). Habituation measured by pattern reversal visual evoked potentials depends more on check size than reversal rate. *Clinical Neurophysiology, 122*(9), 1846–1853, https://doi.org/10.1016/j.clinph.2011.02.025.

Or, C. C.-F., Retter, T. L., & Rossion, B. (2019). The contribution of color information to rapid face categorization in natural scenes. *Journal of Vision, 19*(5), 20, https://doi.org/10.1167/19.5.20.

Rabin, J., Switkes, E., Crognale, M., Schneck, M. E., & Adams, A. J. (1994). Visual evoked potentials in three-dimensional color space: Correlates of spatio-chromatic processing. *Vision Research, 34*(20), 2657–2671, https://doi.org/10.1016/0042-6989(94)90222-4.

Regan, D. (1968a). Chromatic adaptation and steady-state evoked potentials. *Vision Research, 8*(2), 149–158, https://doi.org/10.1016/0042-6989(68)90003-5.

Regan, D. (1968b). A high frequency mechanism which underlies visual evoked potentials. *Electroencephalography and Clinical Neurophysiology, 25*(3), 231–237, https://doi.org/10.1016/0013-4694(68)90020-5.

Regan, D. (1970). Objective method of measuring the relative spectral-luminosity curve in man. *Journal of the Optical Society of America, 60*(6), 856, https://doi.org/10.1364/JOSA.60.000856.

Regan, D. (2009). Some early uses of evoked brain responses in investigations of human visual function. *Vision Research, 49*(9), 882–897, https://doi.org/10.1016/j.visres.2008.01.017.

Rinner, O., & Gegenfurtner, K. R. (2000). Time course of chromatic adaptation for color appearance and discrimination. *Vision Research, 40*(14), 1813–1826, https://doi.org/10.1016/S0042-6989(00)00050-X.

Robson, A. G., & Kulikowski, J. J. (2012). Objective assessment of chromatic and achromatic pattern adaptation reveals the temporal response properties of different visual pathways. *Visual Neuroscience, 29*(6), 301–313, https://doi.org/10.1017/S0952523812000351.

Russo, F. D., & Spinelli, D. (1999). Spatial attention has different effects on the magno- and parvocellular pathways: *NeuroReport, 10*(13), 2755–2762, https://doi.org/10.1097/00001756-199909090-00011.

Saul, A. B., & Cynader, M. S. (1989). Adaptation in single units in visual cortex: The tuning of aftereffects in the spatial domain. *Visual Neuroscience, 2*(6), 593–607, https://doi.org/10.1017/S0952523800003527.

Schiller, P. H., & Malpeli, J. G. (1978). Functional specificity of lateral geniculate nucleus laminae of the rhesus monkey. *Journal of Neurophysiology, 41*(3), 788–797, https://doi.org/10.1152/jn.1978.41.3.788.

Schwartz, S. H., & Loop, M. S. (1982). Evidence for transient luminance and quasi-sustained color mechanisms. *Vision Research, 22*(4), 445–447, https://doi.org/10.1016/0042-6989(82)90192-4.

Sclar, G., Lennie, P., & DePriest, D. D. (1989). Contrast adaptation in striate cortex of macaque. *Vision Research, 29*(7), 747–755, https://doi.org/10.1016/0042-6989(89)90087-4.

Shapley, R., Kaplan, E., & Soodak, R. (1981). Spatial summation and contrast sensitivity of X and Y cells in the lateral geniculate nucleus of the macaque. *Nature, 292*(5823), 543–545, https://doi.org/10.1038/292543a0.

Shibata, K., Yamane, K., Nishimura, Y., Kondo, H., & Otuka, K. (2011). Spatial frequency differentially affects habituation in migraineurs: A steady-state visual-evoked potential study. *Documenta Ophthalmologica, 123*(2), 65–73, https://doi.org/10.1007/s10633-011-9281-2.

Shibata, K., Yamane, K., Otuka, K., & Iwata, M. (2008). Abnormal visual processing in migraine with aura: A study of steady-state visual evoked potentials. *Journal of the Neurological Sciences, 271*(1–2), 119–126, https://doi.org/10.1016/j.jns.2008.04.004.

Siegfried, J. B., Tepas, D. I., Sperling, H. G., & Hiss, R. H. (1965). Evoked brain potential correlates of psychophysical responses: Heterochromatic flicker photometry. *Science, 149*(3681), 321–323, https://doi.org/10.1126/science.149.3681.321.

Skiba, R. M., Duncan, C. S., & Crognale, M. A. (2014). The effects of luminance contribution from large fields to chromatic visual evoked potentials. *Vision Research, 95*, 68–74, https://doi.org/10.1016/j.visres.2013.12.011.

Smithson, H. E. (2005). Sensory, computational and cognitive components of human colour constancy. *Philosophical Transactions of the Royal Society B: Biological Sciences, 360*(1458), 1329–1346, https://doi.org/10.1098/rstb.2005.1633.

Solomon, S. G., Peirce, J. W., Dhruv, N. T., & Lennie, P. (2004). Profound contrast adaptation early in the visual pathway. *Neuron, 42*(1), 155–162, https://doi.org/10.1016/S0896-6273(04)00178-3.

Strasburger, H., Murray, I., & Remky, A. (1993). Sustained and transient mechanisms in the steady-state visual evoked potential: Onset presentation compared to pattern reversal. *Clinical Vision Sciences, 8*, 211–211.

Sun, P., Ueno, K., Waggoner, R. A., Gardner, J. L., Tanaka, K., & Cheng, K. (2007). A temporal frequency–dependent functional architecture in human V1 revealed by high-resolution fMRI. *Nature Neuroscience, 10*(11), 1404–1406, https://doi.org/10.1038/nn1983.

A. Valberg, & B. B. Lee (Eds.). (1991). *From Pigments to Perception: Advances in Understanding Visual Processes*. New York: Springer US, https://doi.org/10.1007/978-1-4615-3718-2.

Vautin, R. G., & Berkley, M. A. (1977). Responses of single cells in cat visual cortex to prolonged stimulus movement: Neural correlates of visual aftereffects. *Journal of Neurophysiology, 40*(5), 1051–1065, https://doi.org/10.1152/jn.1977.40.5.1051.

Wang, J., & Wade, A. R. (2011). Differential attentional modulation of cortical responses to S-cone and luminance stimuli. *Journal of Vision, 11*(6), 1–1, https://doi.org/10.1167/11.6.1.

Webster, M. A., & Mollon, J. D. (1991). Changes in colour appearance following post-receptoral adaptation. *Nature, 349*(6306), 235–238, https://doi.org/10.1038/349235a0.

Webster, M. A., & Mollon, J. D. (1994). The influence of contrast adaptation on color appearance. *Vision Research, 34*(15), 1993–2020, https://doi.org/10.1016/0042-6989(94)90028-0.

Werner, A. (2014). Spatial and temporal aspects of chromatic adaptation and their functional significance for colour constancy. *Vision Research, 104*, 80–89, https://doi.org/10.1016/j.visres.2014.10.005.

Werner, A., Sharpe, L. T., & Zrenner, E. (2000). Asymmetries in the time-course of chromatic adaptation and the significance of contrast. *Vision Research, 40*(9), 1101–1113, https://doi.org/10.1016/S0042-6989(00)00012-2.

Xing, D., Ouni, A., Chen, S., Sahmoud, H., Gordon, J., & Shapley, R. (2015). Brightness-color interactions in human early visual cortex. *Journal of Neuroscience, 35*(5), 2226–2232, https://doi.org/10.1523/JNEUROSCI.3740-14.2015.

Yeh, T., Lee, B. B., & Kremers, J. (1996). The time course of adaptation in macaque retinal ganglion cells. *Vision Research, 36*(7), 913–931, https://doi.org/10.1016/0042-6989(95)00332-0.

2. The execution of saccadic eye movements suppresses visual processing of both color and luminance in the early visual cortex of humans

J Neurophysiol 131: 1156–1167, 2024.
First published May 1, 2024; doi:10.1152/jn.00419.2023

american physiological society

JNP JOURNAL OF NEUROPHYSIOLOGY

RESEARCH ARTICLE

Sensory Processing

The execution of saccadic eye movements suppresses visual processing of both color and luminance in the early visual cortex of humans

Yuan Zhang,[1] Matteo Valsecchi,[2] Karl R. Gegenfurtner,[3] and Jing Chen[4]

[1]*School of Psychology, Shanghai University of Sport, Shanghai, China;* [2]*Dipartimento di Psicologia, Universitá di Bologna, Bologna, Italy;* [3]*Abteilung Allgemeine Psychologie, Center for Mind, Brain & Behavior, Justus-Liebig-Universität Gießen, Gießen, Germany; and* [4]*School of Psychology, Research Center for Exercise and Brain Science, Shanghai University of Sport, Shanghai, China*

Abstract

Our eyes execute rapid, directional movements known as saccades, occurring several times per second, to focus on objects of interest in our environment. During these movements, visual sensitivity is temporarily reduced. Despite numerous studies on this topic, the underlying mechanism remains elusive, including a lingering debate on whether saccadic suppression affects the parvocellular visual pathway. To address this issue, we conducted a study employing steady-state visual evoked potentials (SSVEPs) elicited by chromatic and luminance stimuli while observers performed saccadic eye movements. We also employed an innovative analysis pipeline to enhance the signal-to-noise ratio, yielding superior results compared to the previous method. Our findings revealed a clear suppression effect on SSVEP signals during saccades compared to fixation periods. Notably, this suppression effect was comparable for both chromatic and luminance stimuli. We went further to measure the suppression effect across various contrast levels, which enabled us to model SSVEP responses with contrast response functions. The results suggest that saccades primarily reduce response gain without significantly affecting contrast gain and that this reduction applies uniformly to both chromatic and luminance pathways. In summary, our study provides robust evidence that saccades similarly suppress visual processing in both the parvocellular and magnocellular pathways within the human early visual cortex, as indicated by SSVEP responses. The observation that saccadic eye movements impact response gain rather than contrast gain implies that they influence visual processing through a multiplicative mechanism.

NEW & NOTEWORTHY The present study demonstrates that saccadic eye movements reduce the processing of both luminance and chromatic stimuli in the early visual cortex of humans. By modeling the contrast response function, the study further shows that saccades affect visual processing by reducing the response gain rather than altering the contrast gain, suggesting that a multiplicative mechanism of visual attenuation affects both parvocellular and magnocellular pathways.

color; luminance; saccade; saccadic suppression; steady-state visual evoked potentials

INTRODUCTION

When viewing the environment, our eyes constantly shift gaze rapidly in a ballistic way through saccadic eye movements. These saccades are crucial, as they allow us to direct the high-resolution fovea toward objects of interest (1–3). The execution of saccades, however, poses a challenge to visual perception. Visual sensitivity is severely suppressed from ~100 ms before until 100 ms after saccade onset (4–7). Saccadic suppression has been studied extensively both psychophysically and neurophysiologically. Nevertheless, the neural mechanism of saccadic suppression remains elusive.

There are conflicting results on whether saccadic suppression occurs exclusively in the magnocellular visual pathway or extends to the parvocellular pathway as well. Several psychophysical studies have found that saccades do not suppress the processing of chromatic information, suggesting that saccades do not affect the parvocellular pathway. Burr et al. (8) showed that saccades reduced the

Correspondence: J. Chen (chenjingps@gmail.com).
Submitted 13 November 2023 / Revised 10 April 2024 / Accepted 28 April 2024

sensitivity of luminance-modulated gratings at low spatial frequencies but did not affect the perception of equiluminant color gratings. Most following studies found similar results and concluded that saccades selectively suppress visual processing in the magnocellular pathway (4, 9–16). Two recent studies with a large number of observers showed significant saccadic suppression for equiluminant stimuli, but suppression was less pronounced at equiluminance and there were notable individual differences in the strength of suppression (17, 18). However, the evidence is mixed in neurophysiological studies. Human functional (f)MRI studies revealed a comparable saccadic suppression effect on luminance and color in the relatively early stages of visual processing, such as the LGN, V1, and V2 (19, 20), whereas studies on nonhuman primates showed that saccade suppresses luminance more strongly than color in early areas such as LGN (21–23). At the superior colliculus (SC) of primates, visual motor neurons showed selective suppression for low-spatial frequency luminance stimuli, but visual neurons showed a general suppression effect independent of stimulus spatial frequency (24). In higher visual areas, such as V4, hMT+, and V7, human fMRI results have also shown that saccadic suppression was more pronounced for luminance than color (19, 20). In contrast, at the frontal eye field (FEF) of nonhuman primates, the suppression effect is comparable for luminance and color (25). Thus, further studies are required on whether saccadic suppression occurs in the parvocellular pathway in the visual cortex.

A potential problem of previous fMRI studies lies in the fact that blood oxygen level-dependent (BOLD) signals have extremely low temporal resolution. As saccadic suppression occurs in tens of milliseconds, the fMRI technique is not ideal for capturing such a time-resolved phenomenon. Here, we used steady-state visual evoked potentials (SSVEPs) to track neural activities across saccadic eye movements. Previously, Chen et al. (26) showed that SSVEPs can track the time course of saccadic suppression successfully, despite the neural processing delays involved in measuring neural activities from V1. Compared with fMRI, SSVEPs have good temporal resolution and are relatively immune to eye movement-related artifacts because of their narrowband responses located at the stimulation frequency (for review, see Ref. 27). Here, across two experiments, we consistently find a comparable saccadic suppression effect for SSVEP responses elicited by color- and luminance-defined stimuli, indicating that the suppression effect is comparable in the parvocellular and magnocellular pathways.

Furthermore, the present study aimed to investigate how saccades exert the modulation on the parvocellular and magnocellular neurons. To elucidate the underlying computational mechanism, we accessed the contrast response function with SSVEPs in *experiment 2*. This is inspired by previous research conducted with luminance stimuli (e.g., see Refs. 28–30). By modeling the contrast sensitivity at various levels of noise, it has been suggested that the most parsimonious mechanism underlying saccadic suppression is a reduction in response gain (29, 30). Consistently, Chen et al. (28) recorded the neuronal firing rates in the superior colliculus during microsaccades and found a significant reduction in response gain with no alteration in contrast gain. Remarkably, our *experiment 2* yielded similar results with SSVEPs in human observers, regardless of whether the stimuli were color or luminance based. Thus, these results strongly support the notion that saccadic eye movements impact visual processing through a multiplicative mechanism in both the parvocellular and magnocellular pathways.

METHODS

Experiment 1: Suppression of SSVEP

The purpose of *experiment 1* was to investigate the effect of saccades on SSVEP responses elicited by color and luminance stimuli.

Participants.

Thirteen observers (5 females and 8 males; mean age: 21.4 yr, age range: 18–27 yr) took part in *experiment 1*. They all had normal or corrected-to-normal vision and had normal color vision, as tested by the Ishihara plates (31). They had no history of neurological or eye-related disorders. They gave written informed consent before the experiment. The study was approved by the local ethics committee (no. 102772019RT009).

Apparatus and stimuli.

Experimental procedures were controlled by the Psychophysics Toolbox (32, 33) in MATLAB (MathWorks, Natick, MA). Stimuli were displayed on a 60-Hz LCD monitor (Eizo Corporation, Hakusan, Japan). The monitor has a spatial resolution of 1,920 × 1,200 pixels and a diagonal size of 61 cm (519.1 mm × 324.4 mm, which corresponds to 47° horizontally and 29° vertically at a viewing distance of 60 cm). The screen was calibrated with a spectrophotometer (I1 Basic Pro2; X-Rite, United States). Two blue dots (0.5° in radius) were separated horizontally by 12° remaining on the screen to serve as the saccade spots. Full-screen horizontal gratings (spatial frequency = 1.03 cycles/°) in the background were defined by either luminance or equiluminant red-green color and were flickering at a pattern-reversal rate of 7.5 Hz to elicit SSVEP responses. The "Stimuli" image in Fig. 1 shows the stimuli used in the experiment, and the "Analysis" image in Fig. 1 shows the stimulus cycles along the timescale. We employed horizontal gratings intended to reduce stimulus motion generated by horizontal saccades, as prior research has indicated the significance of this visual factor in saccadic suppression (34). The level of contrasts was defined as the maximally possible modulation achievable in Derrington–Krauskopf–Lennie (DKL) color space on the monitors (for a detailed description of the DKL color space, see the Appendix of Ref. 35). Both the luminance and color stimuli were presented against a gray background of our monitor: CIE xy = (0.26, 0.28, and 56.5 cd/m^2). The luminance flickering grating bars ranged from 52.9 to 59.6 cd/m^2 at 6% contrast and from 42.8 to 69.7 cd/m^2 at 24% contrast. For the red-green stimuli, luminance was held constant at 56.5 cd/m^2, whereas color was varied at 12% and 48% chromatic contrast between CIE xy = (0.27, 0.27) and (0.25, 0.28) and between CIE xy = (0.30, 0.26) and (0.22, 0.29), respectively. The root-mean-square cone contrast for the 12% and 48% red-green stimuli was 1.6% and 6.3%, respectively. These levels of contrast ensured that the

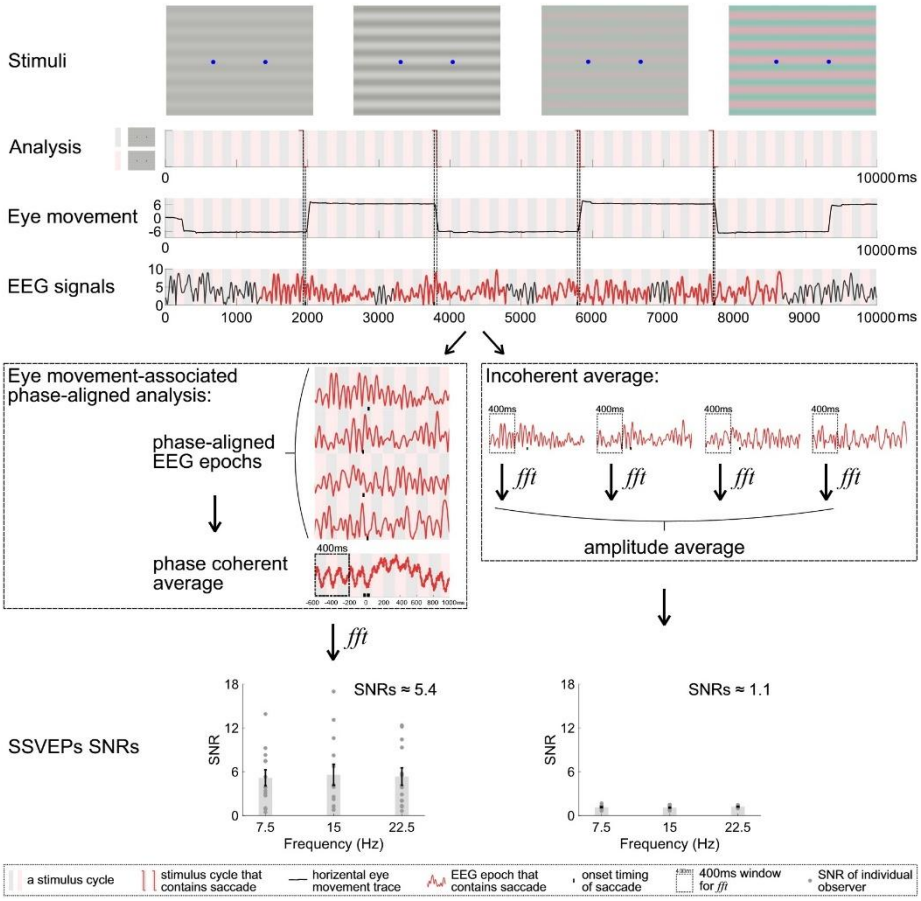

Figure 1. Stimuli: the schematic of the stimuli used in *experiments 1* and *2*: from *left* to *right*, low-contrast luminance, high-contrast luminance, low-contrast color, and high-contrast color. Analysis: the stimulus cycle along the timescale used in *experiments 1* and *2*. The gratings in the background were flickering in pattern reversal at a rate of 7.5 Hz to elicit steady-state visual evoked potential (SSVEP) responses; 1 cycle for the stimulus lasted ~133 ms. The red line indicates the stimulus cycle containing saccade onset. Eye movement: an example eye trace for the first 10 s of a trial. The *y*-axis is the horizontal eye position (°) relative to the center of the screen. EEG signals: the example EEG signals for the first 10 s of a trial after detrending. The red line indicates the extracted EEG epoch, and the black dot on the *x*-axis shows the onset timing of the saccade. The cut-out EEG epochs were phase aligned. Eye movement-associated phase-aligned analysis: coherent averaging of the phase-aligned EEG epochs. Incoherent average: application of short-term fast Fourier transformation (FFT) to each EEG epoch separately (e.g., see Ref. 26). SSVEPs SNRs: the signal-to-noise ratios (SNRs) of example EEG epoch from [−600 − 200] ms relative to the midpoint of the stimulus cycle that contains saccade. Filled circles are 13 individual observers. Coherent averaging of the phase-aligned EEG epochs increased the SNRs. Error bars indicate SEs across observers.

SSVEP amplitudes were roughly equivalent for luminance and color, as shown in Chen et al. (36).

Procedures.

We used the same experiment design as Chen et al. (26). Each trial lasted for 90 s. The experiment has 2 (type of stimuli: color vs. luminance) × 2 (contrast: low vs. high) = 4 conditions and has eight trials in total (2 trials for each condition). Observers were required to make horizontal saccades back and forth between two spots (Stimuli in Fig. 1), at a rate of once every 1–2 s. They made saccades voluntarily without any instruction during the experiment. The order of trials was randomized. Observers took a short break (at least 30 s) after each trial. They performed a 9-point calibration for the eye tracker at the beginning of the experiment and recalibrated it after each break.

Eye movement recordings and analyses.

Eye movements from the right eye were recorded with a video-based eye tracker (EyeLink Portable Duo; SR Research Ltd., Ottawa, ON, Canada), at a sampling rate of 1,000 Hz. The observer's head was rested on a chin rest to minimize

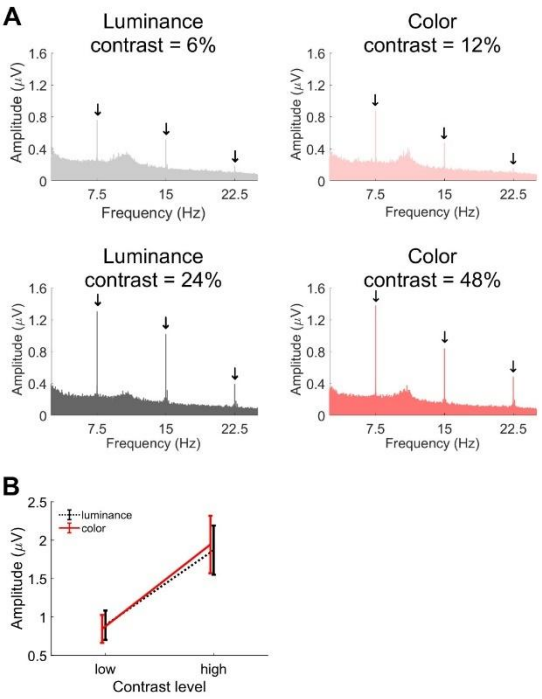

Figure 2. *A*: average amplitude spectra in 4 conditions over all observers ($N = 13$). Steady-state visual evoked potential (SSVEP) responses are elicited by luminance and color stimuli. Peak responses at 7.5 Hz and its harmonics (e.g., 15 and 22.5 Hz) are visible, as indicated by black arrows. *B*: SSVEP amplitudes in 4 conditions over all participants. Error bars indicate the SEs across observers. Overall, the color and luminance stimuli elicited comparable SSVEP responses.

head movements. Saccades were detected by the default algorithm from EyeLink, which uses a velocity threshold of 30°/s and an acceleration threshold of 8,000°/s^2. Customized scripts in MATLAB were used to analyze eye movement data. The analysis procedures were largely the same as in Chen et al. (26). To ensure that the analyzed saccades were larger saccades made toward the two saccade targets, we excluded any saccades with an amplitude smaller than 9° or larger than 15°. The example eye trace for the first 10 s of a trial is shown in the "Eye movement" image in Fig. 1. The mean saccade numbers (mean ± SE) in color and luminance trials were 52 ± 2 and 54 ± 2, whereas the saccade amplitude was 12.79 ± 0.21° and 12.78 ± 0.18°, respectively.

EEG recording and analyses.

We recorded EEG signals from three electrodes (O1, Oz, and O2) with a BrainAmp amplifier (Brain Products, Munich, Germany) sampling at 1,000 Hz. SSVEP responses are mainly confined to these three electrodes in paradigms similar to ours (26, 36–38). The ground electrode was placed at the AFz, and the online reference at the FCz. We kept electrode impedances below 10 kΩ. EEGLAB toolbox (39) and customized scripts in MATLAB were used to analyze EEGs. The EEG signals were first detrended by removing the linear fit (40). For the amplitude we used fast Fourier transformation (FFT; *fft*.m in MATLAB), and the frequency resolution differs when the length of the EEG epoch varies. In the analysis of 90-s EEG signals (e.g., Fig. 2), the frequency resolution was 1/90 = 0.011 Hz. When we utilized short-term FFT in a 400-ms EEG epoch (e.g., Fig. 5), the resulting frequency resolution was 1/0.4 = 2.5 Hz. For the EEG waveforms (e.g., Fig. 3), the signals were passed to a fourth-order low-pass Butterworth filter (41) with a cutoff frequency of 40 Hz (*ft_preproc_lowpassfilter*.m in the FieldTrip toolbox in MATLAB).

Eye movement-associated phase-aligned analysis.

To increase the signal-to-noise ratios (SNRs) of SSVEP responses during saccades, we performed eye movement-associated phase-aligned analysis to reduce the non-phase-locked EEG activities. Specifically, we coherently averaged the phase-aligned EEG epochs at the time of saccades in the time domain separately for each condition and each observer in the following steps. First, we pinpointed the onset time of the stimulus cycle within the whole trial (e.g., 90 s). For a pattern-reversal rate of 7.5 Hz, each cycle for the stimulus lasts ~133 ms. Next, we identified the timing of saccade onset within the stimulus cycle and used the midpoint of this cycle for alignment. Then, we extracted the EEG epochs from −600 to 1,000 ms relative to the midpoint timing of the stimulus cycle containing the saccade, resulting in 1,600-ms EEG epochs (as shown by the red line in the "EEG signals" image in Fig. 1). The EEG epoch was excluded if there was an overlap between it and the epochs before or after. After averaging these phase-aligned EEG epochs, we cut out short time windows (400 ms each, with a 1-ms step) and obtained the amplitude spectrum of the epoch by short-term FFT (as shown in the "Eye movement-associated phase-aligned analysis" image in Fig. 1). Then, the SSVEP SNRs were calculated

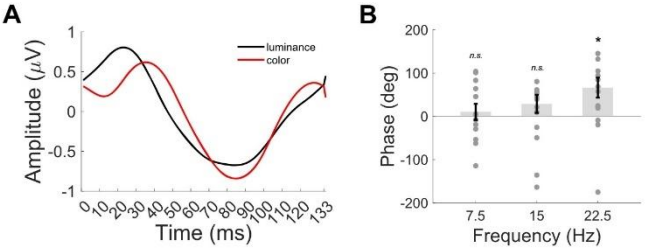

Figure 3. *A*: the average EEG waveforms for luminance and color stimuli within 1 stimulus cycle. *B*: the phase difference between luminance and color at the first 3 harmonics (i.e., 7.5, 15, and 22.5 Hz). Filled circles are 13 individual observers. Error bars indicate the SEs across observers. Significance of the phase difference from 0, established with 1-sample tests: n.s., $P > 0.05$, $*P < 0.05$.

by dividing the peak amplitude at the harmonics (e.g., 7.5 Hz) by the average amplitude of the two nearby bins (e.g., 5 and 10 Hz). The SSVEP amplitudes were calculated by subtracting the average amplitude of the two nearby bins from the peak amplitude at each harmonic and summing the amplitudes at the first three harmonics (i.e., 7.5, 15, and 22.5 Hz) for further analysis.

To illustrate the benefit of our phase alignment, the "SSVEPs SNRs" image in Fig. 1 shows the SNRs obtained from example EEG epochs from [−600 −200] ms relative to the midpoint of the stimulus cycle that contains saccades, displaying the SNRs of the harmonics resulting from eye movement-associated phase-aligned analysis on the left and SNRs from the EEG processing pipeline from Chen et al. (26) on the right. It was evident that the SNRs on the left were significantly higher than those on the right, though both were derived from a 400-ms window using short-term FFT. Compared with the incoherent averaging of the amplitude spectra (26), eye movement-associated phase-aligned analysis increases the SNRs at all harmonics. This improvement arises from the reduced noise achieved through coherent averaging of phase-consistent EEG epochs.

Experiment 2: Suppression of CRF

The purpose of *experiment 2* was to investigate the effect of saccades on SSVEPs to color and luminance stimuli at a number of contrast levels, i.e., on the SSVEP contrast response function (CRF).

Participants.

Fourteen observers (8 females and 6 males; mean age: 21.6 yr, age range: 18–25 yr) took part in *experiment 2*.

Apparatus and stimuli.

Experiment 2 used the same monitor as in *experiment 1*. The stimuli in *experiment 2* were largely the same as in *experiment 1* (Stimuli in Fig. 1), with the exception that more levels of contrast were tested. The contrast for luminance-defined stimuli was at 1.25%, 1.70%, 2.31%, 3.15%, 4.29%, 5.83%, 7.94%, 10.80%, 14.70%, and 20% (log spaced), and the contrast for color stimuli was 2.50%, 3.40%, 4.63%, 6.30%, 8.57%, 11.67%, 15.87%, 21.60%, 29.39%, and 40% (log spaced).

Procedures.

We manipulated the contrast of stimuli (i.e., 10 contrast levels) and type of flickering stimuli (i.e., color- or luminance-defined stimuli), which resulted in 20 combinations of conditions in total. Each observer accomplished 40 trials in total. Each trial lasted for 60 s. The procedures were the same as in *experiment 1*.

Eye movement recordings and analyses.

Eye movement recording and analysis were the same as in *experiment 1*. The mean saccade numbers (means ± SE) among 14 observers in color and luminance trials were 38 ± 2 and 37 ± 2, whereas the saccade amplitude was 11.74 ± 0.09° and 11.73 ± 0.10°, respectively.

EEG recording and analyses.

We recorded EEG signals from three electrodes (O1, Oz, and O2), using an actiCHamp amplifier (Brain Products) sampling at 1,000 Hz. The ground electrode was placed at the FPz and the online reference at the FCz. We kept electrode impedances below 10 kΩ. EEG analysis procedures were the same as in *experiment 1*.

Bayesian Statistical Analysis

In *experiment 1*, we conducted Bayesian statistical analysis with JASP (42) to evaluate the null hypothesis and identify the strength of the evidence. BF_{01} is the index of how strongly the data support the null hypothesis that there is no difference between the two conditions. Based on Lee and Wagenmakers (43), $BF_{01} > 3$ provides moderate evidence for H_0 and >10 provides strong evidence for H_0.

In *experiment 2*, we used a Bayesian model to analyze the contrast response function of SSVEP responses. *Experiment 2* measured SSVEPs elicited by color and luminance stimuli at a large number of contrast levels. The contrast response function was described with a modified version of the hyperbolic ratio function (44, 45):

$$R = R_{\max}\frac{c^n}{c_{50}^n + c^n} - R_0 \qquad (1)$$

In *Eq. 1*, R is the SSVEP amplitude, c is the contrast of stimulus, $R_{\max}$ is the asymptotic response to a high-contrast stimulus, n is the slope term, c_{50} is the contrast at the half-maximum response, and R_0 is a constant of the response. $R_{\max}$ changes reflect response gain adjustments, whereas c_{50} changes indicate alterations in contrast gain. We fitted this model to the normalized SSVEP amplitude at the time point of fixation (i.e., −400 ms relative to the midpoint of the stimulus cycle that contains the saccade) and saccade (i.e., 200 ms after the midpoint of the stimulus cycle that contains the saccade) in each contrast for color and luminance stimuli. The data from all subjects and conditions were fit with a Bayesian model. We used Gibbs sampling to estimate the posterior probability distribution of the unknown parameters based on the observed data. JAGS package was used for Gibbs sampling to implement the model (42). The model was sampled in one chain and contained 20,000 iterations for both color and luminance stimuli analyses, respectively. The 99% highest density interval (99% HDI) was computed from the samples for the variables of interest and differences across conditions. These 99% HDIs were utilized to estimate the credible ranges for the values and differences.

RESULTS

Experiment 1: SSVEP Responses to Color and Luminance

Experiment 1 recorded SSVEPs while the observer made saccadic eye movements. There were 4 conditions in *experiment 1*, which were 2 (type of stimuli: color vs. luminance) × 2 (contrast: low vs. high). We adopted a single-trial design, where each trial for one condition lasted for 90 s. To access the overall SSVEP responses, we did a fast Fourier transformation on the whole 90-s EEG signals in four conditions of all observers. Figure 2*A* displays the grand average spectra. We can see the peak response amplitude in 7.5 Hz and its harmonics (e.g., 15 and 22.5 Hz) for both the color- and luminance-defined stimuli. Next, we summed SSVEP amplitudes

at 7.5, 15, and 22.5 Hz for each condition, as Fig. 2*B* shows. The high-contrast stimuli elicited significantly higher SSVEP responses than low-contrast stimuli [$F(1,12) = 26.66$, $P = 2.356e{-}04$, $\eta_p^2 = 0.690$]. The SSVEP responses elicited by color and luminance were comparable [$F(1,12) = 0.003$, $P = 0.956$, $\eta_p^2 = 0.0001$].

It is known that the response latency of parvocellular neurons is delayed compared with that of magnocellular neurons, by no more than ~10 ms in the LGN and less in V1, by ~5 ms (46–48). If SSVEP responses to color and luminance can really segregate the two pathways, we would also expect that color SSVEPs show delayed visual response latency compared with luminance. We first visualized the waveforms of luminance and color response. We classified all trials into luminance and color subsets and then averaged the EEG signals in the time domain. Next, we segmented the 90-s EEG signals into 133-ms (i.e., the duration of 1 cycle for 7.5 Hz) epochs, resulting in 675 epochs. After separately averaging all epochs of luminance and color, a slight temporal offset can be observed, as depicted in Fig. 3*A*. In addition to waveforms, we extracted the phase information of the first three harmonics (i.e., 7.5, 15, and 22.5 Hz) by applying FFT to the 90-s EEG signals in each individual trial. We calculated the phase difference between luminance and color and conducted a one-sample test on it (*circ_dist*.m and *circ_mtest*.m in the circular statistics toolbox in MATLAB), as shown in Fig. 3*B*. The average phase differences at 7.5, 15, and 22.5 Hz are 10.57°, 29.02°, and 66.48°, corresponding to 3.91 ms, 5.37 ms, and 6.16 ms in time, respectively. For 7.5 and 15 Hz, the phase difference was not significantly different from 0, with a 95% confidence interval of [−39.19, 60.32°] and [−14.89, 72.94°], respectively. At 22.5 Hz, the phase difference was significantly different, with a 95% confidence interval of [24.84, 108.11°]. Therefore, the phase at 22.5 Hz showed a delay for color compared with luminance. This indicates that SSVEP signals from the two types of stimuli can indeed segregate the parvocellular and magnocellular pathways.

Experiment 1: Comparable Suppression on SSVEPs Elicited by Color and Luminance

To indicate how saccades modulate the SSVEP responses, we computed SSVEP power in short time windows (400 ms) centered at variable latencies relative to the midpoint of the stimulus cycle that contains saccade. Figure 4*A* displays the

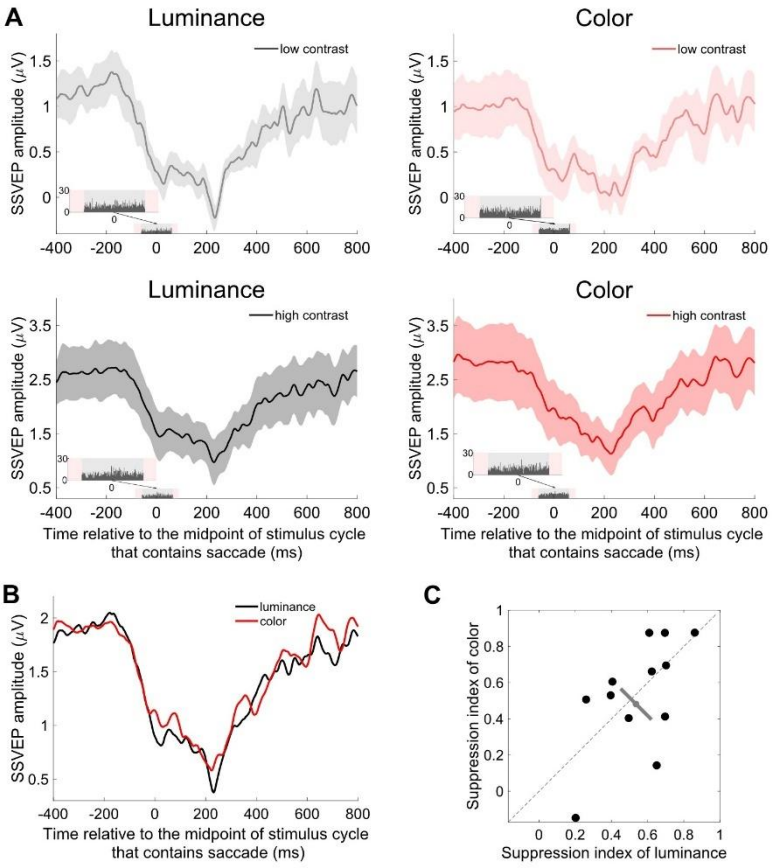

Figure 4. *A*: the grand average of steady-state visual evoked potential (SSVEP) amplitudes at different time points relative to the midpoint of the stimulus cycle that contains saccade in 4 conditions. Shaded areas indicate SE across all observers. *Insets*: *x*-axis corresponds to main image, and *y*-axis indicates the number of saccade onset times for all observers relative to *time 0*. These histograms showed that the onset times were evenly spread out and confined in 1 stimulus cycle. The background in gray and light red indicates the stimulus phase. *B*: average SSVEP amplitude of color and luminance at different time points relative to the midpoint of the stimulus cycle that contains saccade among all observers. The data from conditions with different contrasts were aggregated. *C*: the index of suppression effect for color and luminance in SSVEPs. Filled circles are 13 individual observers. All observers fell along the diagonal line, indicating that the SSVEP suppression effect is comparable in color and luminance. The gray line shows the average value and the 95% confidence interval.

time course of SSVEP responses in four conditions. We can see that saccades did reduce SSVEP responses strongly among all four conditions. As the low and high contrast had a similar suppression effect, we combined the two levels of contrast in further analyses. Figure 4*B* shows the average SSVEP amplitudes of color and luminance at different time points relative to the midpoint of the stimulus cycle that contains the saccade among all observers. The SSVEP response pattern is largely similar in color and luminance.

Previously, SSVEP measurements revealed that the maximum suppression occurred ~150 ms after saccade onset, because of the neural processing delay in transmitting visual stimuli to V1 activity (26). In our eye movement-associated phase-aligned analysis, we used one stimulus cycle (i.e., ~133 ms) that contains the saccade onset for phase alignment, resulting in a jitter where the saccade onset times were evenly spread (as shown in Fig. 4*A*, *insets*). In addition, the monitor we used differs from that in Chen et al. (26), which may introduce an uncertain delay in presenting the visual stimulus. Consequently, the maximum suppression for SSVEP responses in our time course occurred around 200 ms relative to the midpoint of the stimulus cycle that contains the saccade. In light of this, we indexed the saccadic suppression effect by evaluating SSVEP responses at two specific time points: the fixation SSVEPs at −400 ms relative to the midpoint of the stimulus cycle that contains saccade and the saccade SSVEPs at 200 ms after the midpoint of the stimulus cycle that contains saccade. Figure 4*C* shows the index of suppression effect, which was calculated by taking the amplitude difference between the two time points and divided by the amplitude at fixation. Each filled circle represents data of an individual observer, with the *x*-axis representing the suppression index of luminance and the *y*-axis the suppression index of color. The data points fell along the diagonal line, indicating that the SSVEP suppression effect is comparable on color and luminance [$t(12) = 0.57$, $P = 0.583$, Cohen's $d = 0.16$]. Bayesian factor analysis indicated that there is moderate evidence supporting the null hypothesis ($BF_{01} = 3.13$, the prior distribution is a zero-centered Cauchy distribution with a default scale parameter of $r = 0.707$). Therefore, the result suggests that saccadic eye movements suppress the processing of both color and luminance in the early visual cortex as measured by SSVEPs.

Could the suppression effect be the result of SSVEP response reduction due to the saccade-related noise? Unlike the SSVEP responses observed at the stimulation frequency and its harmonics (e.g., 7.5 and 15 Hz), EEG signals at broadband frequencies (e.g., 5 and 10 Hz) encompass saccade-related EEG artifacts, lambda response, and visual reafferent responses. By calculating the amplitude difference between the fixation and saccade epochs, we assessed the suppression effect at the first three harmonics (i.e., 7.5, 15, and 22.5 Hz) and their nearby bins (i.e., 5 and 10 Hz, 12.5 and 15 Hz, 17.5 and 25 Hz) and averaged each pair of nearby bins. Figure 5 shows the amplitude difference between fixation SSVEPs and saccade SSVEPs. Each filled circle represents data of an individual observer, with the *x*-axis representing the suppression effect of the harmonic and the *y*-axis the suppression effect of its nearby bins. Most of the data points fell below the diagonal line, indicating that the suppression effect at harmonics is stronger than that at the nearby bins. These results suggest that the impact of saccade-related broadband noise on the SSVEP suppression effect is limited. Therefore, the observed suppression effect in SSVEP responses cannot be attributed to the saccade-related EEG noise.

Experiment 2: Saccades Reduce Response Gain in SSVEP Contrast Response Function to Color and Luminance

Experiment 2 measured SSVEPs in response to color and luminance stimuli at various contrast levels. Similar to *experiment 1*, we used a single-trial design where each trial for a condition lasted for 60 s while observers made saccadic eye movements voluntarily. The aim of *experiment 2* was to investigate the effect of saccades on the SSVEP contrast response function. We employed a Bayesian model for data analysis, using a uniform distribution as the prior for all parameters. Initially, we normalized the SSVEP amplitudes by

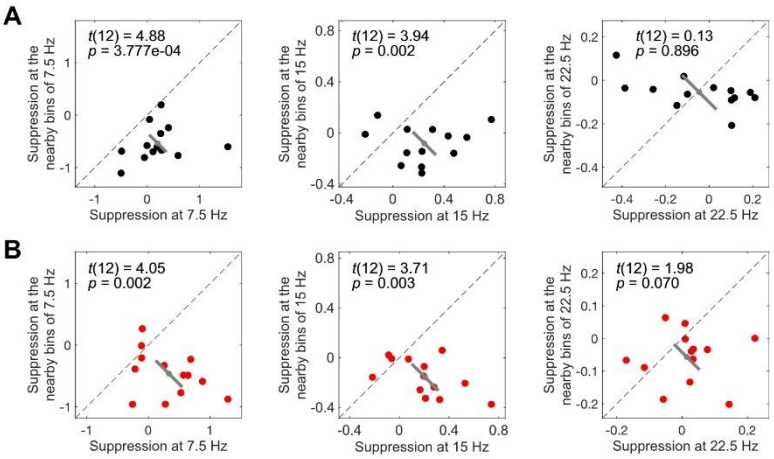

Figure 5. The suppression effect at the first 3 harmonics (i.e., 7.5, 15, and 22.5 Hz) and their nearby bins (i.e., 5 and 10 Hz, 12.5 and 15 Hz, 17.5 and 25 Hz) for luminance (*A*) and color (*B*). Filled circles are 13 individual observers. *x*-Axis represents the suppression effect of the harmonic and *y*-axis the suppression effect of its nearby bins. Most observers fell below the diagonal line, indicating that the suppression effect at the harmonic is stronger than that at nearby bins. The gray line shows the average value and the 95% confidence interval.

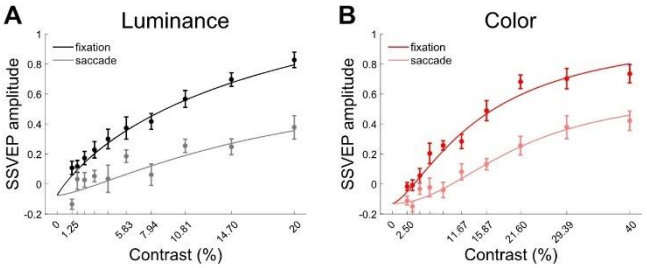

Figure 6. The normalized steady-state visual evoked potential (SSVEP) amplitudes as a function of contrast, at the time of fixation or saccade. The curves were fit with contrast response functions. Saccades suppress the contrast responses for both luminance (*A*) and color (*B*). Error bars show the SEs across observers. Compared with fixation, the SSVEP amplitudes at saccade are scaled down, rather than shifted to the right, indicating that the saccades reduce response gain but do not affect contrast gain. This suppression effect is similar for both color and luminance.

the maximum response in each observer to reduce between-observer variability in the data. Subsequently, the fitting was performed using the data from all 14 observers. Since we normalized the SSVEP amplitudes, and given that the mean SSVEP responses across all observers in the fixation epoch were approximately two times higher than in the saccade epoch, we set the prior scaling of $R_{\max}$ to [0.0001 1.5] for fixation and [0.0001 0.75] for saccade, for both luminance and color conditions, whereas the prior scaling of c_{50} was set to [0.0001 1] for all four conditions.

Figure 6 shows the normalized SSVEP amplitudes and fitting curves for all conditions. These curves fit our data satisfactorily, accounting for 93.32% of the variance on average. The parameters for fitting the respective curves are for luminance at fixation: $n = 1.06$, $c_{50} = 0.13$, $R_{\max} = 1.33$, $R_0 = 0.04$; for luminance at saccade: $n = 1.69$, $c_{50} = 0.14$, $R_{max} = 0.57$, $R_0 = 0.04$; for color at fixation: $n = 1.54$, $c_{50} = 0.15$ $R_{\max} = 1.09$, $R_0 = 0.10$; for color at saccade: $n = 2.49$, $c_{50} = 0.19$, $R_{\max} = 0.62$, $R_0 = 0.10$.

Figure 7, *A* and *B*, show the Bayesian estimated posterior distributions for c_{50} and $R_{\max}$ at fixation and saccade on luminance and color, respectively. We computed the distribution of differences by subtracting c_{50} and $R_{\max}$ values between fixation and saccade, as depicted in Fig. 7, *C* and *D*. The horizontal bar indicates the 99% HDI. For c_{50} on luminance and color, both of the HDIs for the difference contain zero, indicating there is no significant difference in contrast gain between fixation and saccade. However, for $R_{\max}$ on luminance and color, both of the 99% HDIs for the difference fall well above zero, indicating that the response gain is significantly larger for fixation than for saccade ($P < 0.01$). Therefore, these results indicate that saccades reduce response gain but do not affect contrast gain, and the

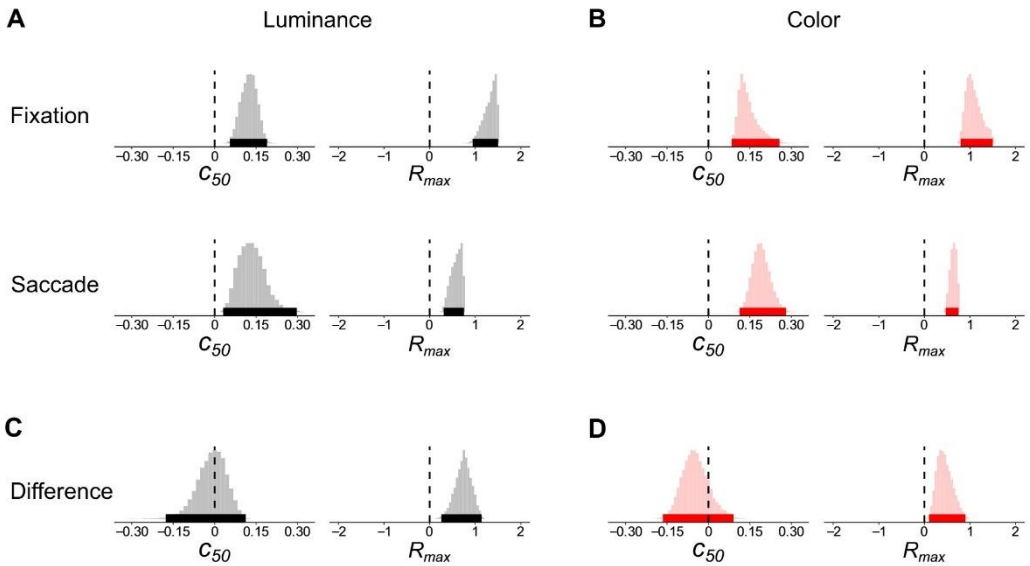

Figure 7. *A* and *B*: the Bayesian estimated posterior probability distributions of contrast at the half-maximum response (c_{50}, *left*) and asymptotic response to a high-contrast stimulus ($R_{\max}$, *right*) in fixation and saccade conditions on luminance (*A*) and color (*B*). *C* and *D*: the Bayesian estimated posterior probability distributions of the mean difference between fixation and saccade (i.e., fixation minus saccade condition) of c_{50} and $R_{\max}$ on luminance (*C*) and color (*D*). The horizontal bar indicates the 99% highest density interval (99% HDI). The *x*-value for the black dashed line is 0.

suppression effect on response gain is similar for both color and luminance.

DISCUSSION

In the present study, two experiments were conducted on human participants to investigate saccadic suppression. This was achieved by recording SSVEPs in response to chromatic and luminance stimuli. Our findings revealed a comparable reduction in SSVEP amplitudes during saccades for both types of stimuli, indicating that saccades have a similar impact on the visual processing of color and luminance information. The SSVEP amplitude reduction is not due to artifacts or visual reafferent response, as the amplitudes of broadband noise increased during saccades whereas the amplitudes at SSVEP harmonics decreased. We also calculated the baseline-corrected SSVEP responses at the stimulation frequency to mitigate the influence of the broadband noise. Additionally, SSVEPs were measured at various contrast levels during saccades, and the contrast response function was modeled. The results demonstrated that saccades primarily reduce the response gain while leaving the contrast gain unaffected, irrespective of the type of stimuli (chromatic or luminance). These observations provide compelling evidence suggesting that saccadic eye movements exert a suppressive effect on both the parvocellular and magnocellular pathways within the early visual cortex of humans.

Previous physiological studies have reported inconsistent results regarding the extent to which saccades suppress color processing. Investigations conducted on nonhuman primates with single-neuron recordings have shown a stronger saccadic suppression of luminance compared with color in early visual areas like the LGN (21–23). However, in V1 neurons similar microsaccadic suppression of luminance and color has been observed (13). Human fMRI studies have indicated comparable suppression effects for color and luminance in regions such as the LGN, V1, and V2 (19, 20). It is worth considering that this discrepancy may stem from the limitations of the fMRI technique because its low temporal resolution makes it less suitable for investigating saccadic suppression. To address this issue, the present study employed the SSVEP technique, which offers a higher temporal resolution that allows us to trace the temporal dynamics of neural activity during saccades in humans. Our results consistently demonstrated comparable saccadic suppressions for both color and luminance stimuli. Consequently, the underlying reason for the previous discrepancy between human fMRI results and single-neuron findings in nonhuman primates warrants further examination. One possibility is that there are species-specific differences in saccadic suppression, as previously observed by Klingenhoefer and Krekelberg (49). However, it is important to note that comparable suppression effects between color and luminance have been observed in nonhuman primates within the frontal eye field (25). These findings emphasize the necessity of reevaluating the similarities and differences between humans and nonhuman primates in the field of visual neuroscience.

Previous psychophysical studies have reported that either saccadic suppression does not occur for color stimuli or, at the very least, the effect is significantly weaker for color compared with luminance stimuli (8–18). However, if the present result, along with previous fMRI findings (19, 20), suggests that the suppression effect is comparable for both color and luminance in the early visual cortex, then the question arises: where does the difference in perception originate? Notably, previous fMRI studies have examined neural activities in higher visual areas such as V5 and MT, revealing a stronger saccadic suppression effect for luminance-defined stimuli compared with color-defined stimuli (19, 20). This observation may indicate that saccades exert a more pronounced suppression of luminance processing in the higher-level visual cortex beyond V1/V2. However, because of the limited temporal resolution of fMRI, further investigations are warranted to delve deeper into this matter. Alternatively, Chen and Hafed (24) showed that visual motor neurons in the superior colliculus had a spatial frequency-specific saccadic suppression effect, similar to perception. Thus, the superior colliculus could also be a neural locus for the perceptual effect. Further studies could use color stimuli to test this hypothesis.

The most popular view for saccadic suppression is that it is caused by an active suppressive signal originating from premotor areas, including corollary discharge signals associated with saccadic eye movements (for review, see Ref. 4). However, there is an alternative view that saccadic suppression is a visual phenomenon due to masking (see Ref. 50 for a review). The present study did not intend to argue about the two hypotheses, but it is interesting to point out the findings in a recent study by Idrees et al. (34). They showed that selective suppression of low-spatial frequency luminance stimuli can be observed even when no saccade was required and only the visual flow was presented to the observer. Furthermore, the selective suppression effect can be easily violated by using a fine-texture background. Their result indicates that the selective suppression of low-spatial frequency information reported in the literature (e.g., see Refs. 8, 51) is probably a visual phenomenon and does not provide enough evidence for the magnocellular suppression hypothesis. This is consistent with our main message in the present study that, at least in the early visual cortex, there is no evidence for selective suppression of the magnocellular pathway.

The findings from *experiment 2*, showing a reduction in response gain but no impact on contrast gain during saccades, provide valuable insights into the computational mechanisms underlying saccadic suppression. By employing contrast response function modeling, it becomes possible to differentiate between two potential mechanisms of top-down modulation: an additive mechanism affecting contrast gain and a multiplicative mechanism affecting response gain. For instance, Li et al. (52) utilized contrast response functions to compare the effects of overt presaccadic and covert spatial attention on perceptual sensitivities. They observed that presaccadic attention exclusively induced changes in response gain, whereas covert spatial attention resulted in a combination of response gain and contrast gain changes. Our results mirror this effect, as we found that saccades solely affected response gain without impacting contrast gain. These findings are in line with previous studies conducted with nonhuman primates (28),

where neural activities were recorded in the SC during microsaccades, which share similar underlying mechanisms with saccades (53, 54). Chen et al. (28) reported a significant reduction in response gain and no substantial change in contrast gain during microsaccades. These results concur to support the notion that saccadic eye movements modulate neural activities through a multiplicative mechanism.

Since we used a spectrophotometer to measure luminance and did not access equiluminance psychophysically for individual observers, there may be residual luminance artifacts in our large-field equiluminant stimuli. One might raise the question of whether these potential luminance artifacts could account for our findings. Specifically, one could argue that the comparability of the saccadic suppression effect to color and luminance stimuli may be attributed to the luminance artifacts present in the equiluminant color stimuli. However, this explanation is unlikely for two reasons. First, it is widely recognized that humans exhibit a greater sensitivity to color compared with luminance (see Refs. 55, 56). Our measures of SSVEP contrast response indicate that even a luminance artifact of 5% contrast would be invisible to luminance-based processing. Second, our stimuli closely resemble those used by Chen et al. (36). In their study, Chen et al. (36) demonstrated that smooth pursuit eye movements, as opposed to fixation, enhance SSVEPs to color stimuli but have no effect on SSVEPs to luminance stimuli. This result indicates that such stimuli sufficiently isolate color and luminance to reveal dissociation effects, if present. Consequently, it is unlikely that the residual luminance in the stimuli can account for the findings observed in our study.

In our SSVEP analysis pipeline, we employed an innovative method, which we named "eye movement-associated phase-aligned analysis." It is an improved version of the analysis pipeline presented in Chen et al. (26) and has resulted in significantly enhanced SNRs. Previously, Chen et al. (26) employed incoherent averaging of amplitude spectra obtained from short-term FFT to calculate the time course of SSVEP responses during saccades. In eye movement-associated phase-aligned analysis, we use the saccade onset timing to identify the midpoint of stimulus cycle timing for extracting phase-aligned EEG epochs. This ensures that the saccade onset timing is confined within one stimulus cycle, as shown in Fig. 4*A*, *insets*, where they are evenly distributed within the cycle. After coherently averaging the phase-aligned EEG epochs, the non-phase-locked noise was reduced, resulting in increased SNRs and SSVEP amplitudes. Eye movement-associated phase-aligned analysis is based on the concept of coherently averaging SSVEP signals to minimize noise (e.g., see Refs. 57–62). Here, we applied this concept to examine SSVEP responses during eye movements. Previous studies did not implement phase-aligned analysis while simultaneously recording eye movement and SSVEPs (e.g., see Refs. 26, 36), presumably because of the inherent uncertainty in the timing of eye movements relative to the stimulus phase. Here, the issue was addressed by using eye movement to precisely identify the stimulus cycle for phase alignment, enabling the capture of SSVEP responses of higher SNRs during eye movement events.

The present study provides the basis for several lines of future work. For instance, it would be interesting to test the effect of saccades on luminance stimuli with various spatial frequencies, given that previous psychophysical studies selectively showed saccadic suppression for low-spatial frequency stimuli (e.g., see Refs. 8, 51). It is also worth testing whether there is a correlation between the suppression effect obtained in SSVEP and the suppression effect in perception, by measuring the saccadic suppression effect using both the SSVEP paradigm as in the present study and the perceptual paradigm (such as in Refs. 17, 18).

To summarize, the present study provides strong evidence supporting that saccades suppress both the parvocellular and magnocellular pathways in the early visual cortex of humans. Our results further suggest that saccadic eye movements modulate neural activities, in both the parvocellular and magnocellular pathways, through a multiplicative mechanism.

DATA AVAILABILITY

Data will be made available upon reasonable request.

ACKNOWLEDGMENTS

During the preparation of this work, the authors used ChatGPT (OpenAI, Inc., https://openai.com/) to improve readability and language. After using this tool, the authors reviewed and edited the content as needed and took full responsibility for the content of the publication.

GRANTS

J.C. was supported by the National Natural Science Foundation of China (No. 31900758) and a research project of the Shanghai University of Sport (A1-3G01-23-0008-25). K.R.G. was supported by the Deutsche Forschungsgemeinschaft (DFG, German Research Foundation; project number 222641018—SFB/TRR 135 Project A1) and the European Research Council Advanced Grant Color3.0 project number 884116.

DISCLOSURES

No conflicts of interest, financial or otherwise, are declared by the authors.

AUTHOR CONTRIBUTIONS

M.V., K.R.G., and J.C. conceived and designed research; Y.Z. performed experiments; Y.Z. analyzed data; Y.Z., M.V., K.R.G., and J.C. interpreted results of experiments; Y.Z. prepared figures; Y.Z. drafted manuscript; Y.Z., M.V., K.R.G., and J.C. edited and revised manuscript; Y.Z., M.V., K.R.G., and J.C. approved final version of manuscript.

REFERENCES

1. **Goettker A**, **Gegenfurtner KR.** A change in perspective: the interaction of saccadic and pursuit eye movements in oculomotor control and perception. *Vision Res* 188: 283–296, 2021. doi:10.1016/j.visres.2021.08.004.
2. **Grünert U**, **Martin PR.** Cell types and cell circuits in human and non-human primate retina. *Prog Retin Eye Res* 78: 100844, 2020. doi:10.1016/j.preteyeres.2020.100844.
3. **Østerberg G.** Topography of the layer of rods and cones in the human retina. *Acta Ophthalmol* 13: 6–97, 1935.

4. **Binda P**, **Morrone MC.** Vision during saccadic eye movements. *Annu Rev Vis Sci* 4: 193–213, 2018. doi:10.1146/annurev-vision-091517-034317.
5. **Ibbotson M**, **Krekelberg B.** Visual perception and saccadic eye movements. *Curr Opin Neurobiol* 21: 553–558, 2011. doi:10.1016/j.conb.2011.05.012.
6. **Latour PL.** Visual threshold during eye movements. *Vision Res* 2: 261–262, 1962. doi:10.1016/0042-6989(62)90031-7.
7. **Sommer MA**, **Wurtz RH.** Brain circuits for the internal monitoring of movements. *Annu Rev Neurosci* 31: 317–338, 2008. doi:10.1146/annurev.neuro.31.060407.125627.
8. **Burr DC**, **Morrone MC**, **Ross J.** Selective suppression of the magnocellular visual pathway during saccadic eye movements. *Nature* 371: 511–513, 1994. doi:10.1038/371511a0.
9. **Anand S**, **Bridgeman B.** An unbiased measure of the contributions of chroma and luminance to saccadic suppression of displacement. *Exp Brain Res* 142: 335–341, 2002. doi:10.1007/s00221-001-0937-0.
10. **Bridgeman B**, **Macknik SL.** Saccadic suppression relies on luminance information. *Psychol Res* 58: 163–168, 1995. doi:10.1007/BF00419631.
11. **Bruno A**, **Brambati SM**, **Perani D**, **Morrone MC.** Development of saccadic suppression in children. *J Neurophysiol* 96: 1011–1017, 2006. doi:10.1152/jn.01179.2005.
12. **Diamond MR**, **Ross J**, **Morrone MC.** Extraretinal control of saccadic suppression. *J Neurosci* 20: 3449–3455, 2000. doi:10.1523/JNEUROSCI.20-09-03449.2000.
13. **Hass CA**, **Horwitz GD.** Effects of microsaccades on contrast detection and V1 responses in macaques. *J Vis* 11: 1–17, 2011. doi:10.1167/11.3.3.
14. **Knöll J**, **Binda P**, **Morrone MC**, **Bremmer F.** Spatiotemporal profile of peri-saccadic contrast sensitivity. *J Vis* 11: 15, 2011. doi:10.1167/11.14.15.
15. **Ross J**, **Morrone MC**, **Goldberg ME**, **Burr DC.** Changes in visual perception at the time of saccades. *Trends Neurosci* 24: 113–121, 2001. doi:10.1016/S0166-2236(00)01685-4.
16. **Uchikawa K**, **Sato M.** Saccadic suppression of achromatic and chromatic responses measured by increment-threshold spectral sensitivity. *J Opt Soc Am A Opt Image Sci Vis* 12: 661–666, 1995. doi:10.1364/JOSAA.12.000661.
17. **Braun DI**, **Schütz AC**, **Gegenfurtner KR.** Visual sensitivity for luminance and chromatic stimuli during the execution of smooth pursuit and saccadic eye movements. *Vision Res* 136: 57–69, 2017. doi:10.1016/j.visres.2017.05.008.
18. **Braun DI**, **Schütz AC**, **Gegenfurtner KR.** Age effects on saccadic suppression of luminance and color. *J Vis* 21: 11, 2021. doi:10.1167/jov.21.6.11.
19. **Kleiser R**, **Seitz RJ**, **Krekelberg B.** Neural correlates of saccadic suppression in humans. *Curr Biol* 14: 386–390, 2004. doi:10.1016/j.cub.2004.02.036.
20. **Sylvester R**, **Haynes JD**, **Rees G.** Saccades differentially modulate human LGN and V1 responses in the presence and absence of visual stimulation. *Curr Biol* 15: 37–41, 2005. doi:10.1016/j.cub.2004.12.061.
21. **Bartlett JR**, **Doty RW**, **Lee BB**, **Sakakura H.** Influence of saccadic eye movements on geniculostriate excitability in normal monkeys. *Exp Brain Res* 25: 487–509, 1976. doi:10.1007/BF00239783.
22. **Reppas JB**, **Usrey WM**, **Reid RC.** Saccadic eye movements modulate visual responses in the lateral geniculate nucleus. *Neuron* 35: 961–974, 2002. doi:10.1016/S0896-6273(02)00823-1.
23. **Royal DW**, **Sáry G**, **Schall JD**, **Casagrande VA.** Correlates of motor planning and postsaccadic fixation in the macaque monkey lateral geniculate nucleus. *Exp Brain Res* 168: 62–75, 2006. doi:10.1007/s00221-005-0093-z.
24. **Chen CY**, **Hafed ZM.** A neural locus for spatial-frequency specific saccadic suppression in visual-motor neurons of the primate superior colliculus. *J Neurophysiol* 117: 1657–1673, 2017. doi:10.1152/jn.00911.2016.
25. **Krock RM**, **Moore T.** Visual sensitivity of frontal eye field neurons during the preparation of saccadic eye movements. *J Neurophysiol* 116: 2882–2891, 2016. doi:10.1152/jn.01140.2015.
26. **Chen J**, **Valsecchi M**, **Gegenfurtner KR.** Saccadic suppression measured by steady-state visual evoked potentials. *J Neurophysiol* 122: 251–258, 2019. doi:10.1152/jn.00712.2018.
27. **Norcia AM**, **Appelbaum LG**, **Ales JM**, **Cottereau BR**, **Rossion B.** The steady-state visual evoked potential in vision research: a review. *J Vis* 15: 4, 2015. doi:10.1167/15.6.4.
28. **Chen CY**, **Ignashchenkova A**, **Thier P**, **Hafed ZM.** Neuronal response gain enhancement prior to microsaccades. *Curr Biol* 25: 2065–2074, 2015. doi:10.1016/j.cub.2015.06.022.
29. **Guez J**, **Morris AP**, **Krekelberg B.** Intrasaccadic suppression is dominated by reduced detector gain. *J Vis* 13: 4, 2013. doi:10.1167/13.8.4.
30. **Watson T**, **Krekelberg B.** An equivalent noise investigation of saccadic suppression. *J Neurosci* 31: 6535–6541, 2011. doi:10.1523/JNEUROSCI.6255-10.2011.
31. **Ishihara S.** *Ishihara's Tests for Color Deficiency*. Tokyo: Kanehara Trading, 2004.
32. **Brainard DH.** The Psychophysics Toolbox. *Spat Vis* 10: 433–436, 1997.
33. **Kleiner M**, **Brainard D**, **Pelli D**, **Ingling A**, **Murray R**, **Broussard C.** What's new in psychtoolbox-3. *Perception* 36: 1–16, 2007.
34. **Idrees S**, **Baumann MP**, **Franke F**, **Münch TA**, **Hafed ZM.** Perceptual saccadic suppression starts in the retina. *Nat Commun* 11: 1977, 2020. doi:10.1038/s41467-020-15890-w.
35. **Hansen T**, **Gegenfurtner KR.** Higher order color mechanisms: evidence from noise-masking experiments in cone contrast space. *J Vis* 13: 26, 2013. doi:10.1167/13.1.26.
36. **Chen J**, **Valsecchi M**, **Gegenfurtner KR.** Enhanced brain responses to color during smooth-pursuit eye movements. *J Neurophysiol* 118: 749–754, 2017. doi:10.1152/jn.00208.2017.
37. **Chen J**, **Valsecchi M**, **Gegenfurtner KR.** Attention is allocated closely ahead of the target during smooth pursuit eye movements: evidence from EEG frequency tagging. *Neuropsychologia* 102: 206–216, 2017. doi:10.1016/j.neuropsychologia.2017.06.024.
38. **Chen J**, **Gegenfurtner KR.** Electrophysiological evidence for higher-level chromatic mechanisms in humans. *J Vis* 21: 12, 2021. doi:10.1167/jov.21.8.12.
39. **Delorme A**, **Makeig S.** EEGLAB: an open source toolbox for analysis of single-trial EEG dynamics including independent component analysis. *J Neurosci Methods* 134: 9–21, 2004. doi:10.1016/j.jneumeth.2003.10.009.
40. **Bach M**, **Meigen T.** Do's and don'ts in Fourier analysis of steady-state potentials. *Doc Ophthalmol* 99: 69–82, 1999. doi:10.1023/A:1002648202420.
41. **Butterworth S.** On the theory of filter amplifiers. *Wirel Eng* 7: 536–541, 1930.
42. **Plummer M.** JAGS: a program for analysis of Bayesian graphical models using Gibbs sampling. *Proceedings of the 3rd International Workshop on Distributed Statistical Computing (DSC 2003)*, Vienna, 20–22 March 2003, 1–10.
43. **Lee MD**, **Wagenmakers EJ.** *Bayesian Cognitive Modeling: a Practical Course* (1st ed.). Cambridge, UK: Cambridge University Press, 2014.
44. **Naka KI**, **Rushton WA.** S-potentials from luminosity units in the retina of fish (Cyprinidae). *J Physiol* 185: 587–599, 1966. doi:10.1113/jphysiol.1966.sp008003.
45. **Solomon SG**, **Peirce JW**, **Dhruv NT**, **Lennie P.** Profound contrast adaptation early in the visual pathway. *Neuron* 42: 155–162, 2004. doi:10.1016/S0896-6273(04)00178-3.
46. **Kaplan E**, **Shapley RM.** X and Y cells in the lateral geniculate nucleus of macaque monkeys. *J Physiol* 330: 125–143, 1982. doi:10.1113/jphysiol.1982.sp014333.
47. **Maunsell JH**, **Gibson JR.** Visual response latencies in striate cortex of the macaque monkey. *J Neurophysiol* 68: 1332–1344, 1992. doi:10.1152/jn.1992.68.4.1332.
48. **Maunsell JH**, **Ghose GM**, **Assad JA**, **McAdams CJ**, **Boudreau CE**, **Noerager BD.** Visual response latencies of magnocellular and parvocellular LGN neurons in macaque monkeys. *Vis Neurosci* 16: 1–14, 1999. doi:10.1017/S0952523899156177.
49. **Klingenhoefer S**, **Krekelberg B.** Perisaccadic visual perception. *J Vis* 17: 16, 2017. doi:10.1167/17.9.16.
50. **Castet E**, **Jeanjean S**, **Masson GS.** 'Saccadic suppression'—no need for an active extra-retinal mechanism. *Trends Neurosci* 24: 316–318, 2001. doi:10.1016/s0166-2236(00)01828-2.
51. **Volkmann FC**, **Riggs LA**, **White KD**, **Moore RK.** Contrast sensitivity during saccadic eye movements. *Vision Res* 18: 1193–1199, 1978. doi:10.1016/0042-6989(78)90104-9.

52. **Li HH**, **Pan J**, **Carrasco M.** Different computations underlie overt presaccadic and covert spatial attention. *Nat Hum Behav* 5: 1418–1431, 2021. doi:10.1038/s41562-021-01099-4.
53. **Hafed ZM.** Mechanisms for generating and compensating for the smallest possible saccades. *Eur J Neurosci* 33: 2101–2113, 2011. doi:10.1111/j.1460-9568.2011.07694.x.
54. **Hafed ZM**, **Goffart L**, **Krauzlis RJ.** A neural mechanism for microsaccade generation in the primate superior colliculus. *Science* 323: 940–943, 2009. doi:10.1126/science.1166112.
55. **Chaparro A**, **Stromeyer CF**, **Huang EP**, **Kronauer RE**, **Eskew RT.** Colour is what the eye sees best. *Nature* 361: 348–350, 1993. doi:10.1038/361348a0.
56. **Gegenfurtner KR**, **Hawken MJ.** Interaction of motion and color in the visual pathways. *Trends Neurosci* 19: 394–401, 1996. doi:10.1016/S0166-2236(96)10036-9.
57. **Ales JM**, **Norcia AM.** Assessing direction-specific adaptation using the steady-state visual evoked potential: results from EEG source imaging. *J Vis* 9: 8, 2009. doi:10.1167/9.7.8.
58. **Candy TR**, **Skoczenski AM**, **Norcia AM.** Normalization models applied to orientation masking in the human infant. *J Neurosci* 21: 4530–4541, 2001. doi:10.1523/JNEUROSCI.21-12-04530.2001.
59. **Gilmore RO**, **Hou C**, **Pettet MW**, **Norcia AM.** Development of cortical responses to optic flow. *Vis Neurosci* 24: 845–856, 2007. doi:10.1017/S0952523807070769.
60. **Hale J**, **Harrad RA**, **McKee SP**, **Pettet MW**, **Norcia AM.** A VEP measure of the binocular fusion of horizontal and vertical disparities. *Invest Ophthalmol Vis Sci* 46: 1786–1790, 2005. doi:10.1167/iovs.04-0954.
61. **Liu-Shuang J**, **Torfs K**, **Rossion B.** An objective electrophysiological marker of face individualisation impairment in acquired prosopagnosia with fast periodic visual stimulation. *Neuropsychologia* 83: 100–113, 2016. doi:10.1016/j.neuropsychologia.2015.08.023.
62. **Lygo FA**, **Richard B**, **Wade AR**, **Morland AB**, **Baker DH.** Neural markers of suppression in impaired binocular vision. *NeuroImage* 230: 117780, 2021. doi:10.1016/j.neuroimage.2021.117780.

3. Laplacian reference is optimal for steady-state visual-evoked potentials

american physiological society

JNP JOURNAL OF NEUROPHYSIOLOGY

J Neurophysiol 130: 557–568, 2023.
First published July 26, 2023; doi:10.1152/jn.00469.2022

RESEARCH ARTICLE

Sensory Processing

Laplacian reference is optimal for steady-state visual-evoked potentials

Yuan Zhang,[1] Matteo Valsecchi,[2] Karl R. Gegenfurtner,[3] and Jing Chen[1,4]

[1]*School of Psychology, Shanghai University of Sport, Shanghai, China;* [2]*Dipartimento di Psicologia, Universitá di Bologna, Bologna, Italy;* [3]*Abteilung Allgemeine Psychologie, Justus-Liebig-Universität Gießen, Gießen, Germany; and* [4]*Research Center for Exercise and Brain Science, Shanghai University of Sport, Shanghai, China*

Abstract

Steady-state visual-evoked potentials (SSVEPs) are widely used in human neuroscience studies and applications such as brain-computer interfaces (BCIs). Surprisingly, no previous study has systematically evaluated different reference methods for SSVEP analysis, despite that signal reference is crucial for the proper assessment of neural activities. In the present study, using four datasets from our previous SSVEP studies (Chen J, Valsecchi M, Gegenfurtner KR. *J Neurophysiol* 118: 749–754, 2017; Chen J, Valsecchi M, Gegenfurtner KR. *Neuropsychologia* 102: 206–216, 2017; Chen J, McManus M, Valsecchi M, Harris LR, Gegenfurtner KR. *J Vis* 19: 8, 2019) and three public datasets from other studies (Baker DH, Vilidaite G, Wade AR. *PLoS Comput Biol* 17: e1009507, 2021; Lygo FA, Richard B, Wade AR, Morland AB, Baker DH. *NeuroImage* 230: 117780, 2021; Vilidaite G, Norcia AM, West RJH, Elliott CJH, Pei F, Wade AR, Baker DH. *Proc R Soc B* 285: 20182255, 2018), we compared four reference methods: monopolar reference, common average reference, averaged-mastoids reference, and Laplacian reference. The quality of the resulting SSVEP signals was compared in terms of both signal-to-noise ratios (SNRs) and reliability. The results showed that Laplacian reference, which uses signals at the maximally activated electrode after subtracting the average of the nearby electrodes to reduce common noise, gave rise to the highest SNRs. Furthermore, the Laplacian reference resulted in SSVEP signals that were highly reliable across recording sessions or trials. These results suggest that Laplacian reference is optimal for SSVEP studies and applications. Laplacian reference is especially advantageous for SSVEP experiments where short preparation time is preferred as it requires only data from the maximally activated electrode and a few surrounding electrodes.

NEW & NOTEWORTHY The present study provides a comprehensive evaluation of the use of different reference methods for steady-state visual-evoked potentials (SSVEPs) and has found that Laplacian reference increases signal-to-noise ratios (SNRs) and enhances reliabilities of SSVEP signals. Thus, the results suggest that Laplacian reference is optimal for SSVEP analysis.

Laplacian reference; referencing method; signal quality; steady-state visual-evoked potential

INTRODUCTION

Steady-state visual-evoked potentials (SSVEPs) are oscillatory brain responses in the visual cortex, elicited by viewing visual stimuli that are modulated periodically as a function of time (1–5). SSVEP responses confine to narrowband peaks at the stimulation frequency and its harmonics. Due to high signal-noise-ratio (SNR) and robustness to artifacts, SSVEPs have been widely used in human sensory and cognitive neuroscience, clinical applications, and brain-computer interface (BCI) designs (for review, see Refs. 6 and 7).

Signal referencing for EEG data analysis is crucial to eliminate common background noise. A number of studies have tested the effect of using different reference methods on event-related potential (ERP) studies (for recent reviews, see Refs. 8 and 9). The advantages and limitations of each reference method for ERPs have been investigated and discussed extensively. However, no previous study has comprehensively evaluated reference methods for SSVEP signals.

Several reference methods have been used in previous SSVEP studies. We searched SSVEP studies from four representative journals (*NeuroImage, Journal of Neuroscience, Neuropsychologia,* and *Journal of Vision*) over the past 10 years and counted the reference methods these studies used (a total of 114 studies as searched on September 2022; see Supplemental Table S1; Supplemental material is available at

Correspondence: J. Chen (chenjingps@gmail.com).
Submitted 10 November 2022 / Revised 18 July 2023 / Accepted 20 July 2023

https://doi.org/10.6084/m9.figshare.23690046.v1). The most commonly used methods are as follows: common average (65%), monopolar (16%), and averaged-mastoids (14%).

The common average reference is used in most SSVEP studies. This is not surprising since the common average is the most widely used reference for EEG studies in general (9). Common average reference is based on the assumption that the whole head scalp electrical activity over a dipole in the layered spherical surface is zero (10), and it is regarded as a high-pass spatial filter that can eliminate the DC component of the spatial frequency spectrum at a fixed time (11). Based on this assumption, common average is considered the "gold standard" when the following preconditions are met: *1*) a large number of electrodes are recorded (e.g., 64 or 128), and *2*) the electrodes are uniformly distributed over the entirety of the head (12–14). However, for SSVEP studies, there are lots of situations where only a few electrodes are recorded, as SSVEP responses are typically confined to the electrodes above a single sensory cortex (for review, see Ref. 6). By recording a small number of electrodes, the preparation time for experiments is much reduced, which is especially advantageous for studies involving special subjects such as children or clinical patients. In these studies, the monopolar reference is often used, i.e., referring to a single electrode (e.g., Refs. 15–17). It is, however, unknown whether the use of monopolar reference sacrifices signal quality to a certain degree, compared with other reference methods such as the common average reference. Another method, the averaged-mastoids reference, has also been used in previous SSVEP studies (see Supplemental Table S1). Even though it has been found that averaged-mastoids would seriously bias the EEG power and distort the field maps for ERPs (18–20), it remains unknown how averaged-mastoids reference affects SSVEP signals.

The Laplacian reference has been used in SSVEP studies, but only rarely (14, 21–29). The Laplacian is a mathematical function, named after the French mathematician Pierre-Simon de Laplace (1749–1827), which exhibits positive values in the center and negative values in the surround. It estimates the second spatial derivative of the electric potential distribution on the scalp and is used in EEG recordings to estimate the brain generators of scalp electrical activity (30). Laplacian, similar to current source density (CSD) and scalp current density (SCD), is a method aimed at identifying the neuronal generator of scalp EEG. Although Laplacian and SCD are based on the spherical shell head model (31–34), CSD is based on a linear volume-conduction model (35, for review about CSD, see Refs. 31, 36, and 37). In practice, the measured EEG potentials have low spatial resolution and are spatially correlated, and the CSD/SCD estimate is approximately linearly related to the Laplacian estimate. Laplacian is calculated by the difference between the potential at one center electrode and the averaged potential of its nearest neighbors (30). For SSVEPs, Laplacian reference uses signals from the maximal activated electrode, typically in medial occipital region at Oz (6), and subtracts the average of several neighboring electrodes. Mackay et al. (24) found that using Laplacian reference in the analysis allowed for the detection of significant SSVEP signals based on shorter epochs compared with monopolar reference, suggesting that Laplacian reference may increase the signal-to-noise ratio (SNR) for SSVEPs. Laplacian reference has also been found to be the optimal reference for studying oscillatory activities in stereo-electroencephalography (38). Since Laplacian reference is known to be sensitive to shallow local sources (34, 39), and the origin of SSVEPs is typically confined to a single sensory cortex (for review, see Ref. 6), it suggests that Laplacian reference may be a suitable choice for SSVEPs. However, it remains to be tested whether Laplacian reference is also optimal reference method compared with others such as common average reference and averaged-mastoids reference.

In summary, several different reference methods have been used in previous SSVEP studies, which suggest a need for a comprehensive assessment of these reference methods to address the issues as outlined earlier. Therefore, in the present study, we re-analyzed four SSVEP datasets from our previous publications (40–42), as well as three public datasets from other studies (43–45), to evaluate the effect of reference methods on the quality of SSVEP signals. On top of the most common quality metric, i.e., the SNR, we also calculated a reliability index as a measurement of the signal consistency across recording sessions or trials. The rationale is that EEG signals capturing neural representations faithfully should be highly reproducible across trials (46, 47). Our results suggest that SSVEP signals using Laplacian reference have the highest SNR and best reliability, compared with other reference methods (i.e., monopolar reference, common average reference, averaged-mastoids reference).

METHODS

Datasets

We re-analyzed SSVEP data from four experiments in our previous publications (40–42) and also public data from three other studies (43–45). The studies are briefly described here, more details can be found in the published articles.

Dataset no. 1.

The *dataset no. 1* was from the previous study (41), which is publicly available at https://zenodo.org/record/808197. Twenty-five observers (15 females and 10 males) participated in the experiment. They either fixated at the screen center or executed smooth pursuit eye movements to a moving target, against a full-screen background that was counter-phase flickering at 7.5 Hz (7.5 reversals/s) to evoke SSVEPs. Here, we analyzed data from both the fixation and the pursuit condition together. Each trial lasted 150 s, and each observer underwent eight trials in total. An EEG system (Brain Products, Munich, Germany) recorded EEG signals according to the international 10–20 system with 32 channels (FP1, FP2, F3, F4, C3, C4, P3, P4, O1, O2, F7, F8, T7, T8, P7, P8, Fz, Pz, Oz, FC1, FC2, CP1, CP2, FC5, FC6, CP5, CP6, TP9, TP10, HLeo, Veo, HReo), at a sampling rate of 1,000 Hz. The ground electrode was placed at the AFz, and the online reference at the Cz.

Dataset no. 2.

The *dataset no. 2* was from the first experiment of the study (40), which is publicly available at https://zenodo.org/record/817545. The observers (n = 12) either fixated at the screen center or executed smooth pursuit eye movements to an array of flickering targets, which were moving across the

screen back and forth. Here, we analyzed data from both the fixation and the pursuit condition. The left and right sides of a black-and-white checkerboard (8.15° × 8.15°) were pattern-reversal flickering at 6.7 Hz or 7.5 Hz (balanced across trials). Each trial lasted 150 s, and each observer conducted four trials. EEG recording was the same as *dataset no. 1*.

Datasets no. 3 and no. 4.

The *dataset nos. 3* and *4* were from the first and second experiments of the study (42), which is publicly available at https://zenodo.org/record/2636083. During the experiment, observers passively viewed a flickering-filled circle at center of the screen. In *experiment 1* ($n = 8$ observers), the circle was flickering at 8 Hz for 52 s. The circle was presented at two physical viewing distances (40 cm and 80 cm). The size of the circle was changed every 5 s except the first size was presented for 7 s (the first 2 s after stimulus onset would be excluded from analysis to avoid abrupt visual responses). The diameter changed from 1° to 10°, or from 10° to 1° (balanced across trials), at a step of 1°. The EEG was recorded the same as in *dataset no. 1*. In *experiment 2* ($n = 8$ observers), the filled circle was flickering at 8 Hz or 30 Hz at the center visual field. The size of the circle changed from 2° to 8° (or from 8° to 2°, balanced across trials) at a step of 1° every 5 s, with the exception of the first size presented for 7 s. Each trial lasted for 37 s. The number of trials was 24. EEG signals were recorded from 32 active electrodes (actiCAP, Brain Products) according to the international 10–20 system, at sampling rate of 5,000 Hz. The ground electrode was placed at FPz, and the online reference electrode at FCz location.

Dataset no. 5.

The *dataset no. 5* was from a study (44) which is publicly available at https://osf.io/x9zr8/. We reanalyzed the data of 16 healthy control participants (there were 19 participants in total; we did not include 3 of them since we were not able to decode the EEG markers in their data). The stimuli were sine-wave gratings flickering at 4 Hz between 0 and their nominal contrast (i.e., 0, 1.5, 6, 24, and 96%). We analyzed data from all conditions together and took their average SSVEPs response. There were eight blocks in total, with 25 trials in each block. Each trial lasted for 12 s. EEG data were recorded by ANT Neuro system according to the international 10–20 system with a 64-channel Waveguard cap, sampled at 1,000 Hz. The ground electrode was placed at AFz, and the EEG signals in each channel were referenced to the whole head average.

Dataset no. 6.

The *dataset no. 6* was from a study (45) which is publicly available at https://osf.io/y4n5k/. We analyzed the data of 99 healthy control participants (there were 100 participants in total; sub 43 was excluded due to having a number of bad channels that were three times the standard deviation away from the mean). The stimuli were sinewave gratings flickering at 7 Hz between 0% contrast and their nominal Michelson contrast (7 contrast conditions, vary from 0, and 2–64% in logarithmic steps). We analyzed data from all conditions together and took their average SSVEPs response. There were four blocks in total, with 40 trials in each block. Each trial lasted for 11 s. EEG recording was the same as *dataset no. 5*.

Dataset no. 7.

The *dataset no. 7* was from a recent study (43), which is publicly available at https://osf.io/e62wu/. Participants ($n = 12$) fixated at a central marker, which was surrounded by a cluster of 20 sinusoidal grating patches. All target stimuli were sinusoidally flickering at 5 Hz between 0% contrast and their nominal Michelson contrast (0, 6, 12, 24, 48, or 96%). We analyzed data from all conditions together and took their average SSVEPs response. There were 12 blocks, with 42 trials in each block. Each trial lasted for 11 s. EEG recording was the same as *dataset no. 5*.

Reference Methods

Our EEG data were recorded using an online reference at Cz, FCz, or the whole head average. Here, we evaluated four additional (re-)reference methods: monopolar reference, common average reference, averaged-mastoids reference, and Laplacian reference. As SSVEP responses in *datasets no. 1* to *no. 7* were all maximal at the occipital electrode Oz, our analyses focus on Oz only.

For monopolar reference, we re-referenced the signals at Oz to Fz in *datasets no. 1* to *no. 3*, and Cz for *datasets no. 4* to *no. 7*. For common average reference, the signals at Oz were re-referenced to the average of all 29 channels (not including the 3 EOG electrodes) in *datasets no. 1* to *no. 3*, all 32 channels in *dataset no. 4*, and all 64 channels in *datasets no. 5* to *no. 7*. For averaged-mastoids reference, we re-referenced the signals to the average signal of TP9 and TP10 in *datasets no. 1* to *no. 4*, and the average of M1 and M2 in *datasets no. 5* to *no. 7*. For Laplacian reference, we re-referenced the signal from the central electrode to the average of 5–9 nearest neighbor electrodes. The differentiation grid of a standard 10-10 montage with 67-channels for Hjorth Laplacian was shown in Fig. 5 in Ref. 37, and *Eq. 1* in Ref. 48 was used for the calculation. We re-referenced the signals from Oz against the average of 7 or 9 parietal-occipital electrodes. That is, 7 (i.e., O1, O2, P3, P4, P7, P8, Pz) in *datasets no. 1* to *no. 4*, and 9 (i.e., O1, O2, PO3, PO4, PO5, PO6, PO7, PO8, POz) in *datasets no. 5* to *no. 7*.

SSVEP Analyses

The analyses for EEG signals were carried out using EEGLAB toolbox (49) and customized scripts in MATLAB. For all datasets, we detected the noisy channels and performed interpolation using functions from the EEGLAB plugin clean_rawdata() (http://sccn.ucsd.edu/wiki/Plugin_list_process). First, we used clean_flatlines() to detect channels that have no signal variation for a duration longer than 5 s. Then, for the remaining channels, we eliminated slow-wave drifts using clean_drifts() (forward-backward filter with a transition band of 0.5–1 Hz and stop-band attenuation of 80 dB). Second, we used clean_channels() to remove the channels with excessive line noise. This algorithm extracted line noise (signals above 50 Hz) from the raw EEG signal and calculated the noise-to-signal ratio for each channel. The noise-to-signal ratio was computed as the median absolute deviation (MAD) of the difference between the raw EEG and the line noise, divided by the MAD of the line noise. Channels with a z-transformed noise-to-signal ratio above 4 were identified as bad channels. For the removed channels, we applied

eeg_interp() from EEGLAB to perform spherical interpolation. The average number of noisy channels across *datasets no. 1* to *no. 7* was 1.7.

The repetitions of conditions vary across datasets. In *datasets no. 1* and *no. 2*, each observer only has one single 150-s trial for every condition, whereas in *datasets no. 3* to *no. 7*, there were more than two trials in each condition. In *datasets no. 3–7*, the EEG signals from each condition and each individual observer were first averaged in the time domain. This averaging process was performed to increase the signal-to-noise ratio by reducing nonphase-locked EEG noise that is not synchronized with the stimulation (e.g., see Refs. 44 and 50). Subsequently, the EEG signals for each condition were cut out into 5-s epochs, resulting in 30 epochs in *datasets no. 1* and *no. 2*, 10 epochs in *dataset no. 3*, 7 epochs in *dataset no. 4*, and 2 epochs in *datasets no. 5* to *no. 7*. All epochs were first de-trended by removing the linear fit (51). Then we zero-padded the signal to 10 s to get a frequency resolution of 0.1 Hz (e.g., see Refs. 40 and 52). We applied fast-Fourier transform (*fft*.m in MATLAB) to obtain the amplitude spectrum in each epoch. The amplitudes of all epochs in each condition were then averaged for further analysis.

SSVEP Signal Quality Metrics

To evaluate the quality of SSVEP signals after applying the four reference methods, we calculated the signal-noise-ratio (SNR) and reliability of SSVEP responses in all seven datasets.

Signal-Noise-Ratio

The SNR is a metric widely used to evaluate SSVEP signals. In our analysis, we calculated SNR using the EEG amplitude at the target frequency (e.g., 7.5 Hz) divided by the average noise at 10 adjacent frequency bins (e.g., 6.9, 7.0, 7.1, 7.2, 7.3, 7.7, 7.8, 7.9, 8.0, 8.1 Hz, two immediately adjacent bins were not included to avoid frequency leakage of target signals due to zero-padding). Since ratio data such as SNRs tend to be skewed rather than normally distributed, we used log-transformed SNR values in statistical tests.

Reliability

Reliability shows the estimated interitem reliability of measurement obtained from repeated items, typically obtained by calculating the correlation between one half of the measurement and the other half (53). In our analyses, we calculated the correlation between SSVEP responses obtained after splitting EEG epochs or trials within the same condition.

The SSVEP responses were calculated by summing the amplitudes at all harmonics below 45 Hz (54). At each stimulation frequency (e.g., 7.5 Hz), we subtracted from the peak amplitude the mean amplitude of the 10 nearby bins (e.g., 6.9, 7.0, 7.1, 7.2, 7.3, 7.7, 7.8, 7.9, 8.0, 8.1 Hz, two immediately adjacent bins were not included due to frequency leakage after zero-padding), to remove the baseline background noise.

For all datasets, we split the epochs into odd and even subsets and then calculated the mean SSVEP amplitude for odd and even subsets of each observer. The cross-observer Pearson correlation was computed between the two subsets for each condition. The reliability score reported in the result was the average of correlation coefficients across all conditions. With all conditions, the reliability was computed between two EEG recordings each with a duration of 600 s, 300 s, 200 s, 280 s, 1,200 s, 880 s, and 2,772 s, for each subject, in *datasets no. 1* to *no. 7*, respectively.

RESULTS

The present study evaluated the effect of using different reference methods on SSVEP data across seven different existing datasets. Overall, we found that Laplacian reference can effectively reduce broadband EEG noise and enhance the signal-to-noise ratio and reliability of SSVEP responses.

Laplacian Referencing Reduces Broadband Noise

The effect of different reference methods on EEG signals from *dataset no. 1* is illustrated in Fig. 1. Figure 1, *A* and *B*, shows identical EEG epochs from a sample observer after monopolar reference and Laplacian reference, respectively. Epochs with Laplacian reference show less noise. Figure 1*C* shows average spectrums of all observers for four reference methods. The broadband noise in EEG signals is lowest when using Laplacian reference, compared with the other three reference methods. The averaged-mastoids reference is not as effective as common average or Laplacian in terms of reducing noise, and even slightly increases broadband noise at high frequency above 30 Hz. Figure 1*D* depicts the topographic distribution and reveals the occipital origin of SSVEP responses. Figure 1*D*, *left*, displays the topography of SSVEP amplitudes obtained from the raw data, whereas Fig. 1*D*, *right*, shows the topography of SSVEP amplitudes after applying the Laplacian reference on every electrode. The distribution of SSVEP responses in the topography from the raw data is more dispersed compared with the Laplacian-referenced data. Thus, Laplacian reference is useful to remove broad noise and enhance the clarity of the SSVEPs responses' origin.

Laplacian Referencing Increase SNRs

To assess the effect of reference methods on the quality of SSVEP responses, we computed the SNRs at the stimulation frequency and its harmonics. Figure 2 shows the result of *dataset no. 1*. Common average reference outperforms monopolar reference at all harmonics. The averaged-mastoids reference increases the SNR at fundamental frequency, whereas at higher harmonics, the SNRs of the averaged-mastoids reference are not as good as that of the monopolar reference. Importantly, Laplacian reference resulted in the highest SNRs at stimulation frequency as well as harmonics. We conducted a 2 (type of reference method: Laplacian reference vs. common average reference) $\times$ 5 (harmonics: 1st to 5th) repeated-measure ANOVA and simple effects analysis on log-transformed SNRs. There was a significant main effect for reference method, $F(1, 24) = 81.11$, $P < 0.001$, $\eta_p^2 = 0.782$. The pairwise comparison results revealed that the Laplacian reference has significantly higher SNRs in the 1st to 5th harmonics (all Ps < 0.01).

Next, we calculated SNRs in *datasets no. 1* to *no. 4*. Figure 3 shows the results. The SNR values here are the average of all harmonics below 45 Hz. We conducted one-way ANOVA and

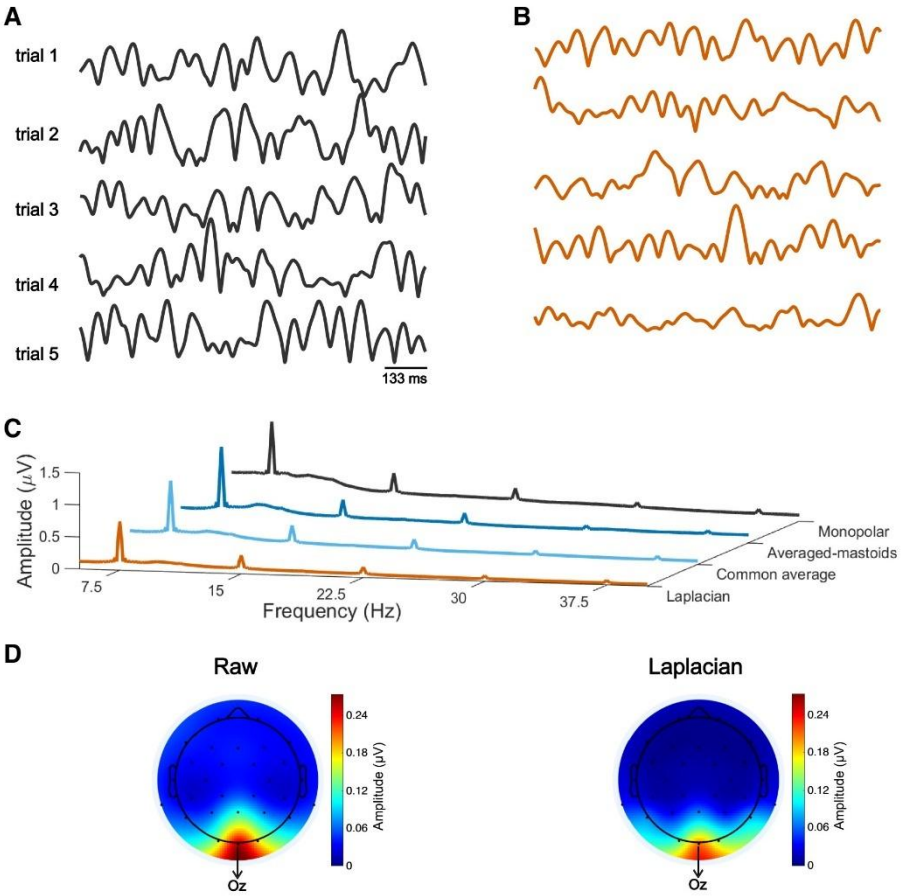

Figure 1. Effect of reference methods on EEG signals in *dataset no. 1* (*A*–*D*). *A* and *B:* example EEG epochs at Oz electrode from a sample subject, with common average reference (*A*) and Laplacian reference (*B*). *C:* average spectra of all subjects for the four reference methods. *D:* the topographic plots that illustrate the occipital origin of these steady-state visual-evoked potential (SSVEP) responses. *Left*: the topography of SSVEP amplitudes obtained from the raw data. *Right*: the topography of SSVEP amplitudes after applying the Laplacian reference on every electrode. Overall, Laplacian reference reduces broadband noise the most, followed by common average, the averaged-mastoids, and monopolar reference.

pairwise comparisons on log-transformed SNRs in *datasets no. 1–4*, respectively. It is worth noticing that in *datasets no. 1* to *no. 4*, Laplacian reference resulted in the highest SNRs, which were significantly higher than monopolar reference, common average reference, and averaged-mastoids reference in *datasets no. 1* to *no. 4* (all Ps < 0.01). As monopolar reference is widely used for SSVEP studies (see INTRODUCTION), one interesting question is whether the use of monopolar reference sacrifices the signal quality compared with common average or averaged-mastoids reference. The statistical results on log-transformed SNRs show that, compared with monopolar reference, common average reference results in higher SNRs in *datasets no. 1* to *no. 4* (all Ps < 0.001); and the averaged-mastoids reference also has higher SNRs in *datasets no. 1* and *no. 2* (Ps < 0.05), but not in *datasets no. 3* and *no. 4* (Ps > 0.4). Therefore, despite the convenience, the use of monopolar reference does have the disadvantage of lower SNRs compared with common average reference and Laplacian reference.

Does Laplacian reference increase SNRs for all observers? Here, we further examined SNR results in individual observers. In Fig. 4, each dot represents data of a single observer, with *x*-axis representing the SNR values using common average reference, and *y*-axis the SNR values using Laplacian reference. Note that most observers fell above the diagonal line, indicating higher SNR with Laplacian reference compared with common average reference. This result suggests that Laplacian reference has a tendency to boost SNRs across observers.

Laplacian Referencing Increases Reliability

We assessed the reliability of SSVEP responses after applying each of the reference methods. The rationale was that

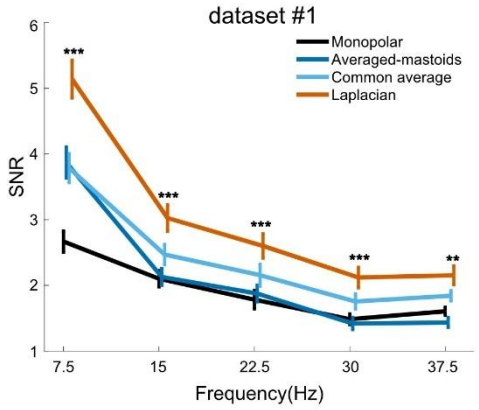

Figure 2. Signal-to-noise ratios (SNRs) of steady-state visual-evoked potential (SSVEP) responses at the fundamental frequency (7.5 Hz) and higher harmonics in *dataset no. 1*. Laplacian reference results in the highest SNRs. Error bars represent standard errors across observers. Asterisks denote the significance of the difference between SNRs of SSVEP responses for common average reference and Laplacian reference, established using paired *t* tests: ***$P < 0.001$, **$P < 0.01$.

high-quality physiological signals should be also highly reproducible across trials (epochs), given identical visual stimulations. Figure 5 shows an illustration for the calculation of reliability index. We calculated the cross-observer correlation between SSVEP amplitudes in the odd/even subsets of epochs of the same condition. The illustration shows an example for the calculation. In this case, Laplacian reference results in more reliable SSVEPs than common average reference with the same raw EEG data.

The average reliability scores after applying each of the reference methods in *datasets no. 1* to *no. 4* are shown in Fig. 6. Most of the reliability indices were high. This means that the quality of SSVEP responses in our datasets was excellent overall. Importantly, SSVEP signals using Laplacian reference show the highest reliability in *datasets no. 1* to *no. 4*, with reliability values of 0.993, 0.952, 0.988, and 0.993, respectively.

The Findings Can Be Replicated in Public Datasets

A further question is how general these findings are, given that we have analyzed data from our own previous studies. Therefore, we tried to find out SSVEP studies that have made their data public and obtain *datasets no. 5*, *no. 6*, and *no. 7* to extend our results. Figure 7 shows the SNRs and reliability after applying each reference method in *datasets no. 5* to *no. 7*. We conducted one-way ANOVA and pairwise comparisons on log-transformed SNRs in *datasets no. 5* to *no. 7*, respectively. SNRs with Laplacian reference are significantly higher than other reference methods in these three datasets (all *P*s < 0.01). In addition, split-half reliabilities with Laplacian reference are the highest in *datasets no. 5* to *no. 7*. Therefore, with public datasets, we could replicate the finding that the Laplacian reference results in better SSVEP signals compared with other methods.

Laplacian Referencing Increase SNRs as a Function of Contrast

In *datasets no. 5* to *no. 7*, which included measurements of full contrast response functions, we further evaluated the effect of reference methods on SNRs in the full contrast response function for the target-only condition (i.e., the contrast of mask is 0). Figure 8 shows the results. At low contrasts (i.e., 0%, 1.5%, and 2%), the SSVEP responses were weak, and the SNRs were close to 1. The four reference methods yielded similar SNRs in this range. We selected contrast levels that had significant SNRs (determined by one-sample *t* tests on common average referenced data, SNRs > 1, $P <$

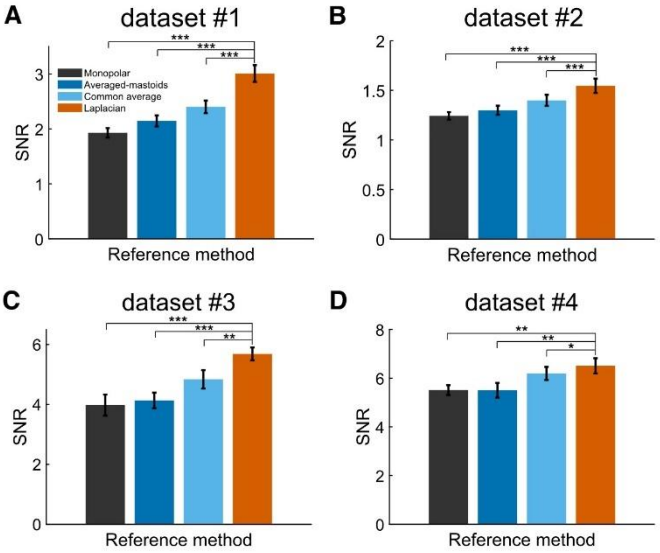

Figure 3. Signal-to-noise ratios (SNRs) for four reference methods in *dataset no. 1* to *no. 4* (*A*–*D*). Laplacian reference led to higher SNRs compared with other three reference methods in all four datasets. Error bars represent standard errors across observers. Asterisks denote the significance of the difference between SNR of steady-state visual-evoked potential (SSVEP) responses for different referencing methods, established using paired *t* tests: ***$P < 0.001$, **$P < 0.01$, *$P < 0.05$.

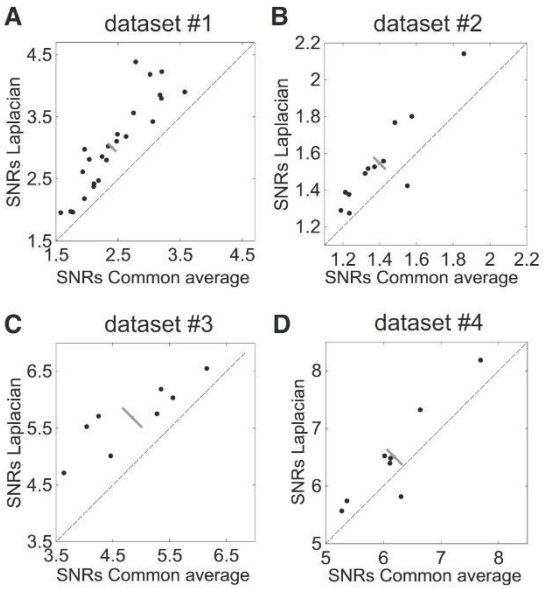

Figure 4. Signal-to-noise ratios (SNRs) of steady-state visual-evoked potential (SSVEPs) in individual observer after common average and Laplacian reference in *dataset no. 1* to *no. 4* (*A–D*). Each filled circle represents data of a single observer. Most of the data points fell above the diagonal line, indicating higher SNR for the Laplacian reference than common average reference. Black bars denote 95% confidence intervals of the mean along the negative-slope diagonal line.

0.05) to examine whether the Laplacian reference outperforms common average reference in terms of SNRs across these contrasts. We conducted a 2 (type of reference method: Laplacian reference vs. common average reference) × *n* (contrast levels, 2, 6, and 5 in *datasets no. 5–7*, respectively) repeated-measure ANOVA and pairwise comparisons on log-transformed SNRs in *datasets no. 5* to *no. 7*. There were main effects for reference method in these three datasets: $F(1,15) = 4.56$, $P = 0.050$, $\eta_p^2 = 0.233$; $F(1,98) = 71.65$, $P < 0.001$, $\eta_p^2 = 0.422$; $F(1,11) = 19.95$, $P < 0.001$, $\eta_p^2 = 0.645$. The statistical results revealed that Laplacian reference led to significant higher SNRs than common average reference at median to high contrast (i.e., 4%, 8%, 12%, 16%, 24%, 32%, 48%, 64%, and 96%), as depicted in Fig. 8. These results suggest that the use of the Laplacian reference offers benefits in terms of SNRs across a broad range of contrast levels.

Optimal Stimulation Durations for Different Referencing Methods

Here, we asked a further question about the optimal stimulation duration for SSVEP studies. As SNRs of SSVEP signals increase with longer stimulation durations, the optimal stimulation duration to achieve a certain SNR would differ for different reference methods. That is, given that Laplacian reference would result in higher SNRs, it would require shorter stimulation durations than other reference methods. We analyzed *dataset no. 1* by using different lengths of epochs. Figure 9 shows SNR values as a function of epoch durations. Overall, SNRs increase with longer epochs. To achieve a certain level of SNR (e.g., 5), Laplacian reference requires an epoch length of 18 s, whereas other reference methods need 1.5 to 3 times longer. Therefore, by using Laplacian reference, SSVEP experiments could afford to use shorter stimulation durations.

DISCUSSION

The present study provides a comprehensive evaluation on the use of different reference methods for SSVEPs. Across four datasets from our own studies and three public datasets, we consistently found that Laplacian reference resulted in SSVEP signals that have the lowest broadband noise, highest SNRs, and best reliability. It suggests that Laplacian reference enhances signal qualities compared with other reference methods such as monopolar, averaged-mastoids, and common average reference. Thus, our results support the use of Laplacian reference for SSVEP studies.

One of the major advantages of SSVEPs is that it provides a neural response with high SNRs, at a predefined narrowband frequency and at a known small brain region (usually at occipital electrodes, especially Oz). A large number of previous studies have taken advantage of this and recorded only a few or even a single occipital electrode (e.g., see Refs. 15, 24, 25, 55, and 56). Preparation time for EEG setups would, therefore, be much reduced, which is especially important for experiments or applications involving special subjects such as children or clinic patients. In most of these cases,

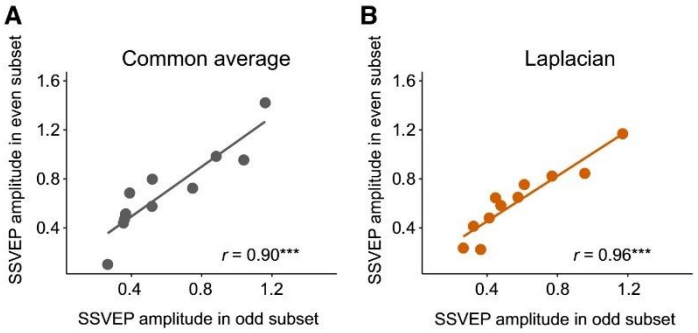

Figure 5. An illustration for the calculation of reliability. *A*: the correlation of steady-state visual-evoked potential (SSVEP) amplitudes in odd and even subset of epochs from the same condition with common average reference (*dataset no. 2*). *B:* the same data with Laplacian reference. Filled circles denote individual observers. SSVEPs are more reliable (i.e., more consistent across trials given identical stimulations) using Laplacian reference. Asterisks denote the significance of the coefficient, established using Pearson correlation: ***$P < 0.001$.

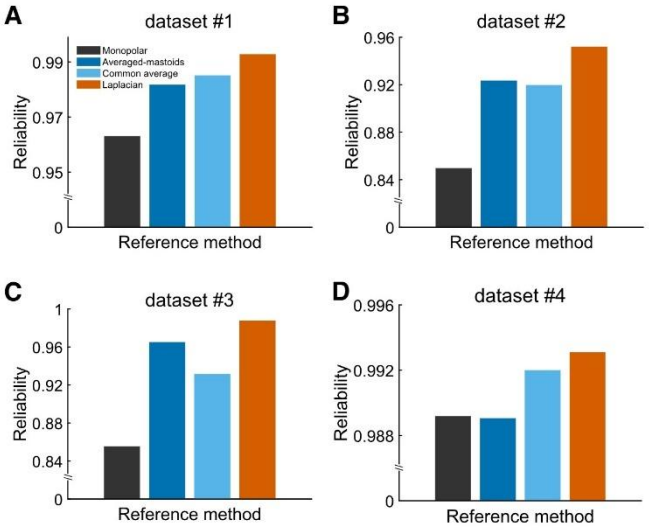

Figure 6. Split-half reliability for four reference methods in *dataset no. 1* to *no. 4* (*A*–*D*). Steady-state visual-evoked potential (SSVEP) signals using Laplacian reference showed the highest reliability in *dataset no. 1* to *no. 4*.

monopolar reference (referring to Cz or FCz) is used. Based on our current results, monopolar reference does sacrifice signal quality compared with the other three methods in terms of the level of noise, SNRs, and reliability (Figs. 1, 2, 3, 6, 7, 8, and 9). Our results indicate that Laplacian reference has the best performance. In terms of preparation time, Laplacian reference is similar to monopolar reference, as only a few occipital electrodes are required (the maximal activated electrode and a few nearby electrodes). But the resulting SSVEP signals with Laplacian reference are better in all the quality metrics we have accessed. The SNRs as a function of the contrast of the four reference methods demonstrates that using the Laplacian reference can provide advantages in terms of SNRs across a wide range of contrast levels (Fig. 8). Furthermore, by using Laplacian reference, SSVEP experiments can afford to use shorter stimulation durations (Fig. 9), which could reduce recording time required or increase the experiment conditions one can test. Thus, based on our current results, Laplacian reference method is strongly recommended for SSVEP studies and applications.

We evaluated only four reference methods that are commonly used and are relatively simple to implement. There are other more sophisticated methods for SSVEPs, which have been used in certain situations, for example, the reliable components analysis (47) and the rhythmic entrainment source separation method (57). These methods require data from all EEG electrodes over the head and have also other requirements or assumptions. For example, the rhythmic entrainment source separation was developed based on the assumption that steady-state activity is spectrally and spatially stationary over time, and also requires high-quality data with many time points. The reliable components analysis decomposes all-channel EEG data into a small number of reliable components by maximizing trial-to-trial consistency, which requires dozens of homogeneous and phase-locked trials. If these requirements are satisfied, the reliable components analysis could be a better choice than Laplacian reference.

As SSVEPs are widely used for BCI designs, previous studies in the field of BCI have also tried to optimize the reference method to improve the recognition accuracy for SSVEP signals. A large number of optimization methods that combines data from multiple EEG channels with various algorithms have been proposed (see Refs. 58 and 59 for recent progress and reviews). In terms of detecting SSVEP signals at certain frequency as in BCI applications, these methods would in principle result in higher detecting accuracy compared with a reference method as simple as the Laplacian. For example, the generated reference filter method has been shown to provide higher accuracy than Laplacian and common average reference (58). For spatial filters such as common average reference and Laplacian reference, Laplacian reference resulted in a higher classification accuracy than common average reference (60). However, stimuli used in neuroscience research are very different from BCI research. Testing these optimization algorithms is outside the scope of the current study. Future studies are needed to examine whether these algorithms developed in the BCI field also benefit SSVEP studies in neuroscience research.

The averaged-mastoids reference has been used more often in some old studies. However, it has been known for decades that averaged-mastoids reference would seriously bias the EEG power and distort the field maps (18–20), and is thus not recommended for ERP studies. Here, we found that the averaged-mastoids reference is better than monopolar reference for SSVEP signals to a certain degree, but does not perform well as the common average or Laplacian reference (Figs. 1, 2, 3, 6, 7, 8, and 9). There seems to be no reason to use the averaged-mastoids reference in future SSVEP studies. The Laplacian is by all means the better choice.

It seems there is no well-accepted principle to the numbers of nearest neighbor electrodes for Laplacian reference in SSVEPs. Previous studies in SSVEPs took the averaged

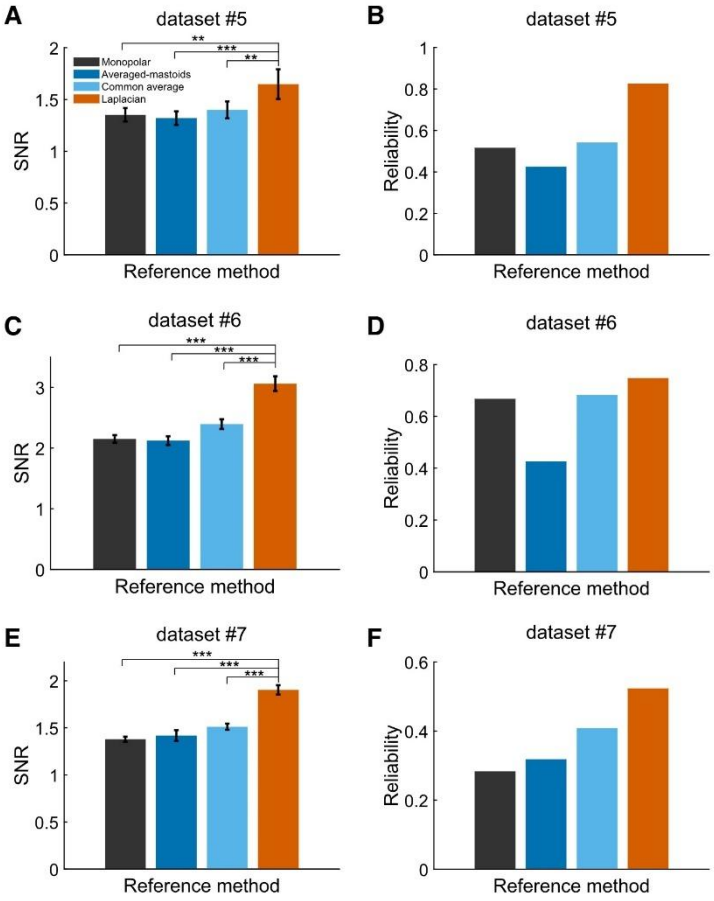

Figure 7. Signal-to-noise ratios (SNRs; *left*) and reliability (*right*) for four reference methods in *dataset no. 5* to *no. 7* (*A*–*F*). A whole head average reference was used in the original analysis in these three datasets. Steady-state visual-evoked potential (SSVEP) signals using Laplacian reference show the highest SNRs and reliability. Error bars represent standard errors across observers. Asterisks denote the significance level: $***P < 0.001$, $**P < 0.01$.

EEG signals from two to nine electrodes surrounding the central electrode for Laplacian reference (e.g., see Refs. 14, 21–25). Traditionally, the Laplacian operator is represented in orthogonal coordinates (30). However, because the Laplacian operator takes the potential difference between the central electrode and the mean of the surrounding electrodes, triangular and hexagonal arrays exist in addition to orthogonal arrays (61, 62). Usually, the number of nearest neighbors for Hjorth Laplacian estimate is 3–5, while any number of "nearest" neighbors can be defined, up to the total number of recording sites minus one (37, 48). Based on these findings, we recommend taking the potential difference between the central electrode and the average of 5–9 nearest neighbor electrodes for Laplacian reference in SSVEPs studies (Fig. 5 in Ref. 37 shows the differentiation grid of a standard 10-10 montage with 67-channels).

The focus of the present study was on the effect of Laplacian reference on SSVEP signals. However, it is a valid question whether Laplacian reference should be used universally for all EEG techniques, including ERPs and spontaneous oscillations. If a study were to analyze SSVEPs, transient ERPs, and spontaneous oscillations together, what reference method should be used? Although a definitive answer to this question goes beyond the scope of the present study, we believe that the choice between different reference methods depends on the specific application scenario. Each reference method has its advantages and limitations, which make them suitable for different scenarios. Laplacian reference is sensitive to shallow local sources but insensitive to distributed deep sources (34, 39). This in principle makes it a preferred reference method for certain ERP components and spontaneous oscillations that are generated by local shallow brain regions. This also explains why Laplacian reference is particularly good for SSVEPs, which are known to be mostly locally generated in a single sensory cortex (e.g., see Refs. 40, 41, 55, 63–66). In future work, it would be beneficial to summarize the most recommended reference method for each EEG component based on the signal origin.

Overall, Laplacian reference provides high-quality SSVEP data and requires only several recording electrodes. Besides,

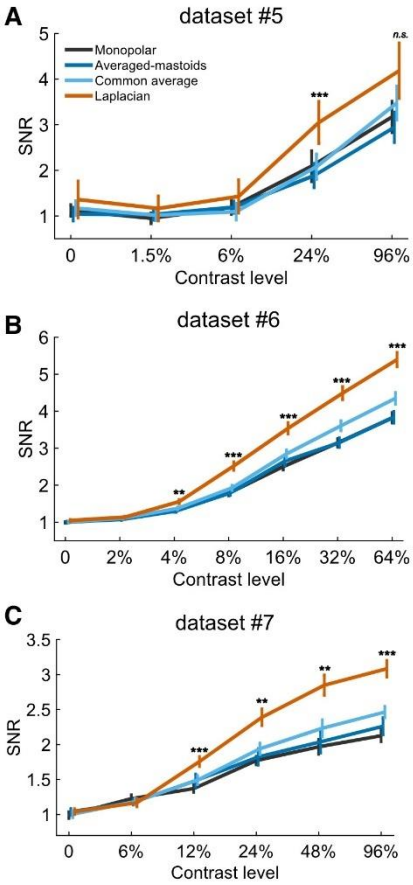

Figure 8. The signal-to-noise ratios (SNRs) as a function of contrast using four reference methods in *dataset no. 5* to *no. 7* (*A*–*C*) at the target only condition (i.e., the contrast of mask is 0). Error bars represent standard errors across observers. Asterisks denote the significance of the difference between SNRs of steady-state visual-evoked potential (SSVEP) responses for common average reference and Laplacian reference, established using paired *t* tests: ***$P < 0.001$, **$P < 0.01$, n.s. for $P > 0.05$.

Laplacian reference can be applied at every electrode on the whole head (Fig. 1*D*). As SSVEPs are not confined in occipital electrodes in other SSVEP paradigms, i.e., periodic stimulations with complex stimuli such as faces or words would elicit responses at other brain areas anterior toward the temporal lobe (e.g., see Refs. 50, 67, and 68), Laplacian reference to the whole head can help find the maximal activated electrode and facilitate the following analysis. However, in the case of recording a limited number of electrodes, the maximal activated electrode should be known before setting up recording electrodes at the maximal and nearby locations in the use of Laplacian reference. In some situations, researchers might choose a cluster of electrodes, instead of a single electrode with maximal responses, for analysis. Does Laplacian referencing outperform other referencing methods in this case? We compared SNR values when the cluster of O1/Oz/O2 was used, and found that Laplacian referencing led to the highest SNRs compared with other reference methods as well. Therefore, the current finding can be generalized to the situation where a cluster of electrodes is used.

Conclusions

The present study provides an empirical assessment on reference methods for SSVEP studies and analyses. Based on quality metrics of SNRs and reliability, the use of Laplacian reference is highly recommended. Laplacian reference is especially advantageous in certain studies or applications where short preparation time is favored as it only requires data from the maximal activated electrode and a few surrounding electrodes.

DATA AVAILABILITY

Data were previously published and links to the data are provided in the METHODS section.

SUPPLEMENTAL DATA

Supplemental Table S1: https://doi.org/10.6084/m9.figshare.23690046.v1.

GRANTS

J. Chen was supported by the National Natural Science Foundation of China under Grant number 31900758. K. R. Gegenfurtner was supported by the Deutsche Forschungsgemeinschaft (DFG, German Research Foundation)—Project Number 222641018—SFB/TRR 135 Project C2, and the European Research Council Advanced Grant Color3.0 Project Number 884116.

DISCLOSURES

No conflicts of interest, financial or otherwise, are declared by the authors.

AUTHOR CONTRIBUTIONS

J.C. conceived and designed research; Y.Z. analyzed data; Y.Z., M.V., K.R.G., and J.C. interpreted results of experiments; Y.Z. prepared figures; Y.Z. drafted manuscript; M.V., K.R.G., and J.C. edited and revised manuscript; Y.Z., M.V., K.R.G., and J.C. approved final version of manuscript.

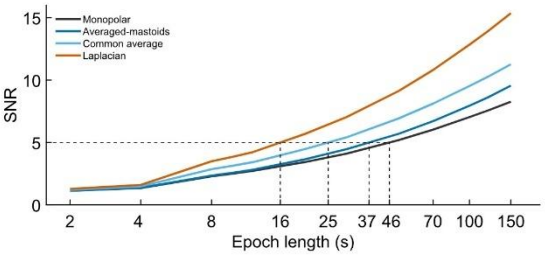

Figure 9. Signal-to-noise ratios (SNRs) as a function of epoch lengths, for four reference methods in *dataset no. 1*. SNRs increase with longer epochs. To achieve a certain SNR, Laplacian reference requires the shortest epoch.

REFERENCES

1. **Adrian ED**, **Matthews BHC.** THE Berger rhythm: potential changes from the occipital lobes in man. *Brain* 57: 355–385, 1934. doi:10.1093/brain/57.4.355.
2. **Kamp A**, **Sem-Jacobsen CW**, **Storm van Leeuwen W**, **van der Tweel L.** Cortical responses to modulated light in the human subject. *Acta Physiol Scand* 48: 1–12, 1960. doi:10.1111/j.1748-1716.1960.tb01840.x.
3. **Regan D.** Some characteristics of average steady-state and transient responses evoked by modulated light. *Electroencephalogr Clin Neurophysiol* 20: 238–248, 1966. doi:10.1016/0013-4694(66)90088-5.
4. **Tweel LH**, **Spekreijse H.** Signal transport and rectification in the human evokedresponse system. *Ann N Y Acad Sci* 156: 678–695, 1969. doi:10.1111/j.1749-6632.1969.tb14007.x.
5. **Van der Tweel LH**, **Lunel HF.** Human visual responses to sinusoidally modulated light. *Electroencephalogr Clin Neurophysiol* 18: 587–598, 1965. doi:10.1016/0013-4694(65)90076-3.
6. **Norcia AM**, **Appelbaum LG**, **Ales JM**, **Cottereau BR**, **Rossion B.** The steady-state visual evoked potential in vision research: a review. *J Vis* 15: 4, 2015. doi:10.1167/15.6.4.
7. **Vialatte F-B**, **Maurice M**, **Dauwels J**, **Cichocki A.** Steady-state visually evoked potentials: focus on essential paradigms and future perspectives. *Prog Neurobiol* 90: 418–438, 2010. doi:10.1016/j.pneurobio.2009.11.005.
8. **Hu S**, **Yao D**, **Bringas-Vega ML**, **Qin Y**, **Valdes-Sosa PA.** The statistics of EEG unipolar references: derivations and properties. *Brain Topogr* 32: 696–703, 2019. doi:10.1007/s10548-019-00706-y.
9. **Yao D**, **Qin Y**, **Hu S**, **Dong L**, **Bringas Vega ML**, **Valdés Sosa PA.** Which reference should we use for EEG and ERP practice? *Brain Topogr* 32: 530–549, 2019. doi:10.1007/s10548-019-00707-x.
10. **Bertrand O**, **Perrin F**, **Pernier J.** A theoretical justification of the average reference in topographic evoked potential studies. *Electroencephalogr Clin Neurophysiol* 62: 462–464, 1985. doi:10.1016/0168-5597(85)90058-9.
11. **Lehmann D**, **Skrandies W.** Spatial analysis of evoked potentials in man—a review. *Prog Neurobiol* 23: 227–250, 1984. doi:10.1016/0301-0082(84)90003-0.
12. **Luck SJ.** *An Introduction to the Event-Related Potential Technique* (2nd ed.). Cambridge, MA: The MIT Press, 2014.
13. **Nunez PL.** REST: a good idea but not the gold standard. *Clin Neurophysiol* 121: 2177–2180, 2010. doi:10.1016/j.clinph.2010.04.029.
14. **Nunez PL**, **Srinivasan R.** *Electric Fields of the Brain*. New York: Oxford University Press, 2006.
15. **Belmonte M.** Abnormal attention in autism shown by steady-state visual evoked potentials. *Autism* 4: 269–285, 2000. doi:10.1177/1362361300004003004.
16. **Marx M**, **Bodis-Wollner I**, **Bobak P**, **Harnois C**, **Mylin L**, **Yahr M.** Temporal frequency-dependent VEP changes in Parkinson's disease. *Vision Res* 26: 185–193, 1986. doi:10.1016/0042-6989(86)90080-5.
17. **Tagliati M**, **Bodis-Wollner I**, **Yahr MD.** The pattern electroretinogram in Parkinson's disease reveals lack of retinal spatial tuning. *Electroencephalogr Clin Neurophysiol* 100: 1–11, 1996. doi:10.1016/0168-5597(95)00169-7.
18. **Faux SF**, **Shenton ME**, **McCarley RW**, **Nestor PG**, **Marcy B**, **Ludwig A.** Preservation of P300 event-related potential topographic asymmetries in schizophrenia with use of either linked-ear or nose reference sites. *Electroencephalogr Clin Neurophysiol* 75: 378–391, 1990. doi:10.1016/0013-4694(90)90083-V.
19. **Feindel W**, **Leblanc R**, **de Almeida AN.** Epilepsy surgery: historical highlights 1909–2009. *Epilepsia* 50, *Suppl 3*: 131–151, 2009. doi:10.1111/j.1528-1167.2009.02043.x.
20. **Stone JL**, **Hughes JR.** Early history of electroencephalography and establishment of the American Clinical Neurophysiology Society. *J Clin Neurophysiol* 30: 28–44, 2013. doi:10.1097/WNP.0b013e31827edb2d.
21. **Bach M**, **Maurer JP**, **Wolf ME.** Visual evoked potential-based acuity assessment in normal vision, artificially degraded vision, and in patients. *Br J Ophthalmol* 92: 396–403, 2008. doi:10.1136/bjo.2007.130245.
22. **Brown RJ**, **Norcia AM.** A method for investigating binocular rivalry in real-time with the steady-state VEP. *Vision Res* 37: 2401–2408, 1997. doi:10.1016/S0042-6989(97)00045-X.
23. **Dong X**, **Du X**, **Bao M.** Repeated contrast adaptation does not cause habituation of the adapter. *Front Hum Neurosci* 14: 589634, 2020. doi:10.3389/fnhum.2020.589634.
24. **Mackay AM**, **Bradnam MS**, **Hamilton R.** Rapid detection of threshold VEPs. *Clin Neurophysiol* 114: 1009–1020, 2003. doi:10.1016/S1388-2457(03)00078-6.
25. **Zhang P**, **Jamison K**, **Engel S**, **He B**, **He S.** Binocular rivalry requires visual attention. *Neuron* 71: 362–369, 2011. doi:10.1016/j.neuron.2011.05.035.
26. **Andersen SK**, **Muller MM**, **Martinovic J.** Bottom-up biases in feature-selective attention. *J Neurosci* 32: 16953–16958, 2012. doi:10.1523/JNEUROSCI.1767-12.2012.
27. **Antonov PA**, **Chakravarthi R**, **Andersen SK.** Too little, too late, and in the wrong place: α band activity does not reflect an active mechanism of selective attention. *NeuroImage* 219: 117006, 2020. doi:10.1016/j.neuroimage.2020.117006.
28. **Adamian N**, **Andersen SK**, **Hillyard SA.** Parallel attentional facilitation of features and objects in early visual cortex. *Psychophysiology* 57: e13498, 2020. doi:10.1111/psyp.13498.
29. **Adamian N**, **Andersen SK.** Attentional enhancement of tracked stimuli in early visual cortex has limited capacity. *J Neurosci* 42: 8709–8715, 2022. doi:10.1523/JNEUROSCI.0605-22.2022.
30. **Hjorth B.** An on-line transformation of EEG scalp potentials into orthogonal source derivations. *Electroencephalogr Clin Neurophysiol* 39: 526–530, 1975. doi:10.1016/0013-4694(75)90056-5.
31. **Babiloni F**, **Babiloni C**, **Fattorini L**, **Carducci F**, **Onorati P**, **Urbano A.** Performances of surface Laplacian estimators: a study of simulated and real scalp potential distributions. *Brain Topogr* 8: 35–45, 1995. doi:10.1007/BF01187668.
32. **Pernier J**, **Perrin F**, **Bertrand O.** Scalp current density fields: concept and properties. *Electroencephalogr Clin Neurophysiol* 69: 385–389, 1988. doi:10.1016/0013-4694(88)90009-0.
33. **Perrin F**, **Pernier J**, **Bertrand O**, **Echallier JF.** Spherical splines for scalp potential and current density mapping. *Electroencephalogr Clin Neurophysiol* 72: 184–187, 1989. doi:10.1016/0013-4694(89)90180-6.
34. **Yao D.** The theoretical relation of scalp Laplacian and scalp current density of a spherical shell head model. *Phys Med Biol* 47: 2179–2185, 2002. doi:10.1088/0031-9155/47/12/312.
35. **Tenke C**, **Kayser J.** Reference-free quantification of EEG spectra: combining current source density (CSD) and frequency principal components analysis (fPCA). *Clin Neurophysiol* 116: 2826–2846, 2005. doi:10.1016/j.clinph.2005.08.007.
36. **Kamarajan C**, **Pandey AK**, **Chorlian DB**, **Porjesz B.** The use of current source density as electrophysiological correlates in neuropsychiatric disorders: a review of human studies. *Int J Psychophysiol* 97: 310–322, 2015. doi:10.1016/j.ijpsycho.2014.10.013.
37. **Kayser J**, **Tenke CE.** Issues and considerations for using the scalp surface Laplacian in EEG/ERP research: a tutorial review. *Int J Psychophysiol* 97: 189–209, 2015. doi:10.1016/j.ijpsycho.2015.04.012.
38. **Li G**, **Jiang S**, **Paraskevopoulou SE**, **Wang M**, **Xu Y**, **Wu Z**, **Chen L**, **Zhang D**, **Schalk G.** Optimal referencing for stereo-electroencephalographic (SEEG) recordings. *NeuroImage* 183: 327–335, 2018. doi:10.1016/j.neuroimage.2018.08.020.
39. **Zhai Y**, **Yao D.** A radial-basis function based surface Laplacian estimate for a realistic head model. *Brain Topogr* 17: 55–62, 2004. doi:10.1023/B:BRAT.0000047337.25591.32.
40. **Chen J**, **Valsecchi M**, **Gegenfurtner KR.** Attention is allocated closely ahead of the target during smooth pursuit eye movements: evidence from EEG frequency tagging. *Neuropsychologia* 102: 206–216, 2017. doi:10.1016/j.neuropsychologia.2017.06.024.
41. **Chen J**, **Valsecchi M**, **Gegenfurtner KR.** Enhanced brain responses to color during smooth-pursuit eye movements. *J Neurophysiol* 118: 749–754, 2017. doi:10.1152/jn.00208.2017.
42. **Chen J**, **McManus M**, **Valsecchi M**, **Harris LR**, **Gegenfurtner KR.** Steady-state visually evoked potentials reveal partial size constancy in early visual cortex. *J Vis* 19: 8, 2019. doi:10.1167/19.6.8.
43. **Baker DH**, **Vilidaite G**, **Wade AR.** Steady-state measures of visual suppression. *PLoS Comput Biol* 17: e1009507, 2021. doi:10.1371/journal.pcbi.1009507.
44. **Lygo FA**, **Richard B**, **Wade AR**, **Morland AB**, **Baker DH.** Neural markers of suppression in impaired binocular vision. *NeuroImage* 230: 117780, 2021. doi:10.1016/j.neuroimage.2021.117780.
45. **Vilidaite G**, **Norcia AM**, **West RJH**, **Elliott CJH**, **Pei F**, **Wade AR**, **Baker DH.** Autism sensory dysfunction in an evolutionarily conserved

system. *Proc Biol Sci* 285: 20182255, 2018. doi:10.1098/rspb.2018.2255.
46. **Dmochowski JP**, **Sajda P**, **Dias J**, **Parra LC.** Correlated components of ongoing EEG point to emotionally laden attention—a possible marker of engagement? *Front Hum Neurosci* 6: 112, 2012. doi:10.3389/fnhum.2012.00112.
47. **Dmochowski JP**, **Greaves AS**, **Norcia AM.** Maximally reliable spatial filtering of steady state visual evoked potentials. *NeuroImage* 109: 63–72, 2015. doi:10.1016/j.neuroimage.2014.12.078.
48. **Tenke CE**, **Kayser J**, **Fong R**, **Leite P**, **Towey JP**, **Bruder GE.** Response- and stimulus-related ERP asymmetries in a tonal oddball task: a Laplacian analysis. *Brain Topogr* 10: 201–210, 1998. doi:10.1023/A:1022261226370.
49. **Delorme A**, **Makeig S.** EEGLAB: an open source toolbox for analysis of single-trial EEG dynamics including independent component analysis. *J Neurosci Methods* 134: 9–21, 2004. doi:10.1016/j.jneumeth.2003.10.009.
50. **Liu-Shuang J**, **Torfs K**, **Rossion B.** An objective electrophysiological marker of face individualisation impairment in acquired prosopagnosia with fast periodic visual stimulation. *Neuropsychologia* 83: 100–113, 2016. doi:10.1016/j.neuropsychologia.2015.08.023.
51. **Bach M**, **Meigen T.** Do's and don'ts in Fourier analysis of steady-state potentials. *Doc Ophthalmol* 99: 69–82, 1999. doi:10.1023/A:1002648202420.
52. **Gray MJ**, **Frey H-P**, **Wilson TJ**, **Foxe JJ.** Oscillatory recruitment of bilateral visual cortex during spatial attention to competing rhythmic inputs. *J Neurosci* 35: 5489–5503, 2015. doi:10.1523/JNEUROSCI.2891-14.2015.
53. **Steinke A**, **Kopp B.** RELEX: an Excel-based software tool for sampling split-half reliability coefficients. *Methods Psychol* 2: 100023, 2020. doi:10.1016/j.metip.2020.100023.
54. **Retter TL**, **Rossion B**, **Schiltz C.** Harmonic amplitude summation for frequency-tagging analysis. *J Cogn Neurosci* 33: 2372–2393, 2021. doi:10.1162/jocn_a_01763.
55. **Chen J**, **Gegenfurtner KR.** Electrophysiological evidence for higher-level chromatic mechanisms in humans. *J Vis* 21: 12, 2021. doi:10.1167/jov.21.8.12.
56. **Liza K**, **Ray S.** Local interactions between steady-state visually evoked potentials at nearby flickering frequencies. *J Neurosci* 42: 3965–3974, 2022. doi:10.1523/JNEUROSCI.0180-22.2022.
57. **Cohen MX**, **Gulbinaite R.** Rhythmic entrainment source separation: optimizing analyses of neural responses to rhythmic sensory stimulation. *NeuroImage* 147: 43–56, 2017. doi:10.1016/j.neuroimage.2016.11.036.
58. **Sözer AT**, **Fidan CB.** Novel spatial filter for SSVEP-based BCI: a generated reference filter approach. *Comput Biol Med* 96: 98–105, 2018. doi:10.1016/j.compbiomed.2018.02.019.
59. **Wu Z**, **Su S.** A dynamic selection method for reference electrode in SSVEP-based BCI. *PLoS One* 9: e104248, 2014. doi:10.1371/journal.pone.0104248.
60. **Syam SH-F**, **Lakany H**, **Ahmad RB**, **Conway BA.** Comparing common average referencing to Laplacian referencing in detecting imagination and intention of movement for brain computer interface. *MATEC Web Conf* 140: 01028, 2017. doi:10.1051/matecconf/201714001028.
61. **Hjorth B.** Multichannel EEG preprocessing: analogue matrix operations in the study of local effects. *Pharmakopsychiatr Neuropsychopharmakol* 12: 111–118, 1979. doi:10.1055/s-0028-1094601.
62. **MacKay DM.** On-line source-density computation with a minimum of electrons. *Electroencephalogr Clin Neurophysiol* 56: 696–698, 1983. doi:10.1016/0013-4694(83)90040-8.
63. **Chen J**, **Valsecchi M**, **Gegenfurtner KR.** Saccadic suppression measured by steady-state visual evoked potentials. *J Neurophysiol* 122: 251–258, 2019. doi:10.1152/jn.00712.2018.
64. **Di Russo F**, **Pitzalis S**, **Aprile T**, **Spitoni G**, **Patria F**, **Stella A**, **Spinelli D**, **Hillyard SA.** Spatiotemporal analysis of the cortical sources of the steady-state visual evoked potential. *Hum Brain Mapp* 28: 323–334, 2007. doi:10.1002/hbm.20276.
65. **Müller MM**, **Teder W**, **Hillyard SA.** Magnetoencephalographic recording of steadystate visual evoked cortical activity. *Brain Topogr* 9: 163–168, 1997. doi:10.1007/BF01190385.
66. **Wittevrongel B**, **Khachatryan E**, **Fahimi Hnazaee M**, **Carrette E**, **De Taeye L**, **Meurs A**, **Boon P**, **Van Roost D**, **Van Hulle MM.** Representation of steady-state visual evoked potentials elicited by luminance flicker in human occipital cortex: an electrocorticography study. *NeuroImage* 175: 315–326, 2018. doi:10.1016/j.neuroimage.2018.04.006.
67. **Cai Y**, **Mao Y**, **Ku Y**, **Chen J.** Holistic integration in the processing of Chinese characters as revealed by electroencephalography frequency tagging. *Perception* 49: 658–671, 2020. doi:10.1177/0301006620929197.
68. **Jacques C**, **Jonas J**, **Maillard L**, **Colnat-Coulbois S**, **Rossion B**, **Koessler L.** Fast periodic visual stimulation to highlight the relationship between human intracerebral recordings and scalp electroencephalography. *Hum Brain Mapp* 41: 2373–2388, 2020. doi:10.1002/hbm.24952.

4. List of publications

Zhang, Y., Valsecchi, M., Gegenfurtner, K. R., & Chen, J. (2023). The time course of chromatic adaptation in human early visual cortex revealed by SSVEPs. *Journal of Vision*, *23*(5), 1–17. https://doi.org/10.1167/jov.23.5.17

Zhang, Y., Valsecchi, M., Gegenfurtner, K. R., & Chen, J. (2024). The execution of saccadic eye movements suppresses visual processing of both color and luminance in the early visual cortex of humans. *Journal of Neurophysiology*, *131*(6), 1156–1167. https://doi.org/10.1152/jn.00419.2023

Zhang, Y., Valsecchi, M., Gegenfurtner, K. R., & Chen, J. (2023). Laplacian reference is optimal for steady-state visual-evoked potentials. *Journal of Neurophysiology*, *130*(3), 557–568. https://doi.org/10.1152/jn.00469.2022

Zhang, Y., Agosti, G., Guan, S., Braun, D. I., & Gegenfurtner, K. R. (2025). Dynamics of S-cone contributions to the initiation of saccadic and smooth pursuit eye movements. *Journal of the Optical Society of America A*, *42*(5), B256–B265. https://doi.org/10.1364/JOSAA.545021

5. Selbstständigkeitserklärung

Hiermit erkläre ich, dass ich die vorliegende Arbeit selbständig und ohne unzulässige Hilfe oder Benutzung anderer als der angegebenen Hilfsmitel angefertigt habe. Alle Textstellen, die wörtlich oder sinngemäß aus veröffentlichten oder nichtveröffentlichten Schriften entnommen sind, und alle Angaben, die auf mündlichen Auskünften beruhen, sind als solche kenntlich gemacht. Bei den von mir durchgeführten und in der Dissertation erwähnten Untersuchungen habe ich die Grundsätze guter wissenschaftlicher Praxis, wie sie in der „Satzung der Justus-Liebig-Universität Gießen zur Sicherung guter wissenschaftlicher Praxis“ niedergelegt sind, eingehalten sowie ethische, datenschutzrechtliche und tierschutzrechtliche Grundsätze befolgt. Ich versichere, dass Dritte von mir weder unmitelbar noch mitelbar geldwerte Leistungen für Arbeiten erhalten haben, die im Zusammenhang mit dem Inhalt der vorgelegten Dissertation stehen, und dass die vorgelegte Arbeit weder im Inland noch im Ausland in gleicher oder ähnlicher Form einer anderen Prüfungsbehörde zum Zweck einer Promotion oder eines anderen Prüfungsverfahrens vorgelegt wurde. Alles aus anderen Quellen und von anderen Personen übernommene Material, das in der Arbeit verwendet wurde oder auf das direkt Bezug genommen wird, wurde als solches kenntlich gemacht. Insbesondere wurden alle Personen genannt, die direkt und indirekt an der Entstehung der vorliegenden Arbeit beteiligt waren. Mit der Überprüfung meiner Arbeit durch eine Plagiatserkennungssoftware bzw. ein internetbasiertes Softwareprogramm erkläre ich mich einverstanden.

_____ _____

Datum Unterschrift

Acknowledgements

I want to thank my co-authors Karl Gegenfurtner, Jing Chen, Matteo Valsecchi, Giulia Agosti, Shuchen Guan, and Doris Braun for their generous support. It has been a long journey to this point, and I am grateful to all the people who have been part of it.